

The Journal of THE BRITISH INSTITUTION OF RADIO ENGINEERS

FOUNDED 1925

INCORPORATED 1932

*"To promote the advancement of radio, electronics and kindred subjects
by the exchange of information in these branches of engineering."*

VOLUME 18

DECEMBER 1958

NUMBER 12

REPORT OF THE 33rd ANNUAL GENERAL MEETING

The Institution's Annual General Meeting, the twenty-fifth since Incorporation, was held at the London School of Hygiene and Tropical Medicine, on Wednesday, 26th November, 1958.

The Chair was taken by the President, Mr. George A. Marriott, B.A., who was supported by other officers of the Institution and members of the Council. 69 corporate members had signed the Minute Book when the meeting opened at 6.5 p.m.

The Secretary, Mr. G. D. Clifford, read the notice convening the meeting as published on page 565 of the September *Journal* and stated that 42 Forms of Proxy vested in the President and himself had been received.

1. To confirm the Minutes of the 32nd Annual General Meeting held on the 27th November, 1957

The Secretary stated that the report of the last Annual General Meeting was published on pages 666-668 of the December 1957 *Journal*. The President's proposal that these Minutes be signed as a correct record of the proceedings was approved unanimously.

2. To receive the Annual Report of the Council

Mr. Marriott stated that the Annual Report of the Council for the year ended 31st March 1958 had been published in the October 1958 *Journal*. He called on Professor Emrys Williams, Vice-President of the Institution, to move the adoption of the Report.

Professor Williams said that the work of each of the Standing Committees was deserving of far greater detail than it was possible to give in the published Report. There were, however, three points in the Report which he felt were outstanding in reflecting the Institution's progress and its affect upon the individual member.

Firstly, Professor Williams referred to the *Journal* which, he said, was the members' link with the Institution, and which, notwithstanding increasing over-all costs, continued to grow in size and in circulation. Today, some 7,000 copies were despatched monthly to some ninety

countries all over the world, and the increasing demand for back numbers was in itself an indication of its importance as an authoritative source of information.

Secondly, there was the advantage to members in having regular Section Meetings, and in Great Britain it would be an isolated case indeed if a member could not pay one or more visits during the course of a year to a local Section Meeting. From personal experience in participating in the founding of two Sections of the Institution, Professor Williams knew that the Council's efforts in this direction were well appreciated. It was also encouraging to note the increase in the number of Sections for members overseas. All these meetings were valuable, not only from the viewpoint of listening to a paper or taking part in discussion, but also in providing opportunity for engineers to meet.

Thirdly, there was the intrinsic advantage of membership itself; maintenance of high standards for admission to the Institution restricted the size of the membership, but it was a necessary restriction for the advantage of members and for the status of the profession.

Commenting on the valuable work of the individual Committees, Professor Williams said that the work of the Programme and Papers Committee was reflected month by month in all the meetings. The Technical Committee continued to show that it was a vigorous and active body which made definite contributions not only to the Institution's own proceedings but to the work of other bodies such as the British Standards Institution. The Library Committee also

endeavoured to give a useful service to members, and should be congratulated on its recent publication "Library Services and Technical Information for the Radio Engineer."

The Membership Committee's task was by no means easy, for although the membership regulations were reasonably well understood, the Committee on several occasions had to adjudicate fairly on qualifications which could not easily be assessed. It was these marginal cases which caused the Committee most difficulty in making a recommendation to the Council.

Professor Williams felt that perhaps the work of the Education and Examinations Committee had the greatest long term influence on Institution activities. He was sure that the Council was right in agreeing to the Committee's proposals for a continual modification of the Examination Syllabus in order to keep abreast of the changes and developments in the science and art of electronics and radio. The fall in entries consequent upon major changes in the Examination Syllabus a year ago was to be expected; now, however, the number of candidates was as high as ever, and Professor Williams regarded the trend in Technical Colleges of basing their Courses on the Institution's Examination Syllabus as a vote of confidence in the standard of the Examination.

All this work required finance—often in advance of revenue. While comment on the Institution's finances would be made by the Honorary Treasurer, Professor Williams said that all Standing and local Section Committees appreciated the way in which the Finance Committee handled all the demands for expenditure. He believed that the way in which the Finance Committee looked ahead was typical of all Committees, and indeed of the Council itself. Professor Williams cited as an example of this forward planning the 1959 Convention which, although not coming within the current report, had been planned during the year under review.

Professor Williams concluded: "During the last two years we have been able to consolidate many of the Institution's aims and have derived much courage to plan for the future. In both respects the Officers, Council and Committees have been much encouraged by the guidance of Mr. Marriott and by his radiant faith in the future of the Institution. It is in this spirit of progress that I move the adoption of the 32nd

Annual Report of the Council." The proposal was seconded by Mr. G. B. Ringham (Member) and the Report adopted unanimously.

3. To elect the President

Mr. Marriott said that it was the unanimous wish of the Council that Professor Eric E. Zepler be elected President for the coming year. Professor Zepler had been a Vice-President for the past six years, an office he had reached after many years' continuous service to the Institution, firstly as a member of the Education and Examinations Committee, and subsequently as its Chairman. The Council regarded him as the inspiration, if not the architect, of many changes which had taken place in the Graduateship Examination requirements since 1944, and his work in this connection had always shown a great understanding of industrial needs and the mind of the undergraduate or student.

The motion that Professor Eric E. Zepler be elected the 15th President of the Institution was carried with acclamation.

4. To elect the Vice-Presidents

Mr. Marriott stated that both Mr. J. L. Thompson and Professor Emrys Williams were well known to members and he was sure that their re-election as Vice-Presidents would be welcomed. This year he was particularly pleased to propose the election of two other Members to the office—Air Vice-Marshal C. P. Brown, C.B., C.B.E., D.F.C., and Colonel G. W. Raby, C.B.E., both of whom had given invaluable service to the Institution.

These proposals were approved unanimously.

5. To Elect the Ordinary Members of Council

Mr. Marriott stated that the Council's nominations for the ten vacancies had been unopposed, and he had pleasure in declaring the following elected to the Council for 1958-59.

A. D. Booth, D.Sc. (Member); F. G. Diver, M.B.E. (Member); A. A. Dyson, O.B.E. (Member); R. H. Garner, B.Sc.(Eng.) (Associate Member); Captain A. J. B. Naish, R.N., M.A. (Member); E. W. Pulsford, B.Sc. (Associate Member); H. F. Schwarz, B.Sc. (Member); T. B. Tomlinson, Ph.D. (Associate Member); Professor D. G. Tucker, D.Sc. (Member); Major P. A. Worsnop (Associate Member).

6. To Elect the Honorary Treasurer

The President said that Mr. G. A. Taylor had served as Honorary Treasurer for five years, and he was pleased to propose that he should be re-elected for a further year. The motion was carried unanimously.

7. To Receive the Auditors' Report, Accounts and Balance Sheet, for the year ended 31st March, 1958

Mr. Taylor expressed his appreciation of the confidence shown in re-electing him as Honorary Treasurer for the sixth year in succession, particularly as last year he had reported some failure. He referred to his last report in having to record the failure of the Institution's endeavours to persuade the Postmaster General to allow learned societies some relief from increased postal charges. Indeed, the Institution's Accounts for the year under review reflected an increase of over £1,000 in the overall expenditure incurred for postage. Mr. Taylor felt, however, that this disappointment had to some extent been offset by the announcement that the Inland Revenue would allow members' subscriptions as a deduction from their earnings for income tax purposes. Whilst this would not affect the Institution's revenue, Mr. Taylor thought that members would welcome the information with just as great enthusiasm as if it did, in fact, assist the Institution's income.

Referring to the Income and Expenditure Account for the year ended 31st March, 1958, Mr. Taylor stated that every member might be well pleased with the Finance Committee's efforts during the year, which had resulted in a substantial amount being placed to the Reserve Account. Dealing firstly with Income, the Treasurer pointed out that all items of revenue had been maintained or increased, and he particularly referred to the record figure of nearly £20,000 received from subscriptions.

The Expenditure Account showed that to offset costs over which the Committee had no control, e.g. postal and telephone costs, printing, etc., some economies had been effected. A most pleasing feature of the accounts was the very low subsidy which had been required to finance the Institution's 1957 Convention: never before had a Convention been held at such a low cost.

The Balance Sheet showed that there had been additions during the year to office and Library equipment, and an increase in investments. In this connection, Mr. Taylor drew particular attention to the fact that all monies received towards the new building were deposited separately and subsequently invested. The Accounts for 1957 showed that the Institution had now received £16,000 for the Building Appeal, excluding monies payable under Deeds

to Covenant. During the year more companies in the radio and electronics industry had covenanted to donate to this appeal, and all these covenants would bring the Building Appeal to over £40,000.

Mr. Taylor concluded by expressing his pleasure at being able to present such satisfactory Accounts, and his thanks for the guidance and help he had received from the Council, Finance Committee, and the President. He then moved the adoption of the Accounts and Balance Sheet for the year ended 31st March, 1958.

The President asked for any comments on the accounts. Mr. J. K. Draper (Associate Member) pointed out that the sum of £40,000 which was still required to purchase a new building represented a very substantial sum when considered in relation to the membership which, according to the Articles of Association, appeared to be limited to 3,000. He therefore felt that an appeal should be made to members for donations on the basis of their rebate of income tax in respect of subscriptions.

Mr. Clifford replied that as far as the Articles of Association were concerned, there was no obligation to register an increase in membership until the figure of 10,000 was reached. This did not mean, however, that membership was now limited to 3,000, and he welcomed Mr. Draper's suggestion which would greatly help the Building Appeal.

The Auditors' Report, Accounts and Balance Sheet were then approved unanimously.

8. To Appoint Auditors and to agree their remuneration

Mr. Marriott moved the re-appointment of Messrs. Gladstone, Jenkins. This proposal was approved, it being agreed that the Auditors' remuneration be left to the discretion of the Council.

9. To Appoint Solicitors

The proposal that Messrs. Braund and Hill be re-appointed as the Institution's Solicitors was approved unanimously.

10. Awards to Premium and Prize Winners

Mr. Marriott congratulated the recipients of Premiums and Examination Prizes for 1957 and presented the awards to the authors and successful examination candidates. A list of recipients was published in the September Journal.

11. Any other business

The Secretary confirmed that notice of any other business had not been received.

ON THE DESIGN OF THE TRANSITION REGION OF AXISYMMETRIC, MAGNETICALLY FOCUSED BEAM VALVES*

by

V. Bevc, M.Sc.,† J. L. Palmer, M.Sc.,†
and C. Süsskind, Ph.D. (Associate Member)†

SUMMARY

Assumption of a particular magnetic-field variation in the transition region of an axially symmetric beam-type device (e.g., klystron, travelling-wave tube) leads to the solution of the equations of electron motion by means of an analogue computer. To illustrate this novel method of solution, beam envelopes are presented for Brillouin flow, periodic magnetic focusing, and space-charge-balanced flow. By matching the beam envelopes with those obtained from the theory of the Pierce gun, dimensions are obtained for an electron gun that produces the required beam.

1. Introduction

The development of beam-type microwave valves has created a need for well-designed electron guns capable of yielding high-density electron beams, usually axially symmetric. To counteract the combined effects of aperture lenses and space-charge spreading, a radially inward directed force is necessary, more often than not provided by a magnetic field. The most frequently used method, that of immersing the entire valve, including the electron gun, in a magnetic field ("confined flow"), has been described in the literature, most recently by Brewer¹. Of the alternative methods proposed in recent years, two have found most favour: "Brillouin" flow and periodic magnetic focusing. Both principles have been widely described in the literature with regard to the behaviour of the beam in the region where it is caused to interact with the microwave "circuit" structure (hereafter designated as the *interaction region*). A large body of literature has also accumulated on the design of the electron *gun region*—a recent review article² lists 88 references. However, very few attempts have been reported dealing with the design of the *transition region* between the gun and interaction regions. The present contribution is an attempt to deal with this problem analytically, with an analogue

computer used to trace out electron trajectories for typical cases.

A similar analysis and computation has been made by Moster and Molnar³ and reported in an unpublished (but widely circulated) Bell Telephone Laboratories Memorandum, for the case of Brillouin flow. This case represents one of the examples used in the present analysis. The essentially identical results are presented here in what is believed to be a more useful form from the designer's viewpoint; the numerical results are in excellent agreement with those of Moster and Molnar. Moreover, a method of matching the design of the transition region to an electron gun designed by the well-known "Pierce" method is also presented.

The second case used to exemplify the present analysis, periodic focusing, has apparently not been previously considered, although Caryotakis and Heffner⁴ have analysed this case (for non-convergent guns) assuming an idealized variation of magnetic-field strength as applicable to a structure of the type described in an analysis by Sterrett and Heffner⁵. Again, a method for matching to a Pierce electron gun is presented.

The third case considered is the general case of space-charge-balanced flow, which is intermediate between Brillouin flow and the aforementioned confined flow in that a portion of the interaction-region magnetic field is permitted to penetrate into the electron-gun region and links the cathode.

* Manuscript first received 10th July 1958 and in final form on 3rd October 1958. (Paper No. 480.)

† Department of Electrical Engineering, University of California, Berkeley, California.

U.D.C. No. 621.385.63/4

One of the results of the present analysis is that the designer is enabled to select the smallest gun that will yield an electron beam of a given beam voltage, current, and radius (and the corresponding magnetic field). Such optimization is especially important from the viewpoint of minimizing the effects of "thermal" velocities, heater-power requirements, and other design factors.

The deleterious effects of "thermal" electron velocities on beam focusing are not considered. The most probable result of the presence of this effect in practice will be that the magnetic-field requirements might be somewhat larger than those predicted by the described design procedures.

2. Equations of Motion

For the axially symmetric case the equations of motion for laminar flow (non-crossing trajectories) can be expressed in cylindrical coordinates in a region free from applied electric fields by

$$\frac{d^2r}{dz^2} + \frac{\eta B^2}{8V} r - \frac{\eta B_c^2 r_c^4}{8V} \frac{1}{r^3} - \frac{I}{4\sqrt{2}\eta\pi\epsilon_0 V^{3/2}} \frac{1}{r} = 0 \dots\dots(1)$$

where *r* and *z* describe the position of an electron on the beam boundary, *I* and *V* are the beam current and voltage, respectively, *r_c* is the radius of the beam at the cathode, *B* and *B_c* are the values of the magnetic field in the beam region and at the cathode, respectively, and $\eta = e/m$. For the purpose of the present analysis, eqn. (1) can be best normalized by making the following definitions:

$$\sigma \equiv r/r_m \dots\dots(2)$$

$$Z \equiv \left(\frac{I}{4\pi\sqrt{2}\eta\epsilon_0 V^{3/2}} \right)^{\frac{1}{2}} \frac{z}{r_m} = 0.1231 P^{\frac{1}{2}} \frac{z}{r_m} \dots\dots(3)$$

$$B_b^2 \equiv \frac{\sqrt{2}I}{\pi\epsilon_0 V^{3/2} r_m^2} \dots\dots(4)$$

$$K \equiv \frac{B_c r_c^2}{\beta B_b r_m^2} \dots\dots(5)$$

where *P* is the microperveance of the beam, *r_m* is a reference radius whose value depends on the particular configuration, *B_b* is the ideal Brillouin field⁶ that would be necessary to focus the same beam, and

$$B(z) = \beta B_b F(z) \dots\dots(6)$$

where β is a scaling factor for the magnetic field, and *F(z)* is a form factor describing the axial variation of the magnetic field. With the above substitutions, eqn. (1) becomes

$$\frac{d^2\sigma}{dZ^2} + [\beta F(z)]^2 \sigma - \frac{\beta^2 K^2}{\sigma^3} - \frac{1}{\sigma} = 0 \dots\dots(7)$$

The form factor *F(z)* can be made to take on any variation desired. Equation (7) thus describes the motion of an electron beam passing through such a field, provided that the beam radius remains small compared with the radial dimensions of the magnetic circuit ("paraxial" beam). The factor *K* accounts for any magnetic field at the cathode.

3. Brillouin Flow

Equation (7) can be applied to the case of Brillouin flow, for which $\beta=1$ and $K=0$. No magnetic flux threads the cathode, the magnetic field in the interaction region is uniform, and eqn. (7) becomes

$$\frac{d^2\sigma}{dZ^2} + [F(z)]^2 \sigma - \frac{1}{\sigma} = 0 \dots\dots(8)$$

The beam is balanced (i.e., $d^2\sigma/dZ^2=0$) if the beam enters the interaction region, in which *F(z)* = 1, with zero slope at the position of minimum radius *r_m*, so that $d\sigma/dZ=0$ when $\sigma=1$.

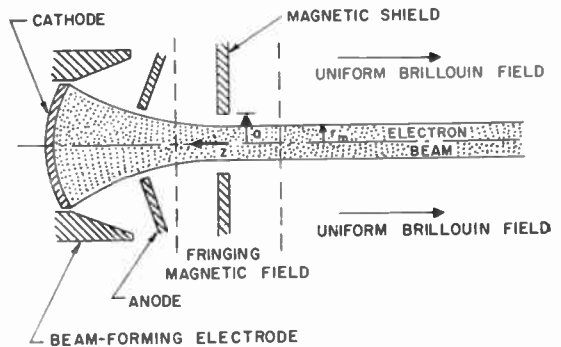


Fig. 1. Typical Brillouin focusing system.

But since the beam must have originated at the cathode in a region free from magnetic field ($K=0$), the beam must have passed through a region in which the magnetic field increased from zero to its final value *B_b*. The behaviour of the electron beam in this transition region is described by eqn. (8), in which *F(z)* is the normalized magnetic-field variation as a function of axial distance (with *z* positive in the

direction toward the cathode). Such a solution has been obtained by Moster and Molnar³. The normalized magnetic-field variation on the axis of a hole of radius a (Fig. 1) in a thin magnetic shield of high permeability with a uniform magnetic field on one side of it is given by

$$F(z/a) = 1 - \frac{1}{\pi} \left[\tan^{-1}(-a/z) + \frac{z/a}{1+(z/a)^2} \right] \quad z/a < 0 \quad \dots\dots(9a)$$

$$F(z/a) = \frac{1}{\pi} \left[\tan^{-1}(a/z) - \frac{z/a}{1+(z/a)^2} \right] \quad z/a > 0 \quad \dots\dots(9b)$$

These expressions appear to be quite insensitive to the thickness of the magnetic shield, as has been established by using electrolytic-trough analogues; the shielding needs to be only thick enough to avoid saturation.

Equations (9) must be put into units of Z , as can be done by the substitution $z/a = Z/\alpha$, where $\alpha = 0.1231 P^{1/2} a/r_m$, so that eqns. (9) become

$$F(Z/\alpha) = 1 - \frac{1}{\pi} \left[\tan^{-1}(-\alpha/Z) + \frac{Z/\alpha}{1+(Z/\alpha)^2} \right] \quad Z/\alpha < 0 \quad \dots\dots(10a)$$

$$F(Z/\alpha) = \frac{1}{\pi} \left[\tan^{-1}(\alpha/Z) - \frac{Z/\alpha}{1+(Z/\alpha)^2} \right] \quad Z/\alpha > 0 \quad \dots\dots(10b)$$

The equation of motion is therefore

$$\frac{d^2 r}{dZ^2} + F(Z/\alpha)^2 r - \frac{1}{r} = 0 \quad \dots\dots(11)$$

A plot of eqns. (10) shows that the magnetic field is essentially uniform for $z/a = -3$ (Fig. 2). This point can be therefore used as the origin of a computation; i.e., the analogue computer is started at the point where $z/a = Z/\alpha = -3$, $r = 1$, and $d r/dZ = 0$, and traces out the beam envelope through the transition region, toward the cathode. Curves of normalized radius and slope vs. distance are shown in Figs. 3 and 4, respectively, both as functions of the parameter $\gamma = P^{1/2} a/r_m$.

The parameters used in plotting Figs. 3 and 4 were selected for ease in adapting or "matching" this design procedure to the design of the electron gun by the Pierce method⁷. For the spherical-cap cathode, Pierce's eqn. (10-12) can be written

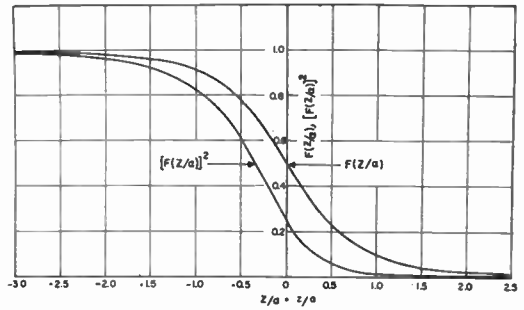


Fig. 2. Normalized magnetic field vs. distance on the axis of an aperture in a magnetic shield.

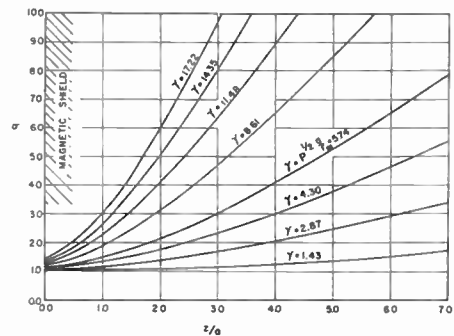


Fig. 3. Normalized beam radius in the transition region vs. axial distance.

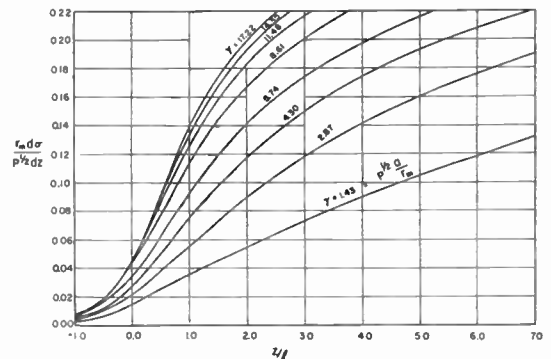


Fig. 4. Normalized beam slope in the transition region vs. axial distance.

$$I = 10^{-6} C V^{3/2} (1 - \cos \theta) \quad \dots\dots(12)$$

where $C = 14.67/(-\alpha)^2$. Since θ is given by $\sin \theta = r_a/\bar{r}$, where r_a is the radius of the beam at the anode, and \bar{r} is the "radius of curvature" of the equivalent anode surface, eqn. (12) can be written

$$P = C [1 - \sqrt{1 - (r_a/\bar{r})^2}] \quad \dots\dots(13)$$

where $P = 10^6 I / V^{3/2}$ is the microperveance. Equation (13) can be solved for \bar{r} and expanded by binomial expansion to give finally

$$\bar{r} = r_a (C/2P)^{1/2} (1 + P/4C) \dots\dots\dots(14)$$

with higher-order terms becoming negligible for cone half angles smaller than 60 deg.

The slope of the beam upon emerging from the anode aperture is given by

$$\left. \frac{dr}{dz} \right|_{r=r_a} = \frac{r_a}{f} \dots\dots\dots(15)$$

which may also be written

$$\bar{r} \left. \frac{d\sigma}{dz} \right|_{r=r_a} = \frac{r_a}{r_m} \frac{\bar{r}}{f} \dots\dots\dots(16)$$

where σ is the normalized radius defined in eqn. (2), and f is the focal length of the anode aper-

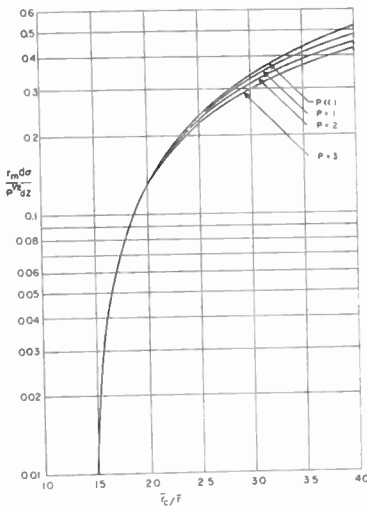


Fig. 5. Normalized beam slope at the anode aperture vs. the ratio of cathode radius of curvature to anode radius of curvature.

ture acting as a thin diverging lens.* By substituting eqn. (14) into (16) and rearranging, we obtain

$$\frac{r_m}{P^{1/2}} \cdot \left. \frac{d\sigma}{dz} \right|_{r=r_a} = \frac{1}{1 + P/4C} \left(\frac{2}{C} \right)^{1/2} \frac{\bar{r}}{f} \dots\dots\dots(17)$$

* Substituting a "thick" electron lens would have the effect of introducing a complicating factor (an aberration produced by the radial variation of the electrostatic field in the anode region, i.e. such as that produced by considering rays that are not paraxial); although a correction can be sometimes worked out for a particular case, it is prohibitively difficult to do so in general.

Values of \bar{r}/f can be obtained from a graph given by Pierce⁷ (Fig. 10, 11).

Equation (17) is plotted in Fig. 5, with microperveance as a parameter. The top curve, for $P \ll 1$, is the result that would be obtained by assuming that $\sin \theta = \theta$ (i.e. very small cone half angles, as assumed by Pierce).

Figure 6 is a plot of the rearranged eqn. (14) in the form

$$P^{1/2} \bar{r} / r_a = (C/2)^{1/2} (1 + P/4C) \dots\dots\dots(18)$$

Again, the curve for $P \ll 1$ is that which would be obtained by assuming $\sin \theta = \theta$.

The design procedure begins with a selection of the anode position, which should be taken to be as near to the magnetic shield as possible (since the resultant minimization of beam convergence serves to reduce the effects of a distribution of initial velocities, and other aberrations), subject only to the requirements that the corresponding emission density at the cathode should not exceed the capabilities of that cathode, and that the anode-to-shield distance should be large enough to locate the anode outside the transition region (say, $z/a > 1$, as shown in Fig. 1). If the beam radius, perveance, and voltage (or current) are given, the next step consists in selecting an appropriate value of the radius a of the shield aperture (usually made as small as outside valve dimensions permit), and calculating $\gamma = P^{1/2} a / r_m$. Knowing γ and the normalized anode position z/a , we obtain the normalized radius σ from Fig. 3 and the normalized slope $(r_m / P^{1/2}) (d\sigma / dz)$ from Fig. 4 at the anode aperture. The "matching" procedure consists of obtaining the normalized cathode radius of curvature (i.e. "spherical" radius) \bar{r}_c / \bar{r} from Fig. 5, and then \bar{r} from Fig. 6, so that both \bar{r}_c and \bar{r} can be determined. The "cylindrical" radius of the cathode r_c is then given by

$$r_c = r_a \bar{r}_c / \bar{r} \dots\dots\dots(19)$$

The final step might be a calculation of the current density from the cathode so designed: if that number should prove to be too large, it would be necessary to begin the computation again with a larger value of anode-to-shield spacing z/a . (The experienced designer might actually prefer to start with a given cathode area, and carry out the above steps in reverse order.)

Since the above procedure does not take radial "thermal" velocities into account, it will probably be necessary to make the usual allowance for this effect⁸ by making the radius of the microwave "circuit" somewhat larger than the value that would correspond to the r_m obtained by the above design procedure.

Incidentally, the above procedure might also be of use in predicting the envelope shape of an electron beam emerging from a Brillouin focusing field, a feature that may be of considerable interest to the designer of the collector electrode.

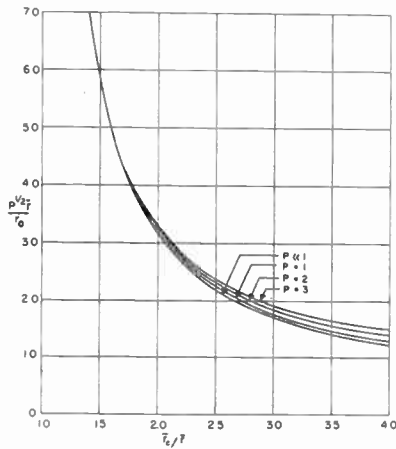


Fig. 6. Normalized anode radius of curvature as a function of the ratio of cathode radius of curvature to anode radius of curvature.

It should be noted that an earlier analysis by Brück⁹ leads to results that are in good agreement with those of the present analysis. Brück considers the case of magnetic distribution of the form $B_z = B_0 \sin^2(\pi z/2l)$, where l is the length of the transition region. It is found that this distribution closely matches the function $F(Z/a) = F(z/a)$ used in the present analysis if $l = 3a$, if the origin is shifted to the point where $F(Z/a) = 0.5$, and if the sign of z is reversed. In other words,

$$F(z/a) = \sin^2 \left[\frac{\pi}{6} \left(\frac{z}{a} - \frac{3}{2} \right) \right]$$

With these transformations, Fig. 3 corresponds to Brück's Fig. 4, which is limited to the range $z/a < 1.5$. A numerical comparison shows agreement to within a few per cent.

A related analysis by Müller¹⁰ confirms that

injection conditions are relatively insensitive to the exact form of the function $F(z/a)$; for functions of the form $\cos z$ and $\exp(-z^2)$, for example, Müller finds that both lead to the neat result that the magnetic shield should be located in such a way that B falls off to 70 per cent. of its full value at the point at which a laminar beam would come to its minimum diameter in the absence of B .

4. Periodic Magnetic Focusing

4.1. Analysis

For a scheme of beam focusing by a periodic magnet of the sort discussed by Sterrett and Heffner (Fig. 4 of Ref. 5), it can be shown that the function $F(z)$ can be represented by an infinite series of cosine terms with the argument $2n\pi z/l$ where n is an odd integer and l is the length of the magnetic structure. Moreover, if the distance d_1 between pole shoes is made approximately equal to $l/3$ (for usual values of the ratio r_1/l , the normalized pole-shoe radius) the $n=3$ term is approximately zero, and the higher-order terms are negligible. This case, which is the simplest from an analytical point of view (since the variation of the magnetic field along the axis in the interaction region corresponds exactly to a simple cosine variation), also turns out to be of considerable practical interest: the radius of the beam is of necessity considerably smaller than the pole-shoe radius at which the axial variation of the magnetic field corresponds to a square wave, so that the magnetic field at the beam edge resembles a simple cosine variation quite closely.

Equation (7) thus becomes

$$\frac{d^2\sigma}{dz^2} + \frac{\beta^2}{2} [1 + \cos(4\pi z/l)]\sigma - \frac{\beta^2 K^2}{\sigma^3} - \frac{1}{\sigma} = 0 \quad \dots\dots\dots(20)$$

where we have also utilized the trigonometric formula $\cos^2 x = (1 + \cos 2x)/2$.

This equation can be normalized by means of the definition $Z/L = z/l$, which defines a reduced period length

$$L = (Z/z)l = 0.1231 P^{1/2} l / r_m \quad \dots\dots\dots(21)$$

where r_m is the maximum radius of the beam in the interaction region. (The beam ripples inward from r_m ; one of the objectives of the design is to make the ripple as small as possible, as described below.)

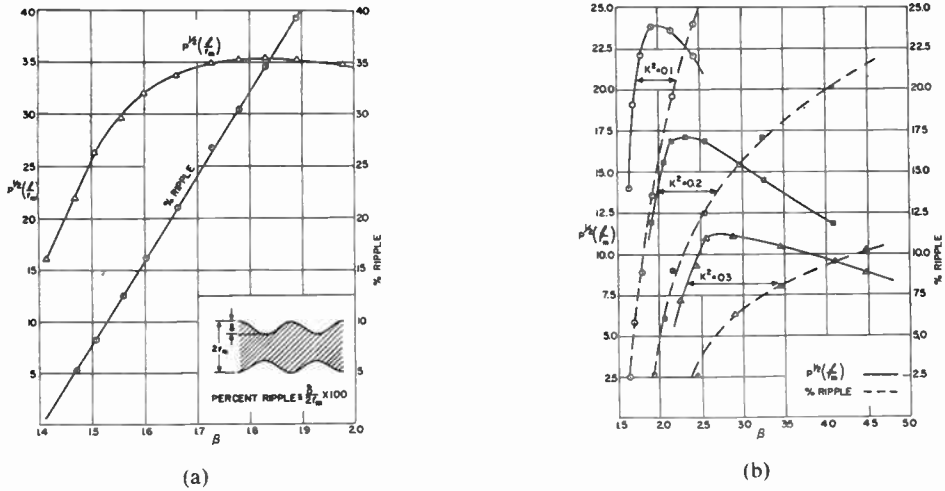


Fig. 7. Period length and percent ripple vs. magnetic field for minimum-ripple solutions for (a) zero magnetic field at the cathode, (b) non-zero magnetic field at the cathode.

The equation of motion can thus be written

$$\frac{d^2\sigma}{dZ^2} + \frac{\beta^2}{2}[1 + \cos(4\pi Z/L)]\sigma - \frac{\beta^2 K^2}{\sigma^3} - \frac{1}{\sigma} = 0 \dots\dots\dots(22)$$

The quantities σ , Z , B_0 , and K are the same as defined in eqns. (2) to (5), and eqn. (6) becomes

$$B(z) = \beta B_0 \cos(2\pi z/l) = B_0 \cos(2\pi z/l) \dots\dots(23)$$

where B_0 is the peak magnetic field on the axis. Equation (23) also defines the scaling factor β , which is the ratio of the peak magnetic field on the axis to the Brillouin field required to focus the same beam.

A solution of eqn. (22) has been carried out with a Beckman EASE computer, and the results are presented in a form that gives information about the beam envelope (radius and slope vs. axial distance) directly. The initial conditions used in the solution are $d\sigma/dZ=0$ and $\sigma=1$ at $Z=0$; i.e., the beam is launched with zero slope at its maximum radius r_m at the centre of the first magnet cell, or half-way between the first two pole shoes.

In the design of the magnet structure for periodically focused beams, it has been shown¹¹ that for a given value of β there is a particular value of L for which the beam envelope has a minimum amplitude of oscillation or ripple. In an analogue-computer solution similar to the present one, Harker¹² has shown that the solutions appear to be of the form

$$\sigma = (1 - R) + R \cos(4\pi Z/L) \dots\dots\dots(24)$$

where, in our notation, R is the percent ripple defined in the insert of Fig. 7(a). This figure also shows a plot of the normalized length of the period of the magnet structure (and percent ripple) vs. β , for the case $K=0$. Similar curves for other values of K are shown in Fig. 7(b). (These curves agree very closely with those of Harker¹², although the present set is normalized differently.) In the design of the magnet structures for periodic focusing, every effort should be made to ensure that the dimensions and other parameters correspond to points *on* these curves; design points not on these curves do not correspond to minimum-ripple solutions.

The curves of Fig. 7 show that if β (and hence the peak magnetic field on the axis) is small, the percent ripple is also small; however, so is the normalized magnet structure period length $P^{1/2}/r_m$, which can then become a limiting factor if the amount of magnetic material per cell should become too small to supply the requisite magnetic-field intensity. (This limitation is particularly serious for large values of P or small values of r_m .)

A schematic representation of the first magnet cell and an electron gun of the shielded Pierce type is shown in Fig. 8. To determine how the magnetic field varies, at least on the axis in the transition region, i.e., to obtain the function $F(z/l)$, an electrolytic-trough analogue was used for convenience. The electric field

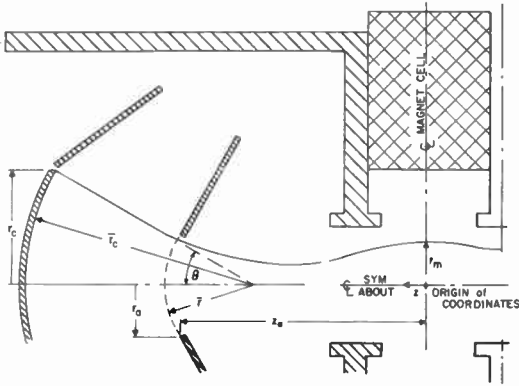


Fig. 8. Pierce gun and first cell of periodic structure.

very near the axis of a wedge of electrolyte (used in the conventional manner to represent an axially symmetric configuration) was measured by a null technique utilizing a double-probe head mounted on a carriage. In order for the analysis to apply exactly, the peak magnetic field in the end cell should be the same as in any cell in the interaction region. This condition can be approximated in the analogue by suitably adjusting the potentials of the two or three cells at the end; a corresponding adjustment is used in the fabrication of actual magnetic structures⁵. The resulting magnetic field on the axis is almost exactly sinusoidal down to the centre of the first cell, which is taken as the origin of the co-ordinates. The normalized magnetic field $F(z/l)$ in the transition region (with z positive in the direction toward the cathode) is shown in Fig. 9; the square of this function, which is one of the terms that occurs in eqn. (7), is also shown in Fig. 9, and is essentially zero for values of $z/l > 0.6$.

In a case of considerable practical interest, a valve containing a periodic magnetic focusing structure and a convergent Pierce gun, the beam originates from an electron gun located outside the magnetic field ($z/l = Z/L > 0.6$), passes through the transition region ($0 < z/l = Z/L < 0.6$),

and arrives at the centre of the first magnet cell ($Z=0$) with its maximum radius ($\sigma=1$) and zero slope ($d\sigma/dZ=0$). In the present solution, the problem is solved in reverse; eqn. (7) is set up on the analogue computer for the case $K=0$, and the function $F(z)$ is replaced by the function $F(Z/L)$ plotted in

Fig. 9. This function is created by a function generator. To obtain curves of normalized radius and slope, we proceed as follows: β , and hence L , are obtained from Fig. 7(a) and eqn. (21). These pairs of values of β and L , each corresponding to a minimum-ripple solution, are the parameters in the input to the computer; the output corresponds to the normalized radius σ and normalized slope ($r_m P^{1/2}$)($d\sigma/dz$). The resulting curves are presented in Figs. 10 and 11, respectively.

The design proceeds very much as in the Brillouin case, except that it is necessary to utilize additional information in the form of the curves of Fig. 7(a). After selecting a value of β as small as is compatible with the capabilities of present-day magnetic materials, and the corresponding value of $P^{1/2}/r_m$, it is possible to determine the magnet structure period length l ,

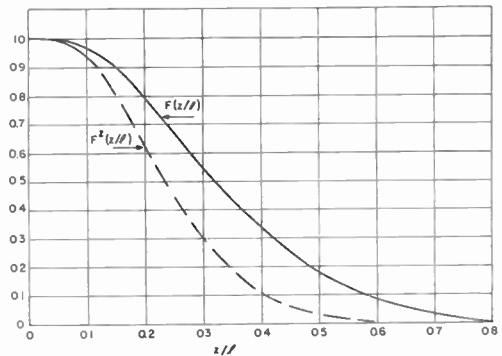


Fig. 9. Normalized magnetic field on the axis in the transition region vs. axial distance.

since P and r_m are assumed to be given parameters of the electron beam. The Brillouin field corresponding to a given beam can be computed from eqn. (4), and the peak magnetic field on the axis from the relationship $B_0 = \beta B_b$. The important physical dimensions of the magnet structure are now determined, and can be checked for the above-mentioned limitation on magnetic-field capability. The complete design can be carried out with the help of the curves given by Sterett and Heffner⁵.

The gun design again consists in matching the radius and slope of the beam emerging from the anode aperture to the radius and slope at some axial position, as predicted by the appropriate curves in Figs. 10 and 11. To attain small

electron-gun dimensions and a small beam-convergence angle, the axial position of the anode should be near the point ($z/l=0.6$) at which the fringing magnetic field has dropped

radius of curvature \bar{r} can be calculated. From the ratio \bar{r}_c/\bar{r} , the cathode radius of curvature \bar{r}_c can be easily obtained. Equation (19) then specifies the radius r_c of the beam at the cathode. The final step is again a calculation of the current density from the cathode so designed; if that number should prove to be too large, it would be necessary to begin the computation again with a larger value of the distance z/l between anode and the centre of the first magnet cell (or to proceed backwards, as previously described in the Brillouin case).

4.2. Experimental Study

An experimental periodically focused valve was designed according to the method developed in the preceding section. A standard convergent Pierce gun with a microperveance of 1.0 was used. In the interaction region the beam is specified by the following design parameters: $V=1,600$ V, $I=64$ mA, $r_m=0.040$ in. A drift tube with 0.125 in. inside diameter and of length 10 in. surrounds the beam in the interaction region.

A periodic electromagnet was constructed with a period length of 1.0 in. By regulating the current through the individual coils (one in each cell) the peak magnetic field on the axis of each cell can be easily adjusted. Measurements employing a magnetic probe reveal that the field along the axis of the magnet structure is very nearly sinusoidal when the peak magnetic fields of all the cells have been equalized. The magnetic-field variation along the axis in the transition region, as shown in Fig. 9, was accurately verified by measurements on the end cell of the magnet structure with a magnetic probe. By this experimental technique the magnetic-field variations assumed in the theoretical treatment were reproduced quite accurately in the experimental apparatus.

The experimental valve behaved quite satisfactorily, exhibiting a beam-current transmission of 95 per cent. through the entire length of the drift tube. The transverse alignment of the tube in the magnet structure affected very critically the current that could be transmitted through the drift tube. This sensitivity to alignment was not surprising, however, since the beam just grazes the wall of the drift tube under conditions of perfect alignment.

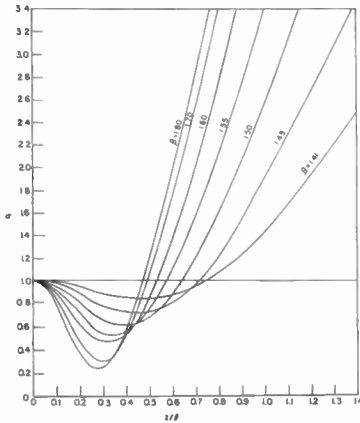


Fig. 10. Normalized beam radius in the transition region vs. axial distance.

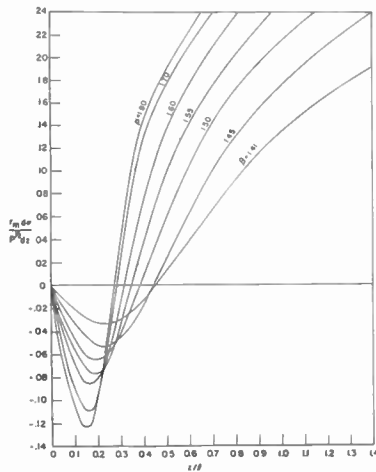


Fig. 11. Normalized beam slope in the transition region vs. axial distance.

essentially to zero. If $z/l=0.6$ is selected as the anode position, the normalized radius and slope at this position can be obtained from Figs. 10 and 11. From the normalized slope, the ratio of cathode radius of curvature to anode radius of curvature \bar{r}_c/\bar{r} can be obtained from Fig. 5, and from it, the parameter $P^{1/2}\bar{r}/r_a$ from Fig. 6. Since the microperveance P and the radius r_a of the beam at the anode are known, the anode

The axial position of the gun with respect to the magnet structure is, of course, a critical adjustment. The highest beam-current transmission was attained when the distance from the gun anode to the centre of the first magnet cell was about 90 per cent. of that predicted by the theory. Either the beam is less convergent as it emerges from the anode aperture than predicted by the simple theory of the Pierce gun, or spherical aberration is introduced by the anode-aperture lens. The latter defect can be greatly reduced by careful design of the electron gun¹³. In the design of a valve employing the proposed injection scheme it would be advantageous to provide an adjustable distance between the gun and the magnet structure, since this distance will probably be, in general, slightly smaller than that predicted by the theory. If such an adjustment is not feasible, a 10 per cent. reduction in the theoretical anode-to-magnet distance is recommended.

By adjusting the field strength in the first cell of the magnet, it is possible to correct, at least partially, for misadjustment of the injection conditions. This effect can be very valuable to the designer, especially if the anode-to-magnet distance is not adjustable. Moreover, by increasing the magnetic field in the first cell, the anode-to-magnet distance may be increased, an effect which may be very desirable for certain applications.

A peak magnetic-field strength 25 per cent. greater than the theoretical value was required to focus the experimental beam. The reason for this discrepancy can be traced to at least four phenomena:

- (1) "Thermal" velocities, not considered in the present analysis.
- (2) Spherical aberration in the anode-aperture lens.
- (3) Imperfect shielding of the cathode from magnetic fields.
- (4) Error in r_m owing to differences between actual and design injection conditions.

All of these factors operate to increase the magnetic-field requirement in the interaction region.

5. Space-Charge-Balanced Flow

The intermediate case between Brillouin flow and confined flow occurs when part of the mag-

netic flux penetrates to the cathode. This general case has been termed *space-charge-balanced flow*^{3, 14}.

The magnetic field in this case varies with axial distance from a given value B_c at the cathode to a different value in the interaction region. This magnetic-field distribution can be composed, for instance, of two distributions given by eqns. (9)—one caused by the field on

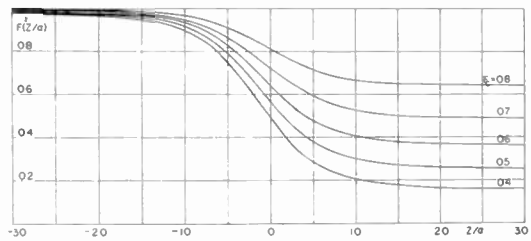


Fig. 12. Assumed distribution of the normalized magnetic-field density along the axis for various values of F_c .

the right of the magnetic shield and the other on the left—and can be readily realized with two solenoids. A graphical representation of the magnetic-field variation is given in Fig. 12 for various ratios of the field in the interaction region to that at the cathode. There is, of course, no fundamental reason for choosing this sort of magnetic-field distribution; other physically realizable distributions could be used.

It is proposed to launch the beam from a linear Pierce gun. The beam emerging from the anode aperture diverges, owing largely to the lens action of the anode; then the beam expands and contracts periodically as it traverses the transition region: it scallops. As the beam enters the interaction region the scallops become smaller because of the stronger magnetic field there. The object of the present investigation is to find such combinations of the parameters of the focusing system (α , β , F_c) for which the beam in the interaction region is smooth.

Equation (7) is again solved with the analogue computer, starting in the interaction region at the full value of the magnetic field, where $F(Z/\alpha)=1$, and working backward toward the cathode. At the initial point, the following conditions exist.

The normalized radius in the interaction region is

$$\sigma = 1 \quad \dots\dots(25)$$

The beam must be smooth throughout the interaction region and its normalized radius must be constant:

$$\frac{d\sigma}{dZ} = 0 \quad \dots\dots(26)$$

Moreover, at equilibrium,

$$\frac{d^2\sigma}{dZ^2} = 0 \quad \dots\dots(27)$$

When these conditions are fulfilled a relation must exist between β and K such that

$$\beta^2 = \frac{1}{1 - K^2} \quad \dots\dots(28)$$

which follows if the condition that is expressed in eqn. (27) is substituted into eqn. (7). Hence

$$K^2 = \frac{\beta^2 - 1}{\beta^2} \quad \dots\dots(29)$$

Recalling eqn. (5) it is seen that

$$K = \frac{r_c^2}{r_m^2} F\left(\frac{Z}{\alpha}\right) \Big|_{z=z_c} \quad \dots\dots(30)$$

The beam must then be launched with a radius r_c if it is to have a radius r_m in the interaction region.

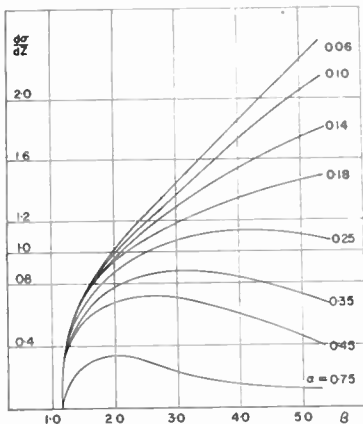


Fig. 13. Normalized slope as a function of β for various values of α at $F_c=0.5$.

It is evident that a considerable number of parameters can be varied in this case: the relative magnetic-field strength at the cathode $F(Z/\alpha)|_{z_c}$, parameter β , and parameter α . Distributions of the magnetic-field density with

$F_c=0.5, 0.6,$ and 0.7 have been used. Parameter α was varied between the values $0.06 > \alpha > 0.75$, and parameter β between $1.4 > \beta > 5.4$.

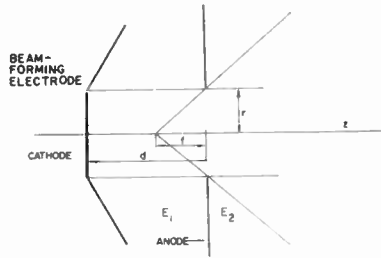


Fig. 14. Linear Pierce electron gun employed in study of space-charge-balanced flow.

For each $F_c, \alpha,$ and $\beta,$ beam envelopes were obtained by solving eqn. (7) on an analogue computer. The normalized slopes $d\sigma/dZ$ at positions along the axis where $r_c/r_m = \sqrt{K/F_c}$ and where the beam diverges, are plotted as a function of $\beta,$ with α held as a parameter. These results are presented in Fig. 13, for the single case of $F_c=0.5$.

A linear Pierce gun (Fig. 14) in which the magnetic and electric lines of force coincide is most amenable to theoretical analysis: the anode is a divergent lens and the slope of the electron beam emerging from the anode can be estimated by the well-known Davison-Calbick formula,

$$\frac{dr}{dz} = \frac{r_c}{f} = \frac{E_2 - E_1}{4V} r_c \quad \dots\dots(31)$$

In the normalized form used in the present contribution, the above formula reduces to

$$\frac{d\sigma}{dZ} \Big|_{z_c} = 1 \quad \dots\dots(32)$$

Exact calculations of the beam slope at the anode aperture, taking into account the effect of space charge and the magnetic field, may result in a value for $d\sigma/dZ|_{z_c}$ somewhat different from unity. However, the diagrams cover a rather wide range of normalized initial slopes, so that matching can be performed to electron guns from which beams emerge at slopes somewhat different from unity.

The normalized length of the transition region Z_c/α is also obtained from the solutions of eqn. (7). The quantity Z_c/α is the normalized length from the beginning of the interaction

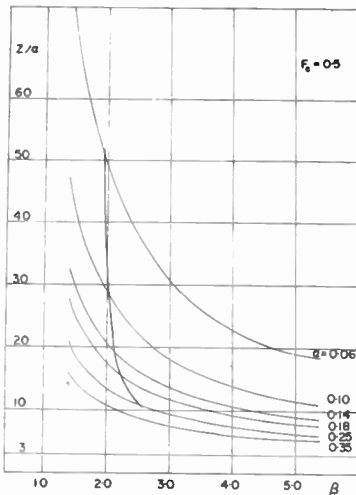


Fig. 15. Normalized length of the transition region as a function of β for various values of α .

region (-3 in Fig. 12) to the plane of the anode aperture. The position of the shield is in all cases at $Z/a = 3$ from the interaction region and a distance $(Z_c/a) - 3$ from the anode aperture. These normalized distances, which correspond to the values of normalized slope on Fig. 13, are shown in Fig. 15. The light curves represent the Z_c/a for which $r = r_c$, and the heavy curve connects the points $r = r_c$ and $d\sigma/dZ = 1$. These points are determined by means of the values of β obtained from Fig. 13. The normalized distance between the shield and the interaction region is also indicated, so that the normalized

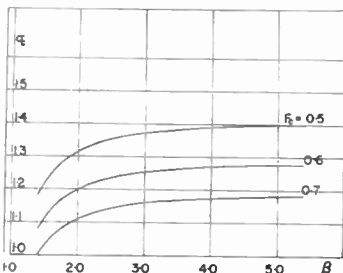


Fig. 16. Normalized radius at cathode as a function of β .

distance between the anode aperture and the magnetic shield, which is of primary interest to the designer, can be readily found from the diagram.

The relationship $\sigma_c = \sqrt{(K/F_c)}$ which is obtained by substituting the definition for K into eqn. (29) is useful for design purposes and is presented graphically on Fig. 16.

For illustration, some beam envelopes that satisfy the above-enumerated conditions are shown in Fig. 17. The same figure also shows how the aperture in the magnetic shield varies with the microperveance, for the case $F_c = 0.5$.

This scheme places a limitation on the perveance. The expression that relates microperveance P to the beam radius r_m , the aperture radius in the magnetic shield a , and the parameter α is the following:

$$P = \left(\frac{\alpha}{0.123 a/r_m} \right)^2 \dots\dots(33)$$

First, the parameter α cannot be arbitrarily increased: it has an upper limit above which the slope of the beam at the anode aperture is

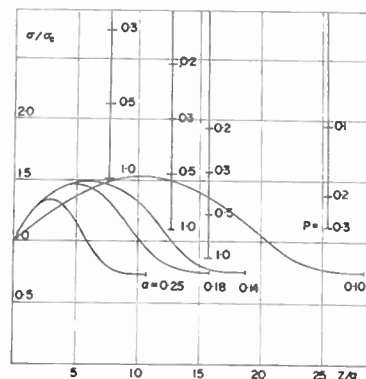


Fig. 17. Variation of the magnetic-shield aperture for various values of microperveance. Scale marks on vertical lines represent actual positions of the aperture for the microperveances indicated; the four lines correspond to the four values of α indicated on the beam envelopes (in the same order).

always less than unity, as is apparent from Fig. 13. Second, the ratio a/r_m must be always maintained greater than unity since the hole in the shield cannot be smaller than the diameter of the beam. It must be concluded from these considerations that the microperveance given in eqn. (33) has an upper limit. An estimate of the highest possible value for the microperveance can be obtained for the following conditions. Let $F_c = 0.5$; then $\alpha = 0.25$ and $a/r_m = 2$ which is reasonable, as some allowance must be made for

the bulging of the beam in the transition region and for the thickness of the vacuum envelope. Then

$$P < \left(\frac{0.25}{0.1231 \times 2} \right)^2 \cong 1 \quad \dots\dots(34)$$

Thus the microperveance cannot be chosen freely; its upper limit is determined by r_m , a , and α . If the microperveance were larger, the magnetic shield would intercept the beam.

It is also apparent from Fig. 15 that Z_c/α , which determines the length of the transition region, increases if β decreases. For low microperveances, the length of the transition region is thus unusually long (up to 10 or 20 times the shield aperture radius).

Examination of the normalized beam envelopes, given by the analogue computer, shows that the bulging beam-envelope radius in the transition region for $F_c > 0.5$ never exceeds twice the value of the beam radius in the interaction region ($\sigma < 2$ for all z). This observation suggests the design criterion that the inner radius of the vacuum envelope in the region between the gun and the magnetic shield of an electron tube employing this focusing system should be at least twice the beam radius in the interaction region ($2r_m$), to ensure that the beam nowhere strikes the vacuum envelope.

6. Conclusions

By the method described, it is possible to trace out the envelope of a "well-behaved" electron beam of high current density through almost any space variation of axially symmetric magnetic fields. To illustrate the method, beam envelopes were obtained with the aid of an analogue computer for Brillouin flow, periodic-magnetic focusing, and space-charge-balanced flow. The particular magnetic-field variations chosen for the transition regions in the three schemes are not, of course, the only ones that can be considered. Those chosen seem to be the most readily realized physically; however, the same method of analysis can be utilized to design tubes employing quite different field variations. In the present contribution, only paraxial conditions are considered. It is possible to account for magnetic-field variations off the axis by using additional terms of the expansion for the magnetic field; however, this modification would complicate eqn. (1), by introducing

additional terms in powers of r , to a point where the analogue-computer solution might become less reliable (owing to the increased probability of error) than the paraxial solution.

From the computer solutions and the well-known Pierce method of electron-gun design, it is possible to specify the parameters of a gun that will produce a beam with the required conditions at the gun anode for the three cases considered. Moreover, the dimensions of the convergent electron guns, which are required for the Brillouin-flow and periodic-focusing cases, can be minimized. The resulting guns also prove to exhibit the least anode-lens aberration and the lowest effective beam temperatures, two effects that are important to the tube designer.

In the case of space-charge-balanced flow a linear Pierce gun was chosen to produce the beam because the magnetic field is uniform in the gun region. It is entirely possible that other gun configurations¹⁵⁻¹⁷ could be chosen for matching at the anode which would lead to more practical designs than that evolved for the present case. However, such alternatives may lead to the difficult task of computing electron trajectories in guns in which trajectories do not coincide with magnetic lines of force. The particular case chosen for space-charge-balanced flow results in a transition region which may be prohibitively long for practical applications; and the microperveance of the resulting beam is restricted to values less than unity.

A treatment of the Brillouin-flow case that is similar to that presented in Section 3 above was presented by W. Veith at the International Convention on Microwave Valves in London in May, 1958. This contribution, which is based on an iterative method operating with power series and applies to very moderately converging (or diverging) beams, was brought to the authors' attention after the present paper was submitted. Veith's paper will be published in the proceedings of the convention¹⁸.

7. Acknowledgment

Part of the material on the periodic-focusing case was presented in a paper read at the Western Electronic Show and Convention of the Institute of Radio Engineers held in San Francisco, California, on August 20-23, 1957, and appears in the *Convention Record* (Part 3, pp.

130-137) under the title "Injection of convergent beams focused by periodic magnetic fields," by J. L. Palmer and C. Süsskind. The present contribution is the outgrowth of two investigations, supported by the U.S. Air Force and monitored by the Air Research and Development Command, both of which are the subjects of separate Scientific Reports published by the Electronics Research Laboratory, University of California, Berkeley, Calif., in Series 60 of the Institute of Engineering Research: Issue No. 197, "Entrance conditions for electron beams focused by axially symmetric magnetic fields," by J. L. Palmer, under Contract AF49(639)-102 (USAF Office of Scientific Research); and Issue No. 204, "Injection of space-charge-balanced beams for microwave tubes," by V. Bevc, under Contract AF19(604)-2270 (USAF Cambridge Research Center).

8. References

1. G. R. Brewer, "Some characteristics of a cylindrical electron stream in immersed flow," *Trans. Inst. Radio Engrs*, **ED-4**, pp. 134-140, April 1957.
2. C. Süsskind, "Electron guns and focusing for high-density electron beams," *Advances in Electronics and Electron Physics*, **8**, pp. 363-402. (Academic Press, New York, 1956.)
3. C. R. Moster and J. P. Molnar, "Some calculations of the magnetic field requirements for obtaining Brillouin flow in cylindrical electron beams." Paper presented at AIEE-IRE Conference on Electron Devices, University of New Hampshire, June 1951.
4. G. A. Caryotakis and H. Heffner, "Periodic Magnetic Focusing for Tubes with Parallel-flow Guns," Stanford University Applied Electronics Laboratory Technical Report 454-1, January 31, 1956.
5. J. Sterrett and H. Heffner, "The design of periodic magnetic focusing structures," *Trans. Inst. Radio Engrs*, **ED-5**, pp. 35-42, January 1958.
6. J. R. Pierce, "Theory and Design of Electron Beams," pp. 152-154, 2nd ed. (D. Van Nostrand, New York, 1954.)
7. *Ibid.*, pp. 182-192.
8. J. R. Pierce and L. R. Walker, "Brillouin flow with thermal velocities," *J. Appl. Phys.*, **24**, pp. 1,328-1,330, October 1953.
9. L. Brück, "Das Verhalten eines Elektronenstrahls beim Eintritt in ein koaxiales Magnetfeld," *Telefunken-Zeitung*, **26**, pp. 85-88, March 1953.
10. M. Müller, "Magnetische Elektronenoptik in Langstrahl-Verstärkerröhren," *Telefunken-Zeitung*, **26**, pp. 95-101, March 1953.
11. J. T. Mendel, C. F. Quate, and W. H. Yocom, "Electron beam focusing with permanent magnetic fields," *Proc. Inst. Radio Engrs*, **42**, pp. 800-810, May 1954.
12. K. J. Harker, "Periodic focusing of beams from partially shielded cathodes," *Trans. Inst. Radio Engrs*, **ED-2**, pp. 13-19, October 1955.
13. G. R. Brewer, "Formation of high-density electron beams," *J. Appl. Phys.*, **28**, pp. 7-15, January 1957.
14. J. T. Mendel, "Magnetic focusing of electron beams," *Proc. Inst. Radio Engrs*, **43**, pp. 327-331, March 1955.
15. J. R. Pierce, "A gun for starting the electrons straight in a magnetic field," *Bell Syst. Tech. J.*, **30**, pp. 825-829, 1951.
16. N. C. Chang, "Beam Perturbations in Confined-flow Electron Beams as a Result of Lens Actions in the Gun Region," Sylvania Electric Products Microwave Tube Laboratory (Mountain View, Calif.) Technical Report 109, November 26, 1956.
17. T. S. Chen and L. Kovach, "Electron beam focusing in three-anode guns for travelling-wave tubes," *J. Electronics and Contr.*, **3**, p. 287, 1957.
18. W. Veith, "A method for the calculation of electron-beam contours in axially symmetrical magnetic fields, including the gun region." I.E.E. Paper 2656. (*Proc. Instn Elec. Engrs*, **105B**, Supplement No. 12, p. 932, January 1959.)

RADAR SYSTEMS WITH ELECTRONIC SECTOR SCANNING*

by

D. E. N. Davies, M.Sc.†

SUMMARY

The application to radar of a system of electronic sector scanning, recently described in relation to underwater acoustic echo-ranging, is discussed.

1. Introduction

A recent paper has given an account of a system of electronic sector scanning which is suitable for application to echo-ranging systems‡. The whole of the sector to be explored is "illuminated" by the transmitted pulses, but on reception a narrow beam is very rapidly swept across the sector. The time of sweep is no greater than the pulse duration, so that the whole sector is explored effectively instantaneously. The previous paper dealt with the system with particular reference to its application to underwater acoustic echo-ranging. The present paper aims to set out briefly some aspects of the application of the system to radar. The particular way in which the radar application differs from the acoustic application is that the received signal frequency, which may be of the order of 10,000 Mc/s, is so high that it is not reasonable to translate received signals upwards in frequency as is done in the acoustic system. Whereas in the latter case the bandwidth of the scanned signal could greatly exceed the signal frequency, clearly this is not possible in the radar system. The approach to the overcoming of scanning distortion must therefore be different in the radar case. It was shown in the previous paper that one source of interference or distortion in the scanning process was the finite delay time of the phase-shifting networks used to produce beam deflection, but with ample bandwidth available the rate of change with frequency could be kept small and the time delay made negligible. This

is not possible in the radar case and other solutions have to be found.

2. Outline of Basic Scanning System

A possible form of the scanning radar system is shown as a block diagram in Fig. 1.

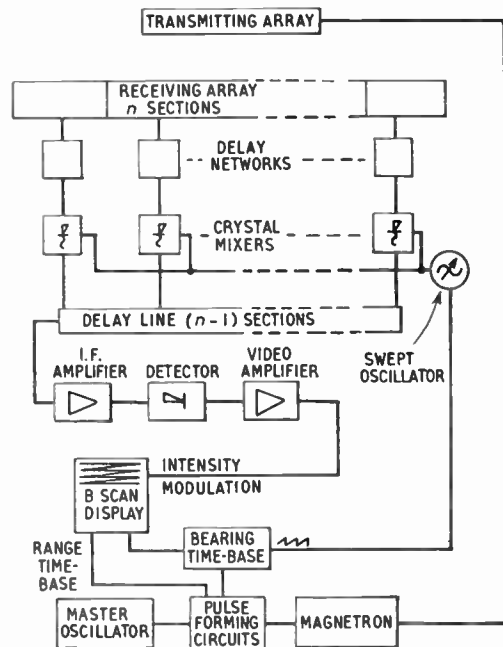


Fig. 1. Schematic diagram of the proposed scanning system.

In general this is similar to the system described in the previous paper. The frequencies at the various parts of the circuit are shown in their

* Manuscript received 2nd October 1958. (Paper No. 481.)

† Electrical Engineering Department, University of Birmingham.

U.D.C. No. 621.396.677:621.396.963.3

‡ D. G. Tucker, V. G. Welsby, and R. Kendell, "Electronic sector scanning", *J. Brit.I.R.E.*, 18, pp. 465-484, August 1958.

relation to time in Fig. 2, and it will be seen that only a few hundred Mc/s can be allocated to the frequency sweep. The restrictions imposed by this are as follows:

(a) It is an obvious requirement, based on elementary information theory, that, if a sector is to have a width of n beamwidths and if the pulse duration is τ sec, then the bandwidth in the intermediate-frequency sweep must be at least n/τ c/s. Thus, if the pulse duration is 0.1 microsec and the scanned sector is ten times the beamwidth, then the i.f. bandwidth must be at least 100 Mc/s.

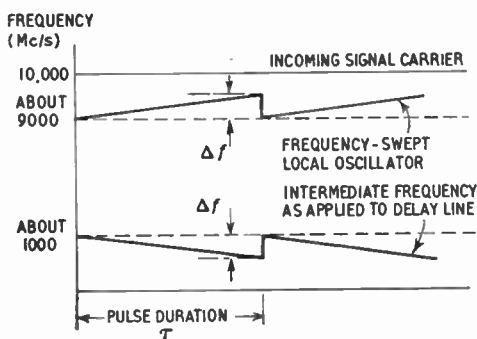


Fig. 2. Frequency diagram.

N.B. It is shown in the text that the use of isosceles-triangular scanning waveforms may often prove advantageous compared with the saw-tooth waveforms shown above.

(b) Since the change of phase-shift per section of the phase-shifting network or delay line is 2π radians over the range of the frequency sweep, Δf , then the delay time of each section is $1/\Delta f$ sec. If $\Delta f = 100$ Mc/s and if $n = 10$, then the delay time through the delay line amounts to about 0.1 microsec, which is of the same order as the pulse duration. This means that, for the given received signal pulses the outputs from the different aerial channels may fail even to overlap (let alone coincide) at the output of the delay lines and no intelligible display can be produced. In the underwater acoustic echanging system this difficulty was easily overcome by making the intermediate frequency exceed the signal frequency and by having a very large bandwidth. As this is not possible in the radar case, special measures have to be taken to eliminate this difficulty and they are discussed in the next section.

(c) Since the i.f. signal consists of n time-staggered frequency-modulated signals, an overlapping period will occur when signals from one scan are being added to signals from the beginning of the next scan. This can be interpreted as an incorrect phasing of the receiving array at the edges of the sector. This effect may be reduced by making the overlapping period small compared to the scanning period,

$$\text{i.e. } (n - 1) \frac{1}{\Delta f} \ll \tau \text{ or } \Delta f \gg \frac{n - 1}{\tau}$$

This means that a bandwidth much larger than the theoretical minimum of n/τ , predicted by information theory, will be required. The use of an isosceles-triangular scanning will evidently reduce this effect, and permit the theoretical minimum bandwidth to be more closely approached.

3. Methods of overcoming Scanning Distortion due to Delay Times

It should be observed that the scanning distortion described in Section 2 arises from the fact that the purpose of the tapped delay line in the scanning system is obviously to produce a phase-shift for beam deflection. Since this phase-shift has to vary with frequency—this being the fundamental requirement of the scanning principle—it is impossible to obtain it without at the same time getting envelope delay. It is possible to compensate for this delay, however, by inserting individual delay lines or networks directly in the connections from the array where the signal carrier is of constant frequency. At this fixed frequency any desired envelope delay can be produced without phase-shift, and, therefore, without interfering with the beam deflection process. In each channel from the array the envelope delay of the additional network is arranged to be exactly complementary to the delay produced in the delay line between the appropriate tapping point and the output to the i.f. amplifier and display. Thus the resultant envelope delays of all the channel components of the output signal are identical and the distortion due to the delay line is corrected. It is clear, of course, that this method of correction can be applied only to the systems in which the output from only one end of the delay line is used, as shown in Fig. 1.

A possible alternative to the above form of correction would be to remove the tapped delay line from the signal path altogether and to put corresponding delay networks in the connections between the local oscillator and the various modulators. The scanning effect will then be unchanged, except for a reversal of direction of scanning, owing to the difference-frequency being selected in the modulator outputs. It may indeed, in practice, prove simpler to effect the scanning in this way, as in the system shown in Fig. 1, it might be difficult to feed the local oscillation to all the modulators without phase errors.

It should be noted that the kind of distortion discussed in Section 2.1 of Part 2 of the previous paper applies to the radar system whether or not either of the above methods of eliminating pulse envelope distortion is adopted. This distortion arises because the different time delays in the various channels cause the instantaneous frequencies of the various channel-components in the combined i.f. output to be different. However, it will be easily seen on putting in typical numerical values that this effect is not likely to be serious in the radar system any more than in the acoustic system. For example, Condition (A) of the previous paper, which is concerned with this form of distortion, requires for freedom from distortion that the time of sweep should be much greater than $(n-1)/f_1$, where n , as before, is the number of beamwidths contained in the scanned sector and f_1 is the lower frequency of the i.f. frequency range. In a typical radar system f_1 will be of the order of 500-1,000 Mc/s and n might be 10. Thus, if the time of sweep, i.e. the pulse duration, is very much greater than about 0.01 microsec, then this form of distortion is negligible. Since radar pulse lengths do not at present generally go below 0.1 microsec, there seems little difficulty here.

Another and more fundamental kind of distortion arises due to the fact that during scanning the beam is deflected without physical movement of the array. This means that a received wave-front (see Fig. 3) will not be parallel to the array and the pulse envelopes received by different sections of the array will arrive at different times. The differential delays (t_1) are proportional to $\sin \theta$, where θ is the angle between the wave-front and the array. These

delays might add to or compensate for the delays (t_2) in the delay line according to whether the deflection is to one side or the other of the normal. In the conditions shown in Fig. 3, it is clear that to obtain compensation at all values of θ , it is necessary that

- (i) t_2 diminishes as t_1 increases, and
- (ii) the narrow-band delay networks have progressively decreasing delays from left to right and are arranged so that the sum of the wide-band delay at zero deflection (i.e. when $t_1=0$) and the narrow-band delay is the same for all channels between the array and the i.f. output.

Since an increase in θ , i.e. in t_1 , corresponds to an increase in frequency on the wide-band delay line, it is clear that the delay line must have a phase/frequency characteristic such that the delay-time decreases with frequency, thus:

$$t_2 = \frac{d\varphi}{d\omega} = A - B\omega$$

giving

$$\varphi = A\omega - B\omega^2/2 + C$$

where A , B and C are constants.

Such a parabolic phase/frequency characteristic is realizable—it has to apply, of course, only over the i.f. frequency-range.

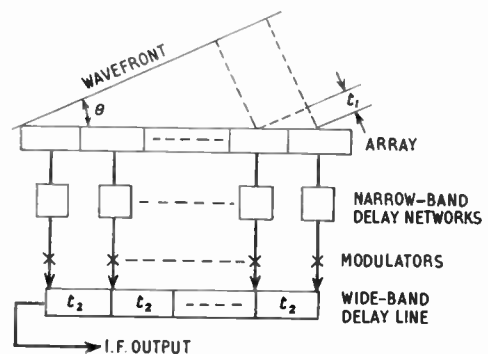


Fig. 3. To illustrate the discussion on pulse envelope distortion.

As discussed above, the use of "parabolic" delay lines provides effective compensation for deflections of the beam only to one side of the centre of the scanned sector. But coverage of the whole sector can be provided for by modifying the phase-shift requirements of the narrow-band networks so that, instead of giving zero

phase-shift, they give progressively increasing phase-shift from left to right; the initial position of the beam is then at one edge of the sector, and deflection from this position over the whole sector is dealt with by the compensating arrangements.

For arrays of length within the limits normally used for centimetric-wave radar, the distortion produced by the delays in the medium is easily seen to be almost negligible, and the provision of "parabolic" delay lines would usually be unnecessary. The radar conditions are, in fact, the opposite of those applying in underwater acoustic echo-ranging, where the effects of t_2 can be made comparatively negligible but, owing to the low velocity of sound in water, t_1 has serious effects making the use of "parabolic" delay lines much more worth-while.

4. Practical Components

The nature of many of the system components would in practice vary with the application of the system. The aerial system would probably consist of an array of equiphase apertures feeding a secondary radiator to increase the gain. The narrow-band delay networks could easily be formed from either cable or resonators as also could the wide-band delay line. Since the i.f. bandwidth is n/τ , this can raise problems of providing wide-band amplification when short pulse lengths are used. As a result of this it is probable that for bandwidths in excess of about 40 Mc/s there might be some advantage in replacing distributed amplifiers by travelling wave tubes.

The swept oscillator provides a novel problem at these frequencies. There is little mention in the literature of the effect of frequency modulation on reflex klystrons at modulation rates of the order of 10 Mc/s. Consequently, experiments have been made and they have shown that such modulation is quite practical and that frequency deviations approaching the 3 db bandwidth of the mode curve are obtainable at modulation rates of 10 Mc/s at X-band. Now a klystron oscillator is itself a resonant structure, since the output electrode is in the form of a resonant cavity. It is therefore impossible for any sidebands of the oscillation to be sustained at frequencies outside the zero power

bandwidth of the klystron mode. As the spectrum tends to spread beyond the mode bandwidth, there is less energy left within the band to sustain oscillations. Therefore beyond a certain frequency deviation, oscillations cease. For a low- Q X-band reflex klystron such as the 723 A/B the maximum frequency sweep obtainable for sinusoidal modulation was found to be of the order of 30 Mc/s.

The large frequency spread shown by the Fourier analysis of a saw-tooth waveform suggests that the adoption of an isosceles-triangular frequency sweep would be preferable, to prevent further severe restriction of frequency deviation. A sinusoidal sweep could also be used but it would result in non-uniform scanning. This would cause the noise factor to vary with deflection. In cases where a large frequency deviation is required the system will have to resort to backward wave oscillators. These oscillators are not resonant structures and can therefore be modulated at high rates. An important factor which may be relevant to the design of the practical system is that it is very difficult to measure instantaneous frequency. All methods of measuring instantaneous frequency (or to be more precise instantaneous rate of change of phase) become more inaccurate as the rate of change of frequency increases.

5. Possible Applications

In practice the signal-to-noise performance of the system will be degraded owing to extra noise introduced by the presence of several modulators. There will on the other hand be more pulses available for integration. The outstanding feature of the scanning system is that an information rate far beyond the capability of conventional pulse radar systems is possible. Two other features are also worthy of mention, namely the elimination of mechanical moving parts and the fact that information from within the scanned sector is continuous in the sense that information regarding the entire sector is available once every pulse repetition period instead of a batch of information being provided once in every mechanical scanning period.

There are some practical radar applications in which there is a need for a large increase of information rate. One of these applications is in aircraft landing systems, and particularly blind

landing systems, where the continuous nature of the information would be an added advantage. For example, in airfield "precision approach radar*", a $\frac{1}{2}$ deg beam is used to scan a 4 deg sector. To effect this electronically would require an array of 8 elements. The mechanical scanning system provides 2 looks per second on an incoming aircraft, though each look will consist of several integrated pulses. The number of looks per second provided by an electronic scanning system would be equal to the p.r.f., in this case 3825 cycles/sec.

One radar application where there is a real need for a large increase in radar information rate is a self-contained aircraft collision-avoidance system†. However no such collision-avoidance system has yet been developed using any radar techniques. This is due to practical limitations on peak power, antenna gain and the difficulty of detecting small aircraft radar echoes against strong ground clutter. Since the range on such a radar would be very limited, the

scanning rate of a complete sphere must be fast enough to provide early collision warning; this therefore requires fast scanning and a high information rate. Scanning with stationary aeri-als would probably enable far greater antenna gains to be employed. Another advantage arises from the fact that if, in an ordinary radar, an echo is missed owing to the other aircraft being just beyond the maximum range of a mechanical scanning radar, then a time equal to the scanning period must elapse before a detectable echo can be obtained. With electronic scanning, where a scanning period is no longer of the same order as the minimum necessary warning time, this situation can be improved upon since a sampled pulse is contributed every pulse repetition period from the limit of the range. It appears however that such applications must await further technical developments such as the production of high-power, low-weight transmitters.

6. Acknowledgments

The author is indebted to Professor D. G. Tucker, who initiated and directed this work, and also to several other colleagues in the Electrical Engineering Department of the University of Birmingham for many helpful discussions.

* G. J. Moorcroft, "Precision approach radar", *Proc. Instn. Elect Engrs*, **105**, Pt. B. Sup. 9, 1958.

† F. C. White, "Is an airborne system of collision avoidance operationally and technically feasible?", *Trans. Inst. Radio Engrs*, **ANE-4**, No. 2, June 1957.

INSTITUTION NOTICES

Physical Society Exhibition Tickets

As stated on page 581 of the October issue of the *Journal*, the Physical Society has kindly offered special admission tickets to enable Brit.I.R.E. members to visit the 1959 Physical Society Exhibition on the morning of Monday, 19th January.

Many members have already notified the Institution of their wish to take advantage of this offer; others wishing to do so should write to the Institution at once.

Tickets for the exhibition, which will take place at the Royal Horticultural Society's Halls, London, S.W.1, from 19th to 22nd January, will not be despatched until a few days before the exhibition is due to open.

Civilian Studentships, Royal Military College of Science

The Ministry of Supply has announced that a number of Studentships at the Royal Military College of Science, Shrivenham, are being offered to civilian students. Successful candidates will join young officers in degree courses, although they will remain civilians in the fullest sense of the word. It is intended that the Studentships will lead to employment in Government Research Establishments in the Scientific Officer class.

Candidates will be selected on the basis of their scholastic record supplemented by written examination in physics, chemistry and mathematics. The standard of entrance will be somewhere between a university scholarship and a county major award. All tuition and examination fees are paid, and the student receives a maintenance allowance of £355 per annum. No means test is imposed, and these allowances are not liable to income tax.

Applications for the 1959 competition, for which the examination will take place in February, must be made by January 15th. Application forms and further information about the scheme may be obtained from the Ministry of Supply, Est. 3 (R) 3, Room 512, The Adelphi, Strand, London, W.C.2.

Awards by the Institution of Radio Engineers, Australia

This year the Brit.I.R.E. has made its biennial recommendation to the Institution of Radio Engineers Australia in connection with the award of the Norman W. V. Hayes Memorial Medal. It will be recalled that recommendations are made in alternate years by the Brit.I.R.E. and the I.R.E. of America.

The Australian Institution has announced that the Medal has been awarded to Mr. W. D. Meewezen for his paper "Some aspects of permeability tuning" which was published in the August 1957 issue of the *Proceedings of the I.R.E. Australia*. Mr. Meewezen who was born in Holland is with the Telecommunication Company of Australia Pty. Ltd. Under the mutual arrangement between the two Institutions it is proposed to reprint Mr. Meewezen's paper in an early issue of the *Journal*.

Completion of Volume

This issue completes Vol. 18 of the *Journal*. An Index to the year's Numbers will be distributed with the January 1959 issue.

Members wishing to have their *Journals* bound by the Institution should send the complete set of twelve issues and Index to 9 Bedford Square, together with a remittance of 15s.

Correction

The following amendments should be made to the paper "Factors in the design of airborne Doppler navigation equipment", published in the July 1958 *Journal*.

Page 426, left hand column, line 2.

For α read φ

Page 441, Appendix 1:

The first three expressions *should read* as follows:—

$$V_1 = [V_H \cos\gamma + V_L \sin\gamma - V_v \tan\varphi] \cos\varphi$$

$$V_2 = [V_H \cos\gamma + V_L \sin\gamma - V_v \tan\varphi] \cos\varphi$$

$$V_3 = [V_L \cos\gamma + V_H \sin\gamma - V_v \tan\varphi] \cos\varphi$$

Delete $\cos\varphi$ from the next three expressions.

The denominator of the twelfth expression *should read* $4 \sin\varphi$.

THE CHARACTERISTIC IMPEDANCE AND PHASE VELOCITY OF HIGH-Q TRIPLATE LINE*

by

K. Foster, M.A.†

SUMMARY

The derivation of the impedance and phase velocity for high- Q triplate line is considered. An exact solution is obtained for the impedance in the absence of the dielectric support sheet. The effect of the sheet is then considered as a perturbation, the analysis resulting in an expression for the phase velocity of the waves in the line. This is compared with experimental values and it is shown that the agreement is sufficiently close for design purposes.

LIST OF PRINCIPAL SYMBOLS

Z_r	characteristic impedance of reduced line.	z, w, t	complex variables.
Z_0	characteristic impedance of the basic line.	$Z(\alpha)$	Jacobi zeta-function.
Z_d	characteristic impedance of the line with dielectric.	$\Theta(t)$	Jacobi theta-function (old notation).
k, γ	moduli of elliptic functions.	$\vartheta_n(\xi, q)$	theta-functions (modern notation).
k', γ'	complementary moduli to k and γ .	χ	susceptibility = $\kappa_e - 1$.
K, I'	complete elliptic integrals of the first kind.	κ_e	dielectric constant.
$\Pi(t, \alpha)$	incomplete elliptic integral of the third kind.	c	velocity of light in free space.
		v	phase velocity of waves in the dielectric supported line.
		a, b, h	the dimensions of the line.
		L	"depolarization factor."

1. Introduction

In recent years considerable interest has been centred on the use of strip transmission lines as alternatives to the more conventional coaxial lines or waveguides for complex microwave systems¹. Various forms of strip lines have been proposed, and used to a greater or lesser extent, and most of the general properties are understood. Unfortunately, the evaluation of basic properties such as characteristic impedance, phase velocity, etc. is extremely difficult for most of these lines and exact solutions are not yet available. One type of line for which this is true is that which Dukes has called High- Q triplate², the cross-section of which is shown in Fig. 1. It comprises two effectively infinite ground planes between which lies a sheet of dielectric medium. Strips

of thin metal foil lie on each side of the dielectric forming the joint inner conductor of the line. Apart from symmetry considerations the main purpose of using two strips of metal for the inner conductor is to ensure that only fringing fields pass through the dielectric thus reducing absorption loss.

It is clear that this line is not a simple line from the analytical point of view. Without the

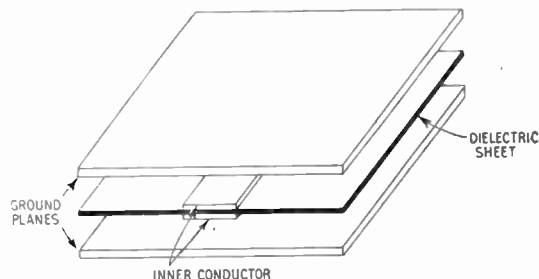


Fig. 1. High- Q triplate line.

* Manuscript received 2nd July 1958. (Paper No. 482.)

† Cossor Radar & Electronics Ltd., Highbury Grove, London, N.5.

U.D.C. No. 621.372.821

dielectric sheet the transmitted wave would be of transverse electromagnetic form with a phase velocity equal to the velocity of light in free space. In the same condition a characteristic impedance could be defined and could be calculated through a calculation of the capacitance per unit length of the line. The presence of the dielectric alters this situation completely, at least from the analytical viewpoint. Field components in the direction of propagation must exist in order to satisfy the boundary conditions at the dielectric/free space interface. The mode of propagation is therefore not of transverse electromagnetic form and a unique characteristic impedance can no longer be defined. The phase velocity will be affected and will now be a function of the dimensions of the line. A direct solution of this modified boundary value problem is very difficult but, since the dielectric is present only in the region of fringing fields, it seems likely that an approximate analysis will produce results useful for design purposes.

Before a systematic design can be carried out using any form of transmission line it is necessary to know the phase velocity of the waves in the line and to have some measure of the impedance of the line. The purpose of this paper is to consider these two properties for the line of Fig. 1. The analytical process employed divides the problem into two distinct parts. In the first instance, the line is considered in the absence of the dielectric sheet. An exact solution for the characteristic impedance of this "basic line" is obtained by means of a conformal transformation, the development of this being outlined in Section 2. (Implicitly the field distribution is also obtained for the line.) The phase velocity of the basic line is simply the velocity of light in free space. This completes the first part of the problem in principle, but because of the difficulty of numerical solution an approximate form of the solution together with its range of validity are considered in Section 3. The second part consists of the insertion of the dielectric sheet which is treated as a small perturbation, in a similar manner to the method employed by Schetzen³ for another type of printed line. Subject to certain assumptions, the phase velocity of the modified line can be calculated. A characteristic impedance can

then be obtained from this phase velocity and the impedance of the basic line. This work occupies Section 4 and in Section 5 the phase velocities calculated for a variety of materials, frequencies and line dimensions are compared with those obtained experimentally. It is shown in this section that with the insertion of one parameter (concerned with dielectric depolarization) agreement between experiment and theory can be adequate for design data.

2. Solution for the Basic Line

The cross-section of this line is shown in Fig. 2(a) and it is apparent from symmetry that its capacitance is four times that of the reduced line of Fig 2(b) in which the dashes indicate magnetic walls (the lines of electric

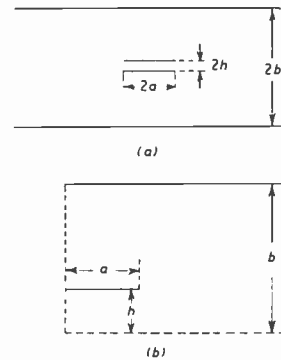


Fig. 2. (a) The basic line (b) The reduced line. Solid lines indicate electric walls. Broken lines indicate magnetic walls.

field being tangential to these walls). The solution of the problem for the reduced line now proceeds by mapping this line onto a complex *z*-plane as shewn in Fig. 3(a). A Schwartz-Christoffel transformation is then sought which maps the contour of the reduced line onto the real axis of a complex *w*-plane as in Fig. 3 (b). The interior of the reduced line is mapped onto the upper half of the *w*-plane and the three points, *w*=0, 1 and ∞, are chosen to correspond with the points *z*=*j**b*, *j* (*h*+0) and ∞ respectively. The quantities *w*₁, *k* and *w*₂ are then determined by the transformation. The impedance problem of the *w*-plane line is standard and, once the parameter *k* is determined, the impedance of the reduced line is given by

$$Z_r = 120\pi K(k)/K(k') \dots\dots\dots(1)$$

where $K(k)$ is the complete elliptic integral of the first kind of modulus k , k' being the complementary modulus. The impedance of the basic line Z_0 is simply one quarter of this and hence

$$Z_0 = 30\pi K(k)/K(k') \quad \dots\dots(2)$$

giving the impedance required.

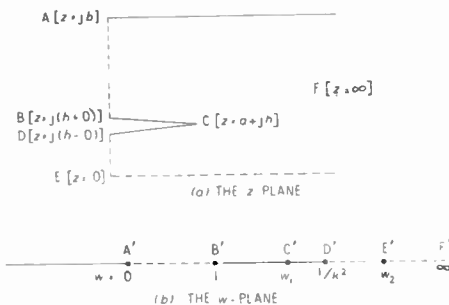


Fig. 3. Correspondence diagram for the transformation (a) The z -plane. The interior angles at B and D are 90° , that at C is 360° . (b) The w -plane.

It is now necessary to determine the parameter k and in order to do this the conformal transformation between z and w is required. The differential equation linking these two variables can be written

$$\frac{dz}{dw} \propto \frac{(w - w_1)}{\sqrt{w(w-1)(k^2w-1)(w-w_2)}} \quad \dots\dots(3)$$

In order to carry out the integration the following substitutions are made:

$$\text{sn}^2(t, \gamma) = \frac{(w_2 - 1)(k^2w - 1)}{(1 - k^2)(w - w_2)} \quad \dots\dots(4a)$$

$$\gamma^2 = \frac{w_2(1 - k^2)}{(w_2 - 1)} \quad \dots\dots(4b)$$

$$\text{sn}^2(a, \gamma) = 1/k^2w_2 \quad \dots\dots(4c)$$

where $\text{sn}(t, \gamma)$ is the elliptic function of modulus γ and a is a new constant, as yet undetermined. (Since elliptic functions of modulus γ are used frequently in this paper this modulus will be assumed henceforth. The complete integral of the first kind will be denoted by Γ and the integral of complementary modulus by Γ^ν . The modulus k which has been introduced in eqn. (1) will be expressly stated in the few instances of its use.)

With the substitutions above the differential equation becomes

$$\frac{dz}{dt} \propto \left\{ 1 + \frac{\gamma^2 \text{cn}^2 a \text{sn}^2 t}{(k^2w_1 - 1)(1 - \gamma^2 \text{sn}^2 a \text{sn}^2 t)} \right\} \dots\dots(5)$$

which can be immediately integrated⁵ to give

$$z = At + \frac{A \text{cn} a}{(k^2w_1 - 1) \text{sn} a \text{dn} a} \text{II}(t, a) + C \quad \dots\dots(6)$$

where $\text{II}(t, a)$ is the elliptic integral of the third kind, A and C being constants to be determined.

Equation (6) can be regarded as a transformation between the z -plane and a complex t -plane which is in turn connected with the w -plane by the transformation given in the first of eqns. (4). The corresponding points of these three planes are given in Table 1.

In this table the value of t_0 is given by

$$\text{sn}^2 t_0 = \frac{(w_2 - 1)(k^2w_1 - 1)}{(1 - k^2)(w_1 - w_2)} \quad \dots\dots(7)$$

Table 1

z	jb	$j(h+0)$	$(a+jh)$	$j(h-0)$	0	∞
w	0	1	w_1	$1/k^2$	w_2	∞
t	$(\Gamma - j\Gamma^\nu)$	Γ	t_0	0	$-j\Gamma^\nu$	$(a - j\Gamma^\nu)$

Use of Table 1 with the points $z=0, jb, j(h-0)$ and $j(h+0)$ in eqn. (6) (and the properties of the elliptic integral) results in the relations

$$\begin{aligned} C &= jh \\ A &= 2bZ(a)/\pi \\ a &= \Gamma(1 - h/b) \end{aligned} \quad \dots\dots(8)$$

$$w_1 = \frac{(1 - \gamma^2)}{\text{dn}^2 a} \left\{ 1 + \frac{Z(a) \text{cn} a}{\text{sn} a \text{dn} a} \right\}$$

where $Z(a)$ is the Jacobian Zeta-function.

With these values the transformation becomes

$$\frac{\pi(z - jb)}{2b} = tZ(a) - \text{II}(t, a) \quad \dots\dots(9)$$

This is not a very convenient form in practice and it can be rewritten in terms of the Jacobi theta-function by using the property⁵

$$\text{II}(t, a) = \frac{1}{2} \log \frac{\Theta(t - a)}{\Theta(t + a)} + tZ(a) \quad \dots\dots(10)$$

giving the final form for the transformation as

$$\Theta(t - \alpha) = \Theta(t + \alpha) \exp \left\{ -\frac{\pi(z - jh)}{b} \right\} \dots\dots(11)$$

The only unknown quantity in this equation is the modulus γ which enters into the theta-functions. (α is determined by eqn. (8) if the modulus is known.) In order to find γ it is necessary to use the point correspondence for $z = a + jh$ and eliminate t_0 by the use of eqn. (7). This last can be cast into a suitable form by using values of k and w_2 from (4) and w_1 from (8).

Omitting the algebra the rearranged equation can be written in the form

$$\frac{\gamma^3 \operatorname{sn} \alpha \operatorname{cn} \alpha \operatorname{dn} \alpha \operatorname{sn}^2 t_0}{(1 - \gamma^2 \operatorname{sn}^2 \alpha \operatorname{sn}^2 t_0)} - Z(\alpha) = 0$$

or

$$\left[\frac{d}{dt} \left\{ \Pi(t, \alpha) - tZ(\alpha) \right\} \right]_{t=t_0} = 0 \dots\dots(12)$$

Comparison with eqn. (10) shows that this is equivalent to

$$\frac{\Theta'(t_0 - \alpha)}{\Theta(t_0 - \alpha)} = \frac{\Theta'(t_0 + \alpha)}{\Theta(t_0 + \alpha)} \dots\dots(13)$$

in which the dash indicates differentiation with respect to the argument.

Direct substitution of the joint correspondence for $z = a + jh$ into eqn. (11) yields

$$\frac{\Theta(t_0 - \alpha)}{\Theta(t_0 + \alpha)} = \exp \left\{ -\frac{\pi a}{b} \right\} \dots\dots(14)$$

From these last two equations t_0 can be eliminated (at least in principle) and the modulus γ determined. Elimination of w_2 from eqns. (4b) and (4c) followed by substitution for α from (8) gives the final answer for k as

$$k = \operatorname{dn} \left\{ 1, \frac{h}{b} \right\} \dots\dots(15)$$

and the characteristic impedance is determined.

Unfortunately the process outlined above cannot, in general, be carried out in a simple fashion and it is necessary to solve the equations for γ numerically. In such a case as this it is of benefit to see if an approximate solution can be obtained which is valid over a reasonably practical range of parameters. The next section is devoted to this problem but before proceeding to this it is of interest to note that the equations can be solved directly for one particular value of h/b , namely when $h/b = \frac{1}{2}$.

In this case, $\alpha = t_0 = \frac{1}{2}1'$ and from the properties of the theta-function $\gamma' = \exp(-2\pi a/b)$. It follows, therefore, from (15) that k is given by

$$k = \exp(-\pi a/b) \dots\dots(16)$$

Values of the characteristic impedance obtained by numerical methods are shown for various of a/b and h/b in Fig. 4. A feature that will be observed in this Figure and which can be established analytically from the properties of the elliptic functions is that

$$Z_0(a/b, h/b=0) = 2Z_0(a/b, h/b=\frac{1}{2})$$

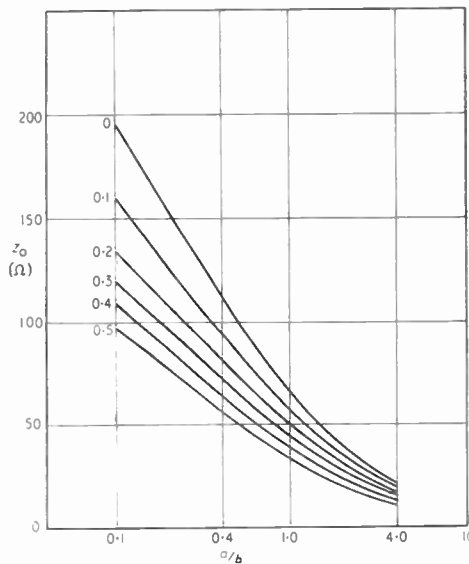


Fig. 4. The characteristic impedance of the basic line.

3. The First Order Approximation

It is possible to obtain two types of first order solutions for the value of k , one of which is suitable for small values of a/b and the other suitable for large values. From the practical point of view it is found that most of the range of importance is covered by the latter solution and this will be the only one considered here. The approximation derives from the fact that for large a/b the modulus γ approaches unity and when this is so, it can be shown (see appendix 1) that the theta-function is given approximately by

$$\Theta(t) = \Theta(0) \exp \left\{ -\frac{\pi t^2}{4\Gamma^2 \nu} \right\} \cosh \left\{ \frac{\pi t}{2\Gamma \nu} \right\} \dots\dots(17)$$

whence

$$\frac{\Theta'(t)}{\Theta(t)} = \frac{\pi}{2\Gamma'} \left[\tanh \frac{\pi t}{2\Gamma'} - \frac{t}{\Gamma'} \right] \dots\dots\dots(18)$$

Using this equation in (13), the subsequent solution for t_0 gives

$$\cosh \frac{\pi t_0}{\Gamma'} = \frac{\Gamma'}{\alpha} \sinh \frac{\pi \alpha}{\Gamma'} - \cosh \frac{\pi \alpha}{\Gamma'}$$

Now in this expression t_0 and α are usually of the order of Γ' and hence the hyperbolic functions can be replaced by their equivalent exponential forms with only the large terms retained. Thus, to a first approximation,

$$\exp \frac{\pi t_0}{\Gamma'} \cong \left\{ \frac{\Gamma'}{\alpha} - 1 \right\} \exp \frac{\pi \alpha}{\Gamma'} \dots\dots\dots(19)$$

Turning attention now to the second of the simultaneous equations for t_0 , namely eqn. (14), the approximate form for the theta-function can be substituted, leading to (after some rearrangement)

$$\log \left\{ \frac{\cosh \frac{\pi(t_0 + \alpha)}{2\Gamma'}}{\cosh \frac{\pi(t_0 - \alpha)}{2\Gamma'}} \right\} - \frac{\pi t_0 \alpha}{\Gamma' \Gamma'} = \frac{\pi \alpha}{b} \dots\dots\dots(20)$$

Before the hyperbolic functions here are replaced by exponential terms it is necessary to eliminate $(t_0 - \alpha)$, since this may be small. The numerator and the denominator inside the logarithm can be multiplied by $\cosh [\pi(t_0 + \alpha)/2\Gamma']$ and the products expanded. When this done and exponential terms substituted the equation becomes

$$\log \left\{ \frac{\exp \frac{\pi(t_0 + \alpha)}{\Gamma'}}{\exp \frac{\pi t_0}{\Gamma'} + \exp \frac{\pi \alpha}{\Gamma'}} \right\} - \frac{\pi t_0 \alpha}{\Gamma' \Gamma'} \cong \frac{\pi \alpha}{b} \dots\dots\dots(21)$$

t_0 can be eliminated from this by substitution from (19), the quantity α/Γ' replaced by $1 - (h/b)$ and the result arranged to give

$$\frac{\Gamma'}{\Gamma'} \cong \frac{\frac{\pi \alpha}{b} - \frac{h}{b} \log \frac{h}{b} - \left(1 - \frac{h}{b}\right) \log \left(1 - \frac{h}{b}\right)}{\frac{\pi h}{b} \left(1 - \frac{h}{b}\right)} \dots\dots\dots(22)$$

Now as the modulus γ approaches unity the elliptic function $\text{dn } t$ can be replaced by $\text{sech } t$ and the approximation for k is finally obtained from (15)

$$k \cong \text{sech} \left\{ \frac{\frac{\pi \alpha}{b} - \frac{h}{b} \log \frac{h}{b} - \left(1 - \frac{h}{b}\right) \log \left(1 - \frac{h}{b}\right)}{2 \left(1 - \frac{h}{b}\right)} \right\} \dots\dots\dots(23)$$

This expression turns out to be quite accurate when used to calculate the impedance of the transmission line, at least in the range which is normally used in practice. Figure 5 shows the error obtained by the use of (23) for a few values of h/b . It is of interest to note that if h/b is put equal to zero in (23) the resulting expression for k , namely $\text{sech} (\pi \alpha / 2b)$, is exact for all values of a/b .

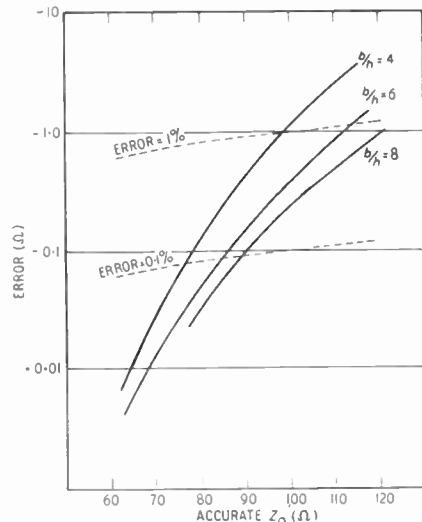


Fig. 5. Error of the first order approximation as a function of the accurate impedance.

4. The Effect of the Dielectric Support

The first part of the analysis, namely the derivation of the impedance of the basic line, has been based on an exact solution of the boundary value problem set by the conducting surfaces. The velocity of propagation of the waves in this line is the velocity of light in free space. In practice, however, the inner conductors are supported by a sheet of dielectric material as shown in Fig. 1 and, although this sheet lies in a region of small field, its presence causes an appreciable modification to the problem. The details of this modification have been outlined in the introduction and it was noted that an exact solution of the modified problem

is very difficult. It is necessary, at present, to extend the analysis by means of an approximate theory resting on the assumption that the effect of the dielectric sheet, although significant from a practical point of view, can be regarded as a relatively small perturbation to the boundary value problem already solved. The effect of this perturbation can then be calculated by one of the usual techniques employed in such problems and in particular the variational approach applied to a similar problem by Schetzen³ can be used*. (The perturbation theory developed by Bethe and Schwinger⁴ for resonant cavities can also be used by the construction of a half-wavelength cavity with subsequent calculation of the change of resonant frequency on introduction of the dielectric sheet. The final result is the same as that obtained from the variational approach.)

The approximate methods use the electric field in the basic line as a first approximation and a direct application is confined to cases for which this field is either parallel to or perpendicular to the dielectric/air interface. In other cases unknown effects are present, due to dielectric depolarization, which prevent a straightforward calculation. A study of the field pattern in the present case shows that the electric field is predominantly parallel to the interface and the basic analysis can be carried out with this assumption, the effect of depolarization being allowed for by the insertion of an unknown constant modifying the susceptibility. Schetzen's expression, rearranged to give phase velocity and modified for depolarization shows that the phase velocity v can be calculated from

$$\frac{v}{c} = \left\{ 1 + L\chi R \left(\frac{a}{b}, \frac{h}{b} \right) \right\}^{-\frac{1}{2}} \dots\dots\dots(24)$$

In the equation c is the velocity of light in free space, L is the "depolarization factor," χ is the susceptibility, and the factor $R(a/b, h/b)$ is defined by

$$R \left(\frac{a}{b}, \frac{h}{b} \right) = \frac{\int_{\Delta} |E|^2 ds}{\int_s |E|^2 ds} \dots\dots\dots(25)$$

* Since reference 3 is not commonly available an outline of this calculation is given in Appendix 2.

where S indicates integration over the whole cross-section of the line and Δ indicates integration over the cross-section occupied by the dielectric only. The electric field used in the integration is that of the basic line.

The factor L can, in principle, be a function of the dimensions a , b and h but it will be shown in the next section that adequate agreement with experimental results is obtained for a wide range of dimensions if L is put equal to 0.8 for all cases.

When the phase velocity is calculated the impedance Z_d of the line with dielectric can be obtained by combining this velocity with the impedance Z_0 of the basic line. It should be noted that in principle the impedance Z_d is not uniquely defined since the true wave in the line is no longer transverse electromagnetic but in practice this form is assumed and the impedance used for design purposes. It is actually the impedance at zero frequency obtained from the static capacitance of the line and is given by the equation

$$\frac{Z_d}{Z_0} = \frac{v}{c} \dots\dots\dots(26)$$

using the fact that the inductance of the lines is not affected by the presence of the dielectric sheet.

5. Comparison with Experimental Results

It is now necessary to compare the results obtained from the analysis of the preceding sections with the results of experimental work on the properties of the line. The comparison undertaken will be restricted to the phase velocity for lines with varying dimensions, dielectric media and frequencies. It is extremely difficult to obtain a reliable measure of impedance at the frequencies used to measure phase velocity and past practice has been to measure the capacitance of the line at some nominal frequency, for instance 25 Mc/s. Experience appears to indicate that it is better for design purposes to measure the phase velocity only, calculating the impedance from eqn. (26).

Five lines are considered for comparison, these lines covering a range of parameters. As far as is known these are the only lines for which a complete set of data is available. In the case of some of the materials which are

Table 2

Case	Material	Frequency	χ	h/b
(a)	Silicone resin bonded fibreglass	3 kMc/s	3.16	0.125
(b)	Resin bonded paper ¹ ...	1 kMc/s	2.7 ⁶	0.17
(c)	Teflon bonded fibreglass ¹ ...	1 kMc/s	2.15 ⁶	0.17
(d)	Silicone resin bonded fibreglass	9 kMc/s	3.16	0.25
(e)	Polythene	3 kMc/s	1.25	0.50

dielectric laminates and are anisotropic, the susceptibility used is that for which the electric field is parallel to the laminate surface. The relevant data are given in Table 2.

The methods by which the phase velocities were measured are somewhat different for the different cases. The first used an open-circuited line following a coaxial standing wave indicator, the strip line being cut to obtain a half or full wavelength as determined by the position of minimum voltage in the coaxial line. The experimental data for cases (b) and (c) were taken from the work of Warren Cooper and Ringenbach¹ and two methods are outlined in the reference. One of these methods uses a short-circuited length of transmission line, the frequency being varied until a minimum reading is observed at a reference probe four wavelengths from the short-circuit. The other method involves the adjustment of two lengths of line for resonance at the same frequency. Full-wave and half-wave resonances were used, the end effects being eliminated by comparison between the two. In case (d) a short-circuited line was used following a waveguide standing wave indicator and a transition. The position of the short-circuit was varied over several half-wavelengths and the minimum of the standing wave pattern in the waveguide followed on the indicator. (c.f. the method of Feenberg⁷ for the measurement of standing wave ratios.) The results can be analysed by integration, the technique also giving a measure of the probable error. The velocities obtained are estimated to be in error by less than 2 per cent. The line in case (e) was measured directly on a standing wave indicator built on the line itself. Unfortunately the lines, being made by hand, were not very consistent along their lengths and the results may be in error by about three or four per cent.

The comparison between theory and experiment is shown in Fig. 6 in which the theoretical curves are calculated for $L=0.8$ for all values of a/b and h/b . In view of the incorrect

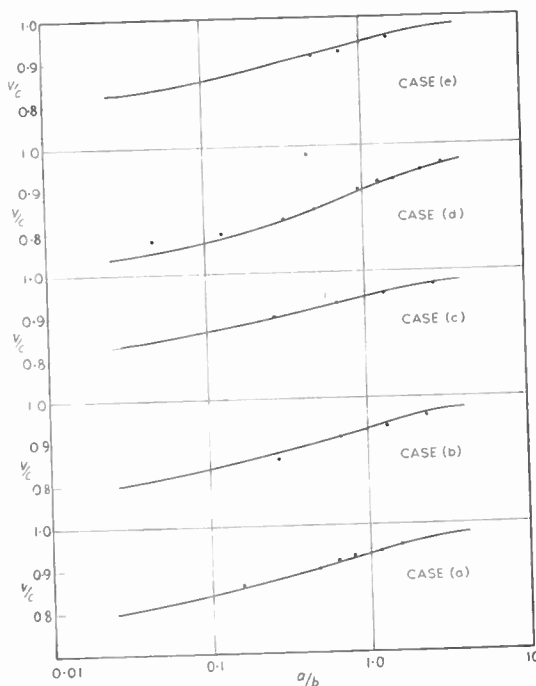


Fig. 6. Comparison between theory and experiment for the cases outlined in the text. The solid curves are those calculated from eqn. (26) with $L=0.8$. The circles are experimental values.

assumption of a constant depolarization effect no attempt was made to obtain a closer fit to the experimental values. In principle the experimental data could be used in conjunction with eqn. (24) to obtain L as a function of the parameters. Unfortunately, an error of about 1 per cent. in the value of phase velocity produces an

error of about 10 per cent. in the calculated value of L (and in some cases more) and this error is probably sufficient to mask any consistent variation of L . However, from the practical point of view, the quantity used in design is v/c and it can be seen that the difference between the theoretical and the experimental values is in most cases within the estimated experimental error.

6. Conclusions

On the basis of the discussion of the previous section it can be seen that the theoretical analysis developed in this paper permits the calculation of the major parameters of the transmission line, namely the phase velocity and characteristic impedance, to an accuracy of probably better than 1 per cent. The calculation of the impedance does depend on the assumption of quasi-transverse magnetic propagation, the quantitative accuracy of which is somewhat difficult to assess. However the experience gained by using this assumption has not indicated any error in the impedance value and, in the absence of an exact solution, it is probably the best value obtainable.

It is possible to estimate the effect of the dielectric sheet on the attenuation of the line by using the complex susceptibility in the calculation of phase velocity. The usual copper loss can be added to this value and the total attenuation coefficient derived. Warren Cooper and Ringenbach¹ have also considered this problem, in their case the effect of the dielectric being obtained from a composite line approach. This approach gives values of the dielectric contribution about one half of those obtained from the use of the complex susceptibility, a difference which would in some part account for discrepancies found by these authors between the calculated and experimental results. The available data are too sparse, however, to make a reliable comparison and the details will not be pursued here.

7. Acknowledgments

The author wishes to acknowledge the assistance of Mr. N. G. Batty and Mr. J. Mangan who carried through all the numerical evaluation necessary for this work and of Mr. J. H. Longley, Mr. B. Graham and Mr. N. Tuck who produced many of the experimental results quoted in the paper. He also wishes to thank

Mr. K. E. Harris, the Technical Director and Mr. A. Allen, the Chief Development Engineer of Cossor Radar and Electronics Ltd., for permission to publish this paper.

8. References

1. "Symposium on Microwave Strip Circuits," *Transactions of the Institute of Radio Engineers*, MTT-3, No. 2, March 1955.
2. J. M. C. Dukes, "The application of printed circuit techniques to the design of microwave components," *Proceedings of the Institution of Electrical Engineers*, 105, Pt B, March 1958.
3. M. Schetzen, "Printed Microwave Systems," M.I.T. Research Laboratory of Electronics Technical Report 289, September 30, 1954.
4. H. Bethe and J. S. Schwinger, "Perturbation Theory for Cavities," M.I.T. Radiation Laboratory Report D1-117, March 4, 1943.
5. E. T. Whittaker and G. N. Watson, "Modern Analysis," (Cambridge University Press, 1952).
6. A. R. von Hippel (Editor), "Dielectric Materials and Applications," (Wiley and Sons, New York, 1954).
7. E. Feenberg, "The relation between the nodal positions and standing wave ratio in a composite transmission system," *Journal of Applied Physics*, 17, p. 530, June 1946.

9. Appendix 1: Expansion for large a/b

The analysis of Section 2 has used the theta-function $\Theta(t)$ which is Jacobi's earlier notation for one of four theta-functions. It is convenient to use in this appendix the more modern notation as in reference 5. In this notation the theta-functions are denoted by $\vartheta_n(\xi, q)$ with n taking the values 1 to 4. The connection with the earlier notation as far as this work is concerned is given by the equations

$$\vartheta_4(\xi, q) \equiv \Theta(t)$$

$$\xi = \frac{\pi t}{2\Gamma}; \quad q = \exp\left\{-\frac{\pi\Gamma'}{\Gamma}\right\} \dots\dots\dots(27)$$

Series expansions for two of these functions are as follows;

$$\vartheta_2(\xi, q) = 2 \sum_{n=0}^{\infty} q \frac{(2n+1)^2}{4} \cos(2n+1)\xi \dots\dots\dots(28a)$$

$$\vartheta_4(\xi, q) = 1 + 2 \sum_{n=1}^{\infty} q^{n^2} \cos 2n\xi \dots\dots\dots(28b)$$

These expansions are useful for small q and, from (27), this is equivalent to small γ . For the present purpose, however, the practical range of a/b more nearly corresponds to γ approaching unity for which q approaches unity. It is pos-

sible to transform the theta-functions by Jacobi's imaginary transformation to construct an expansion suitable for this case. The transformation is

$$\theta_2(\xi, q) = \left(\frac{1'}{1''}\right)^{\frac{1}{2}} \exp\left\{-\frac{1''\xi^2}{\pi 1''}\right\} \theta_2\left(\frac{j\xi 1'}{1''}, q'\right) \dots\dots\dots(29)$$

where

$$q' = \exp\left\{-\frac{\pi 1'}{1''}\right\}$$

Since q' is now small the right-hand side can be expanded in terms of q' by (28a). The first term of this expansion can be written, on changing to the original notation, in the form of eqn. (17).

10. Appendix 2: Variational Calculation of Phase Velocity

The analysis in this appendix outlines Schetzen's variational approach which leads to eqn. (24).

Let the electric and magnetic fields in the transmission line be denoted by $\mathbf{E}(x, y)\exp j(\omega t - \beta z)$ and $\mathbf{H}(x, y)\exp j(\omega t - \beta z)$ respectively. In these expressions x, y, z are space co-ordinates, z being the direction of propagation, and β is the phase constant of propagation.

Substituting the expressions into Maxwell's equations yields

$$\nabla \Delta \mathbf{E} - j\beta \mathbf{k} \Delta \mathbf{E} = -j\omega \mu \mathbf{H} \dots\dots\dots(30a)$$

$$\nabla \Delta \mathbf{H} - j\beta \mathbf{k} \Delta \mathbf{H} = j\omega \epsilon \mathbf{E} \dots\dots\dots(30b)$$

in which \mathbf{k} signifies the unit vector in the direction of propagation. Forming the scalar product of (30a) with \mathbf{H}^* , (30b) with \mathbf{E}^* , subtracting the two resulting equations and integrating over the transmission line cross-section gives

$$\beta \int_s [\mathbf{H}^* \cdot \mathbf{k} \Delta \mathbf{E} - \mathbf{E}^* \cdot \mathbf{k} \Delta \mathbf{H}] ds = \omega \int_s [\mu \mathbf{H} \cdot \mathbf{H}^* + \epsilon \mathbf{E} \cdot \mathbf{E}^*] ds + j \int_s [\mathbf{E}^* \cdot \nabla \Delta \mathbf{H} - \mathbf{H}^* \cdot \nabla \Delta \mathbf{E}] ds \dots\dots\dots(31)$$

whence

$$\beta = \frac{\omega \int_s [\mu \mathbf{H} \cdot \mathbf{H}^* + \epsilon \mathbf{E} \cdot \mathbf{E}^*] ds + j \int_s [\mathbf{E}^* \cdot \nabla \Delta \mathbf{H} - \mathbf{H}^* \cdot \nabla \Delta \mathbf{E}] ds}{\int_s [\mathbf{H}^* \cdot \mathbf{k} \Delta \mathbf{E} - \mathbf{E}^* \cdot \mathbf{k} \Delta \mathbf{H}] ds} \dots\dots\dots(32)$$

This last equation can be shewn to be a variational expression for β with respect to the fields \mathbf{E} and \mathbf{H} . Put

$$\begin{aligned} \mathbf{E} &= \mathbf{E}_0 + \mathbf{e} \\ \mathbf{H} &= \mathbf{H}_0 + \mathbf{h} \\ \beta &= \beta_0 + \delta\beta \end{aligned} \dots\dots\dots(33)$$

denoting the true values by the suffix, \mathbf{e} and \mathbf{h} being small vectors, arbitrary except that they satisfy the boundary conditions on the conducting surfaces. Substitute (33) into (31) and retain only the first order terms. This process leads, after some re-arrangement and simplification by the use of (30), to

$$\begin{aligned} \delta\beta \int_s [\mathbf{H}_0^* \cdot \mathbf{k} \Delta \mathbf{E}_0 - \mathbf{E}_0^* \cdot \mathbf{k} \Delta \mathbf{H}_0] ds \\ = j \int_s \nabla \cdot [\mathbf{h} \Delta \mathbf{E}_0^* - \mathbf{e} \Delta \mathbf{H}_0^*] ds \dots\dots\dots(34) \end{aligned}$$

By conversion of the integral on the right to a volume integral, (which can be done immediately since the integrand is independent of z), and by subsequent application of Gauss' theorem and the boundary conditions it can be shown that the right-hand side of (34) is zero. The integral on the left-hand side can be transformed into an integral proportional to the power flowing along the transmission line and is therefore not zero. It is thus necessary that $\delta\beta = 0$ which establishes (32) as a variational equation for β .

This equation can now be applied to the line with the dielectric sheet. The fields can be taken as those existing in the line in the absence of the dielectric for which $\mathbf{H} = (\beta/\omega\mu)\mathbf{k}\Delta\mathbf{E}$, both \mathbf{E} and \mathbf{H} lying in the cross-sectional plane. Substitution for \mathbf{H} in (32) leads, after simplification and re-arrangement, to the first order expression

$$\left(\frac{\beta}{\beta_a}\right)^2 = 1 + \frac{\chi \int |E|^2 ds}{\int |E|^2 ds} \dots\dots\dots(35)$$

which is essentially eqn. (24) before the depolarization factor L is inserted, β_a being the propagation constant in the line before the dielectric is inserted.

REPORT OF THE ANNUAL GENERAL MEETING OF SUBSCRIBERS TO THE BRIT.I.R.E. BENEVOLENT FUND

The Meeting was held on 26th November, 1958 and the Chair was taken by Mr. George A. Marriott, B.A.(Cantab.).

1. To confirm the Minutes of the Annual General Meeting of subscribers held on 27th November, 1957

The Minutes of the Annual General Meeting dated 27th November, 1957, had been published in the January 1958 Journal. The Chairman's proposal that those Minutes be taken as a correct record was approved unanimously.

2. To receive the Annual Report of the Trustees and

3. To receive the Income and Expenditure Account and the Balance Sheet for the year ended 31st March, 1958

Mr. Marriott stated that as Item 3 of the Agenda was related to Item 2, he felt that subscribers would prefer these two items to be taken together. This was approved, and Mr. Marriott called upon Mr. G. D. Clifford, Honorary Secretary of the Benevolent Fund, to report on these two items.

Mr. Clifford then referred to the Annual Report of the Trustees which had been published in the November 1958 *Journal* and circulated to all subscribers. The Report gave examples of some of the cases handled by the Trustees during the year, which Mr. Clifford felt indicated the work which the limited resources of the Fund endeavoured to do for members of the Institution or their dependants.

Of equal, or perhaps even more importance, was the Trustees' work in ensuring that the children of incapacitated or deceased members did not suffer through lack of the education which they would have received in normal circumstances. In this connection, the decision of the Trustees to support such schools as Reed's School, the Royal Wolverhampton School, and the Royal Wanstead School, had always received unanimous approval from members and subscribers. Indeed, it was heartening to the Trustees to know that quite a number of members were giving support to one or all of those schools quite independently of their donations to the Institution's Benevolent Fund.

It would be obvious from the Report, and borne out by the Income Account, that all this work had only been made possible by the

increase in donations. Mr. Clifford felt, however, that no one could be satisfied with the comparatively small percentage of members who supported the Fund. The Schools referred to should receive larger contributions, and the Trustees were anxious to secure more bursaries to ensure that no child of any member should be deprived of adequate educational opportunities. He therefore appealed to every member to give consideration to the Trustees' work and support the Fund, in the knowledge that they would be rewarded by the appreciation and thanks of those children who received help.

Mr. Clifford stated that the President had always emphasised the necessity for having adequate investments to withstand any sudden demands upon the Fund and the Balance Sheet showed that this had again been achieved during the year.

The Report and Accounts were adopted unanimously.

4. To elect Trustees for the year 1958-59

The Secretary stated that it was the general wish of subscribers that the retiring Trustees, Mr. G. A. Marriott, Rear-Admiral Sir Philip Clarke, Mr. A. A. Dyson, Mr. A. H. Whiteley and Mr. G. A. Taylor should be re-elected.

The nominations were approved unanimously.

5. To appoint the Honorary Solicitors and

6. To appoint the Honorary Accountant

Mr. Marriott referred to the very great help which the Trustees had received from Mr. Charles Hill and from Mr. R. H. Jenkins, and he moved their re-appointment as Honorary Solicitors and Honorary Accountant respectively.

The proposal was carried unanimously.

7. Any other business

The Secretary stated that he had not received notice of any other business. The Chairman again thanked all subscribers for their support and declared the meeting of subscribers to the Benevolent Fund at an end.

PROPERTIES OF HOOK TRANSISTORS IN SWITCHING AND AMPLIFYING CIRCUITS*

by

L. M. Vallese, Dr.Sc.†

SUMMARY

The circuit properties of hook and $p-n-p-n$ transistor configurations are examined for applications to switching circuits and to linear amplifiers. Two- and four-terminal switching circuits of the open-circuit stable or of the short-circuit stable type may be built; in particular, thyatron-like characteristics may be obtained. Some of these circuits may be used also as negative impedance converters in network synthesis applications. Furthermore, stable amplifiers with remarkable characteristics are obtainable, as for example, unilateral amplifiers with very large input impedance or amplifiers with very large input admittance and very large power gain.

1. Introduction

The circuit properties of hook transistor connections (direct cascade of complementary common base and common collector stages) and of $p-n-p-n$ transistors, are of considerable interest for switching and amplifying circuit applications. Although their similarity to point contact transistors has been pointed out^{1,2,3}, a complete analysis of the various obtainable configurations has not been given in the literature.

In the following paper the analysis of the most significant properties of hook transistor connections in common base (Fig. 1(a)), common emitter (Fig. 1(b)) and common collector (Fig. 1(c)) configurations is given. These properties are similar to those of $p-n-p-n$ transistors. For simplification purposes the parameters of the hook component transistors (impedance-type parameters are used in this paper) are assumed to be identical. This assumption is not restrictive with respect to the

methods of analysis used and is valid in most cases of interest. For the cases in which the parameters are unequal (for example because of different bias currents), the generalization of the analysis is straightforward, and, on the other hand, its results remain qualitatively the same.

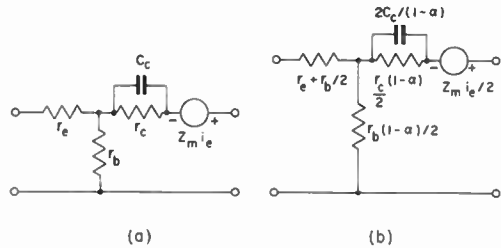


Fig. 2. Low frequency equivalent circuit, (a) of single transistor, (b) of hook transistor.

2. The Hook Common Emitter Configuration

The impedance matrices of the various hook configurations are given in Appendix 1. In particular, the matrix of the hook common base may be written approximately as follows for the forward operation

$$||Z_{ijhb}|| = \begin{vmatrix} r_e + r_b(1-a)/2, & r_b(1-a)/2 \\ (r_b + r_m)/2, & (z_c + 2r_b)(1-a)/2 \end{vmatrix} \dots\dots(1)$$

A corresponding low-frequency equivalent circuit is shown in Fig. 2(b). In this circuit the intrinsic feedback is much smaller than that of the common base configuration; the forward transfer impedance and the open circuit output impedance are both about one half the corresponding values of the common emitter.

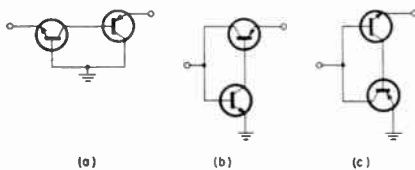


Fig. 1. Hook transistor configurations.

* Manuscript first received 20th March 1958, in revised form on 4th July 1958 and in final form on 1st October 1958. (Paper No. 483.)

† Polytechnic Institute of Brooklyn, Brooklyn 1, New York.

U.D.C. No. 621.382.333:621.318.572:621.375.4

The matrix of the hook common emitter configuration may be written approximately as follows for the forward operation:

$$\begin{vmatrix} |z_{ijhc}| \cong & & \\ r_{e1} + r_b(1 - \alpha/2), & r_{e1} + r_b/2 & \\ r_{e1} + r_b(1 - \alpha)/2 - z_m/2, & r_{e1} + r_{e2} + z_e(1 - 2\alpha)/2 & \end{vmatrix} \dots\dots(2)$$

In the above relation r_{e1} is the emitter resistance of the lower transistor in Fig. 1(b).

If the hook common emitter configuration is used as a transducer with resistor load, the input impedance in the active region at low frequencies assumes the value

$$R_{in} \cong r_{e1} + r_b(1 - \alpha/2) - \frac{[(r_{e1} + r_b/2)(r_m - 2r_{e1} - r_b(1 - \alpha))]}{(2\alpha - 1)r_c - 2(r_{e1} + r_{e2} + R_L)} \dots\dots(3)$$

This quantity is positive or negative depending whether R_L is larger or smaller than the critical value

$$R_L^* \cong r_m - r_c/2 - r_{e1} - r_{e2} \cong r_m - r_c/2 \dots\dots(4)$$

If an external resistance $R_e \gg r_b$ is added in series with r_{e1} , the expression of the input resistance becomes

$$R_{in} \cong -R_e \frac{1 - \alpha + 2R_L/r_c}{2\alpha - 1 - 2(R_e + R_L)/r_c} \dots\dots(5)$$

or roughly $R_{in} \cong -R_e(1 - \alpha)$ if $R_e + R_L \ll r_c/2$, $\alpha \cong 1$; correspondingly the expression of R_L^* becomes

$$R_L^* \cong r_m - r_c/2 - R_e.$$

Experimental verifications of this result are shown in Fig. 3, where the static input characteristics of a 2N27-2N45 hook common emitter stage are shown. The following cases have been considered:

$E_2 = 10 \text{ V}$,	$R_e = 0$,	$R_L = 300 \text{ k}\Omega$	(curve a)
"	"	100 k Ω	" b
"	"	50 k Ω	" c
"	"	25 k Ω	" d
"	10 k Ω	25 k Ω	" e
"	20 k Ω	25 k Ω	" f

Note that a resistance of 1,500 ohms has been connected between base and emitter of the 2N45 transistor.

All of the above curves are of the short-circuit stable type; in first approximation each of them may be represented by means of a three segment broken line, with a cut-off region of very high resistance, an active region of resistance given

by eqn. (5), and a saturation region of resistance $R_e R_L / (R_e + R_L)$. The (V, I) co-ordinates of the two turning points are roughly

$$0, I_{CE0}; \quad \frac{R_e(1 - \alpha)E_2}{(R_e + R_L)(1 - \alpha) + R_L},$$

$$I_{CE0} - \frac{E_2}{(R_e + R_L)(1 - \alpha) + R_L}$$

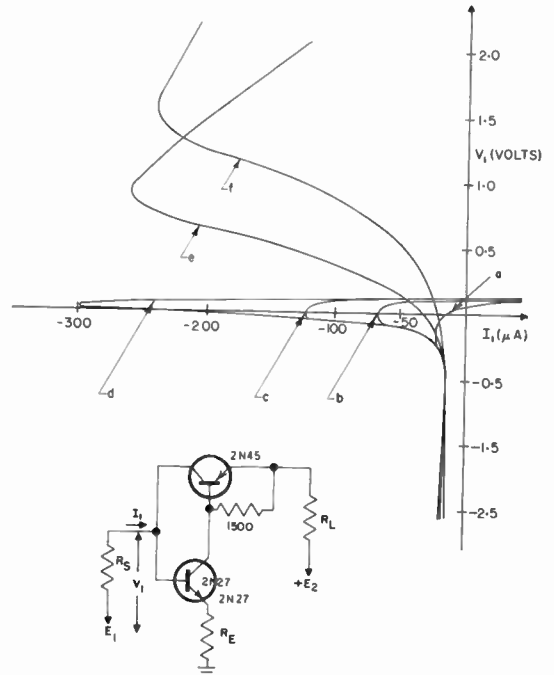


Fig. 3. Input characteristics of hook common emitter stage.

With reference to the circuit of Fig. 3, I_{CE0} is the (negative) reverse collector current of the 2N45 transistor.

The output resistance of the hook common emitter configuration, when a resistive source termination is used, is expressed as follows for the active region

$$R_{out} \cong -r_m + r_c/2 + r_{e1} + r_{e2} + \frac{[(r_{e1} + r_b/2)(r_m/2 - r_{e1} - r_b(1 - \alpha)/2)]}{r_{e1} + r_b(1 - \alpha/2) + R_s} \dots\dots(6)$$

If R_s is increased from zero, R_{out} varies from a positive to a negative value and approaches asymptotically the limit $-r_m + r_c/2$ for R_s very large.

The latter condition corresponds to the operation of the so-called "four-layer diode"⁴. The static output characteristics are of the open-circuit stable type, with peak and valley points depending upon the input bias. The device, therefore, acts like a thyatron. In particular, with reference to Fig. 4(a), letting $V_{bb} = E_1 + V_s$, the peak point occurs when the input voltage $V_1 = V_{bb} + R_s I_1$ assumes the transitional value between the reverse and the forward bias regions. Since in each region I_1 varies directly with I_2 and V_3 , while the transitional V_1 value is approximately constant, it follows that the peak point varies with V_{bb} . A family of characteristics with parameter V_{bb} obtained experimentally for a 2N28-2N45 hook transistor is shown in Fig. 4(c). These curves present a negative resistance of the order of half megohm, except where avalanche phenomena occur, in which case the negative resistance becomes very high. Since germanium transistors were used, the reverse current of these characteristics is high; more convenient conditions are obtained using silicon transistors.

The dynamic behaviour of the hook common emitter switch may be investigated assuming that the device is cut-off initially and that a rectangular pulse is applied at point A of Fig. 4(a); this condition corresponds to "collector triggering". If C_L and R_s are large, the variational differential equation for the output current I_2 in the active region (given in general by $Z_o(p)I_2(p) = 0$) assumes the approximate form

$$[p - \omega_a(2\alpha_0 - 1)]I_2(p) = 0 \quad \dots\dots(7)$$

where α_0 and ω_a are respectively the low frequency value of α and its cut-off frequency. Correspondingly $i_2(t)$ rises exponentially in the

active region with the equation

$$i_2(t) = I_2(0)\exp[\omega_a(2\alpha_0 - 1)t] \quad \dots\dots(8)$$

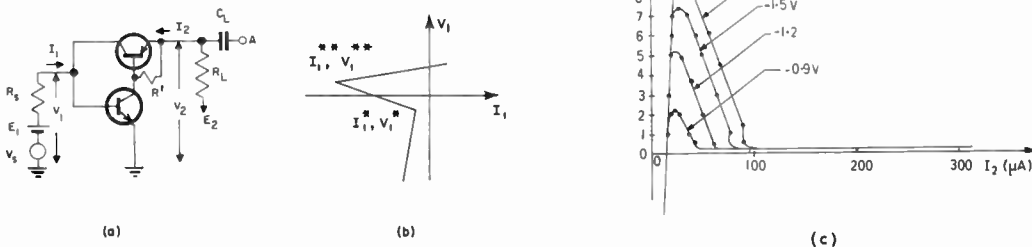
of very high rate of change. Similarly for "base triggering", from the general equation $Z_{in}(p)I_1(p) = 0$ one finds the following variational differential equation for $i_1(t)$ in the active region

$$[p^2 - \omega_a^2(1 - \alpha_0)]I_1(p) = 0$$

Hence $i_1(t) = I(0) \exp(\omega_a \sqrt{1 - \alpha_0} t)$. Since $i_2(t)$ must at best follow $i_1(t)$, it is seen that the rate of increase is somewhat lower than that of eqn. (8). Experimentally, using a 2N28-2N45 thyatron of the type of Fig. 4(a), with $R_L = 5 \text{ k}\Omega$, $R' = 50\Omega$, $E_2 = 6 \text{ V}$, switching times of the order of 0.1 microsec were obtained for collector triggering and of the order of 0.3 microsec for base triggering. The storage time of the device was found to be high, of the order of 15 microsec; it varied proportionately to R' , decreasing to 8 microsec for $R' = 20\Omega$ and increasing to 17 microsec for $R' = 100 \text{ ohms}$.

A direct comparison with single transistor switches cannot be made since these do not possess thyatron-like characteristics and, therefore, would not be used in similar circuits. However, it is instructive to consider the rise and decay times of the pulse response of a simple common emitter stage. The rise time from cut-off depends upon the amplitude of the driving pulse and may be made small if the collector is allowed to saturate. Using a 2N28 transistor and raising the drive-amplitude to the threshold of no-saturation, a rise time of ~ 8 microsec and a decay time of ~ 20 microsec were obtained, with collector resistance of 5 k Ω and collector supply voltage of 6 V.

Fig. 4. Hook transistor thyatron: (a) switching circuit, (b) input characteristic, (c) output characteristics.



Other interesting properties are found in the operation of the hook common emitter configuration as a linear amplifier. In the first place, with reference to Fig. 3 and to eqn. (5), it is seen that the amplifier may be used as a negative impedance converter, since its input impedance is proportional to the negative of an impedance Z_e connected in the emitter lead. This property may find useful applications in the synthesis of active networks.

On the other hand, the current gain of the amplifier is given approximately by the expression

$$A_i \cong - \frac{\alpha - 2R_e/z_c}{2\alpha - 1 - 2(R_e + R_L)/z_c} \dots\dots\dots(9)$$

which reduces to $-\alpha/(2\alpha - 1)$, i.e. a value slightly above one, when $R_e + R_L \ll z_c/2$. When $R_e = r_m/2$, the current gain is zero, and when $R_e + R_L = r_m - r_c/2$, (an identity which can be satisfied for $R_e < r_m/2$) the current gain is infinite. Correspondingly, the amplifier becomes unstable. It is of interest to note that, when $R_L = R_L^* = r_m - r_c/2$, the input impedance, given by eqn. (5), becomes approximately equal to $r_m/2$ and independent of the value of R_e .

In practical applications the performance of the above circuit may be improved by the introduction of suitable modifications⁵. In fact the values of R_L and of R_e are generally too high and require the use of large supply voltages. If a resistance R'' is connected across the two collectors, the critical value of R_L is found to become

$$R_L^* = \frac{(2r_m - r_c)R'' - (r_c - r_m)r_b}{r_b + r_c + 2R''} \dots\dots\dots(10)$$

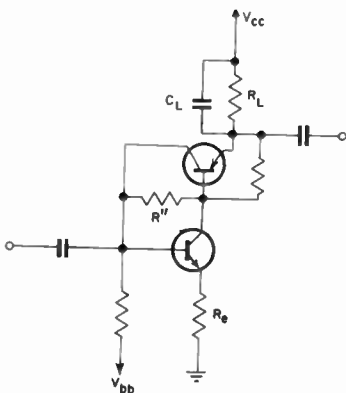


Fig. 5. Hook common emitter amplifier.

which reduces approximately to $(2\alpha - 1)R''$ if $R'' \ll r_c$. The corresponding value of R_{in} also decreases from $r_m/2$ and becomes

$$R_{in} \cong \frac{R''}{1 + (r_b + 2R'')/r_c} \dots\dots\dots(11)$$

The above relations have been written with reference to low-frequency operation. At high frequency the phase angles of $z_m/2$ and of the right hand member of eqn. (10) become less than zero. In order to maintain compensation, the resistance R_L may be replaced with a shunt R_L, C_L impedance. (Fig. 5.)

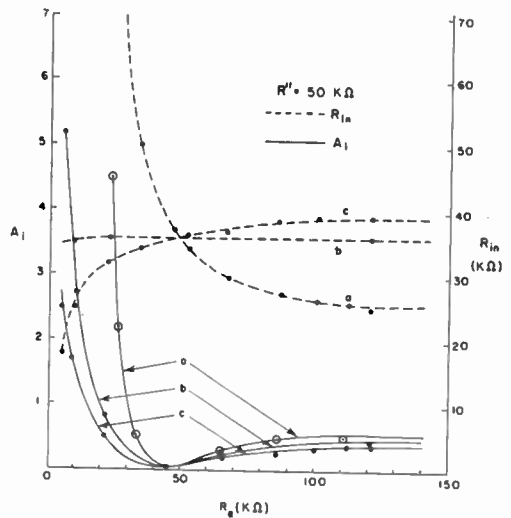


Fig. 6. Input resistance and current gain of hook common emitter amplifier: (a) $R_L = 20$ kΩ, (b) $R_L = 40$ kΩ, (c) $R_L = 50$ kΩ.

Experimental verifications of the properties of hook common emitter amplifiers are shown in Fig. 6. In this case a 2N27-2N45 combination was used, and R'' was made equal 50 kΩ. The critical value of R_L was found to be 40 kΩ (curve b) and the corresponding value of the input resistance 36 kΩ; on the other hand, the current gain was found to be zero at $R_e = 45$ kΩ. In Fig. 6 graphs indicating the variation of the input resistance and of the current gain with R_e are shown also for the cases $R_L = 20$ kΩ (curve a) and $R_L = 50$ kΩ (curve c). The graphs also show the existence of a minimum value of R_e under which the amplifier becomes unstable.

3. The Hook Common Base Configuration

Of the three possible configurations the hook common base (Fig. 1(a)) is the oldest in practical use. From the matrix (1) it is seen that it constitutes a stable amplifier, with current and voltage gains respectively equal approximately to those of the common collector and of the common base. The frequency response may be improved by introduction of an appropriate peaking inductance in series with the ungrounded collector-to-base connection, to resonate with the input capacitance of the common collector stage, and of an appropriate shunt resistance across the two collectors. An example is shown in Fig. 7 for a 2N43-2N27 hook common base, where it is seen that the voltage gain \times bandwidth product is improved from 2.5×10^6 to 4.5×10^6 .

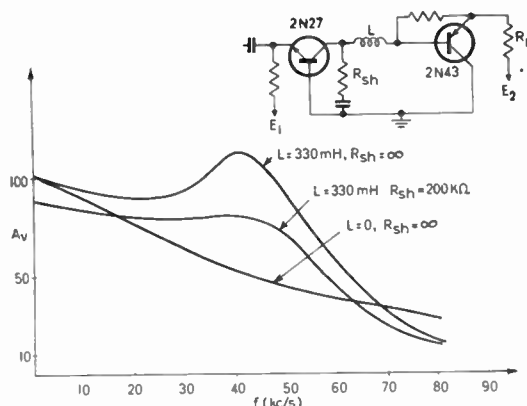


Fig. 7. Hook common base amplifier.

It is well known that the hook common base configuration may be made unstable with the use of positive feedback, such as obtained by inserting a resistance R_F in the ground lead of the circuit of Fig. 1(a). In this case (Fig. 8) the input resistance at audio frequencies is approximately

$$R_{in} \cong -R_F \frac{2\alpha - 1 - 2R_L/r_c}{1 - \alpha + 2(R_F + R_L)/r_c} \dots\dots(12)$$

provided $R_F \gg r_b/2$ and $R' \gg r_b$. If R_F and R_L are much smaller than $r_c/2$, eqn. (12) may be simplified as follows

$$R_{in} \cong -R_F \frac{2\alpha - 1}{1 - \alpha} \dots\dots(13)$$

i.e. the input resistance is proportional to the negative of R_F . This result shows that the

device may be used as a negative impedance converter.

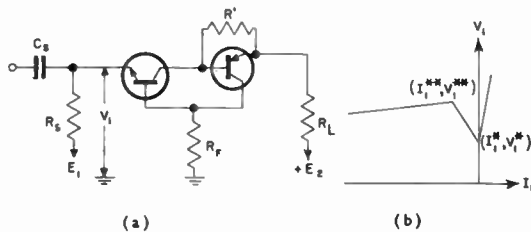


Fig. 8. Hook common base with positive feedback: (a) circuit, (b) input characteristic.

More generally, the static input characteristics are of the open input stable type (Fig. 8(b)) and find useful applications in switching circuits, saw-tooth oscillators, etc⁶. The switching speed is of the same order of that of the hook common emitter thyatron, with the same external resistances. For example, using $R_F = 10 \text{ k}\Omega$, $R_s = 200\Omega$, $R_L = 2,000\Omega$ and feeding the triggering pulse through R , the turn on time was found to be of the order of 0.3 microsec. A shorter turn-on time was obtained for triggering directly at the emitter. The dynamic behaviour in the active region, obtained letting $Z_{in}(p)I_1(p) = 0$, is from eqn. (12)

$$[2\alpha_0 - (1 + 2R_L/r_c)(1 + p/\omega_\alpha)] I_1(p) = 0 \dots\dots\dots(14)$$

This equation reduces to the form (7) when $2R_L/r_c$ is neglected.

Equation (12) shows that the input resistance depends upon the load R_L . By appropriate choice of the latter resistance, R_{in} may be made positive. In particular, if $R_L = r_m - r_c/2$, R_{in} is zero and the amplifier is stable; its input voltage and input power are zero, its current gain is -1 , its voltage and power gains are infinite. From an academic point of view this result is interesting, because it points out dramatically that the transistor is primarily a current controlled device which may be operated with zero input voltage, but not with zero input current. In particular, it cannot have infinite input impedance; on the other hand the vacuum tube cannot have zero input impedance. In practice the power gain of the above amplifier is found to be very large, but infinite, because of limitations of the dynamic range. The performance of the amplifier may be improved from the point of view of practical applications, using the

same modifications indicated for the case of the hook common emitter amplifier. The final circuit used for experimental verifications is shown in Fig. 9, where $R_F = 60\Omega$, $R_L = 3,000\Omega$, $R'' = 500\Omega$. The input bias was adjusted for a collector current of about 0.5 mA. The compensation was obtained by adjusting R'' for given values of R_F and of R_L . A 1 kc/s generator was applied at the input terminals and it was found that the input voltage, although not zero, was very small. With $V_1 = 1\text{ mV}$ an output voltage across $R_L = 3,000\Omega$ of 1.1 V, corresponding to a gain of 1,100, was obtained. This gain was found to be about five times larger than the gain obtainable with a conventional cascade combination common base-common collector of the same transistors with similar load and bias. It must be added that the above experimental verifications were made primarily with the purpose of verifying the theory and no special effort was made to obtain

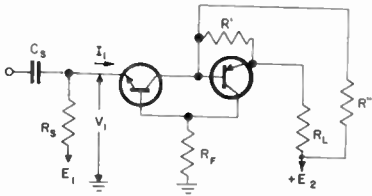


Fig. 9. Hook common base amplifier with "zero" input impedance.

optimum results. Using different transistors and different values of the components of the compensating network, higher gains may be obtained.

4. The Hook Common Collector Configuration

The impedance matrix of the hook common collector configuration (Fig. 1(c)) may be written approximately as follows for the active region of operation

$$\begin{aligned}
 ||z_{ijhc}|| &\cong \\
 \begin{vmatrix} r_{e1} + z_c(1 - \alpha)/2, & r_{e1} + r_b/2 - z_c(2\alpha - 1)/2 \\ r_{e1} + z_c(1 - \alpha)/2, & r_{e1} + r_{e2} - z_c(\alpha - \frac{1}{2}) \end{vmatrix} & \\
 \dots\dots\dots(15) &
 \end{aligned}$$

Here r_{e1} is the emitter resistance of the transistor with collector connected to the input terminals. Ordinarily, the hook common collector possesses a negative input resistance, which is

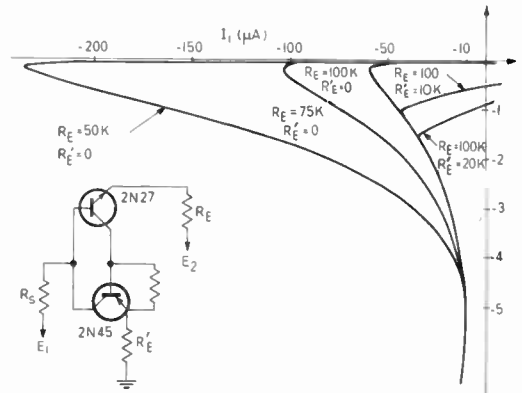


Fig. 10. Experimental input characteristics of hook common collector amplifier.

function of the load R_E (Fig. 10) and is given approximately by the expression

$$R_{in} = -R_E(1 - \alpha)/(2\alpha - 1) \dots\dots\dots(16)$$

This formula is equivalent to eqn. (5) [if the terms $2R_L/r_c$, $2(R_c + R_L)/r_c$ in the latter are neglected], and to eqn. (13) [where the resistance R_F corresponds to R_c]. The overall static input characteristics are of the short circuit stable type; their form is modified when a resistance R_E is placed in series with the grounded emitter terminal. This reduces the range of the negative resistance region without changing its slope; on the other hand the saturation resistance becomes R_E . In particular, if R_E is made equal $r_m - r_c/2$, the resulting configuration is unilateral and the input impedance is $\sim z_m/2$. The circuit is not different from that of Fig. 5, except for the terminal which is used as output. For this reason the practical modifications indicated for the circuit of Fig. 5 may be used in the present case also.

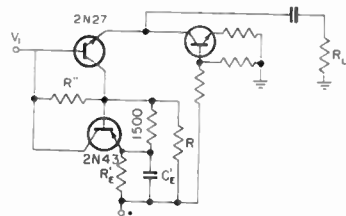


Fig. 11. Unilateralized common collector amplifier.

For experimental verifications the circuit of Fig. 11 was used, with $R_E = 3,000\Omega$, $C_e = 2,400\text{ pF}$, $R'' = 50\text{ k}\Omega$, $R = 75\Omega$. The input

resistance of this amplifier at 1,000 c/s varies with R'' , approaching asymptotically the value $r_m/2$ for very large values of R'' (Fig. 12). At the same time, since the amplifier is unilateralized, the reverse voltage gain, obtained applying a generator at the output terminals and measuring the resulting voltage at the input terminals, should be zero. In practice the reverse voltage gain is found to be very small and varies with R'' as shown in Fig. 12. In the same figure the values of the output resistance are also plotted.

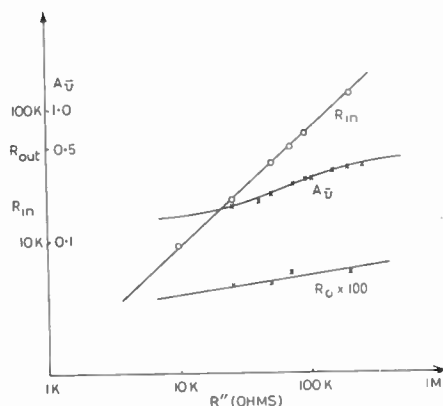


Fig. 12. Input resistance, reverse voltage gain and output resistance of the unilateralized common collector amplifier versus R'' .

In Fig. 13 the variation of the reverse voltage gain $A_{\bar{v}}$ as a function of the value of the resistance R is shown. It is seen that, when R is

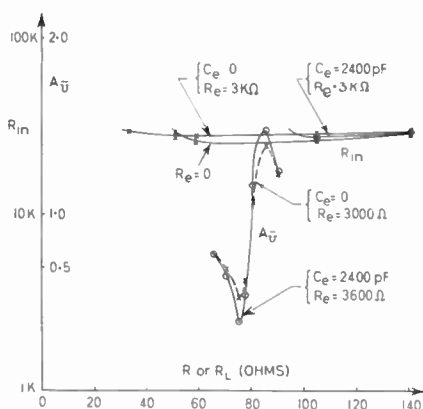


Fig. 13. Reverse voltage gain as a function of R ; input resistance as a function of R_L .

about 75Ω , $A_{\bar{v}}$ is minimum. This critical value of R corresponds to compensation obtained at a room temperature of $30^\circ C$; it is found to decrease at a constant rate as the temperature increases. In particular, for the circuit investigated this rate of variation was found to be 2% per degree, a value which can be easily realized by means of thermistors.

In the same Fig. 13 the variation of the input resistance as a function of the load resistance R_L is shown. It is seen that R_{in} is approximately constant, for all values of R_L larger than a critical value (of about 90Ω); when R_L is made smaller than such critical value, the amplifier becomes unstable.

5. Conclusion

The circuit properties of the hook common emitter, common base and common collector configurations have been examined for application to switching circuits and to linear amplifiers. It has been shown that open-circuit stable as well as short-circuit stable negative resistance characteristics may be obtained. In particular, the hook common emitter and the hook common collector may be used as switches with thyatron-like characteristics and with very high switching-on speed, depending upon the cut-off frequency. The four-layer diode is a particular application of the above result.

As a stable linear amplifier the hook configuration provides unusual characteristics:

- it may be used as a negative impedance converter.
- it may be used as a unilateral three-terminal, transformerless amplifier with very large input resistance.
- it may be used as an amplifier with very small input impedance and input power and very large voltage and power gains.

The properties derived for hook transistor connections also apply at least qualitatively in the case of $p-n-p-n$ transistors.

6. Acknowledgment

This work was supported by the Office of Naval Research, U.S.A.

7. References

1. W. Shockley, M. Sparks and G. K. Teal, "The p-n junction transistor", *Physical Review*, **83**, pp. 151-162, 1951.

2. J. J. Ebers, "Four-terminal p-n-p-n transistors", *Proc. Inst. Radio Engrs*, **40**, pp. 1,361-1,364, November 1952.
3. J. J. Moll, M. Tanenbaum, J. M. Goldey and N. Holonyak, "P-n-p-n transistor switches", *Proc. Inst. Radio Engrs*, **44**, pp. 1,174-1,182, September 1956.
4. W. Shockley, "Unique properties of the four-layer diode", *Electronic Industries and Tele-Tech*, August 1957, p. 58.
5. L. M. Vallese, "Unilateralized common collector transistor audio amplifier", *Proc. Nat. Electronics Conf., Chicago*, **13**, pp. 55-68, 1957.
6. A. E. Joel, "An experimental remote controlled line concentrator", *Bell. Syst. Tech. J.*, **35**, No. 2, pp. 249-293, March 1956.

8. Appendix 1: impedance Parameters of the Hook Transistor Configurations

Indicating with z_{ijb} , z_{ijc} respectively the impedance parameters of the common base and of the common collector configurations, those of the hook common base are written

$$||z_{ijhb}|| = \begin{vmatrix} z_{11b} - \frac{z_{12b} z_{21b}}{z_{22b} + z_{11c}} & \frac{z_{12b} z_{12c}}{z_{22b} + z_{11c}} \\ \frac{z_{21b} z_{21c}}{z_{22b} + z_{11c}} & z_{22c} - \frac{z_{21c} z_{12c}}{z_{22b} + z_{11c}} \end{vmatrix}$$

$$\cong \begin{vmatrix} r_e + \frac{r_b(2z_c - z_m + r_b)}{2(z_c + r_b)} & \frac{r_b(z_c - z_m)}{2(z_c + r_b)} \\ \frac{z_c(r_b + z_m)}{2(z_c + r_b)} & r_e + \frac{(z_c - z_m)(z_c + 2r_b)}{2(z_c + r_b)} \end{vmatrix}$$

For the forward operation these parameters may be approximated as follows

$$||z_{ijhb}|| = \begin{vmatrix} r_e + r_b(1 - \alpha/2), & r_b(1 - \alpha)/2 \\ (z_m + r_b)/2, & (z_c + 2r_b)(1 - \alpha)/2 \end{vmatrix}$$

Similarly the impedance matrix of the hook common emitter configuration, expressed in terms of the hook common base parameters, is

$$||z_{ijhe}|| = \begin{vmatrix} z_{11hb}, & z_{11hb} - z_{12hb} \\ z_{11hb} - z_{21hb}, & z_{11hb} + z_{22hb} - z_{12hb} - z_{21hb} \end{vmatrix}$$

In first approximation and for the forward operation the expressions of these parameters may be simplified as follows

$$||z_{ijhe}|| \cong \begin{vmatrix} r_{e1} + r_b(1 - \alpha/2), & r_{e1} + r_b/2 \\ r_{e1} + r_b(1 - \alpha)/2, & z_m/2 + r_{e1} + r_{e2} + (z_c/2)(1 - 2\alpha) \end{vmatrix}$$

where r_{e1} is the emitter resistance of the transistor having its base connected to the input terminal.

Finally the impedance matrix of the hook common collector configuration, expressed in terms of the impedance parameters of the hook common base is

$$||z_{ijhc}|| = \begin{vmatrix} z_{22hb}, & z_{22hb} - z_{21hb} \\ z_{22hb} - z_{12hb}, & z_{11hb} + z_{22hb} - z_{12hb} - z_{21hb} \end{vmatrix}$$

In first approximation the expressions of the parameters of the latter matrix may be simplified as follows for the operation in the forward direction

$$||z_{ijhc}|| \cong \begin{vmatrix} r_{e1} + z_c(1 - \alpha)/2, & r_{e1} + r_b/2 - z_c(\alpha - \frac{1}{2}) \\ r_{e1} + z_c(1 - \alpha)/2, & r_{e1} + r_{e2} - z_c(\alpha - \frac{1}{2}) \end{vmatrix}$$

Here r_{e1} is the emitter resistance of the transistor having its collector connected to the input terminal.

ELECTROMAGNETIC WAVE PROPAGATION IN CYLINDRICAL WAVEGUIDES CONTAINING GYROMAGNETIC MEDIA

by

R. A. Waldron, B.A. (Cantab.) (Associate Member)†

PART 3*

8. Solutions of the Characteristic Equation

We have solved the characteristic equation for $\bar{\beta}$, for certain values of the parameters a/λ_0 , b/a , ϵ , μ , and α , for certain of the lowest modes. The solutions were obtained by means of the electronic computer "DEUCE" (Digital Electronic Universal Computing Engine); the details of the computation are of little interest, and will not be discussed in the present work, except for one or two points having a bearing on the accuracy of the results, which are dealt with in Section 13. In Tables 4-14‡, the results are given with $\bar{\beta}$ tabulated against the radius ratio b/a , for stated values of the other parameters, for stated modes. Curves have also been drawn for certain cases (Figs. 17, 18, 19) in order to illustrate more clearly the general behaviour of the phase constant, although these curves do not give any information which is not contained in the tables.

We are most interested in the H_{11} mode. For large values of a/λ_0 , such that propagation takes place in the empty guide, $\bar{\beta}$ does not change greatly, at first, as b/a is increased from zero, but later it increases more rapidly. As a/λ_0 approaches the value at which the guide becomes cut off when empty ($b/a=0$), the flat region of the curve becomes shorter, eventually disappearing when $a/\lambda_0=0.29303$, where the empty guide becomes cut off. This behaviour is illustrated in Fig. 19, and is also apparent on comparing, for example, Table 12(d) with Table 9(e). As a/λ_0 decreases further, below the cut-off value for the empty guide, the value of b/a for which propagation begins to take

place increases from zero, and at the same time the phase constant curves rise more and more steeply, as can be seen from Fig. 19.

An interesting phenomenon now makes its appearance—the initial slope of a phase constant curve may not only increase indefinitely, but even pass through infinity and become negative. This is apparent from Fig. 19, but for discussion it is convenient to consider Fig. 17(a), when it is seen that for sufficiently large values (algebraically) of α , a value of $\bar{\beta}$ can be obtained for a value of b/a less than the "cut-off" value. This "bulging" effect increases with increasing α , ϵ , or μ ; for sufficiently small values of ϵ it disappears altogether, as can be seen on comparing Tables 6(a), (b), (c), and (d). Tables 5(b), 6(c), and 7(b) may also be compared, illustrating the dependence of the effect on μ .

In order to interpret the "bulges" physically, it is necessary to consider the continuation of the phase constant curves in the imaginary β plane. This is illustrated in Fig. 20 for the case $\epsilon=10$, $\mu=1$, $\alpha=+0.5$, with several values of a/λ_0 . For $a/\lambda_0 \geq 0.29303$, $\bar{\beta}$ is always real. For a curve such as that shown for $a/\lambda_0=0.25$, $\bar{\beta}$ is single-valued for all values of b/a , and there is no difficulty. For a curve such as that shown for $a/\lambda_0=0.2$, the form of the curve in the imaginary $\bar{\beta}$ plane may be expected to be as shown, and $\bar{\beta}$ is three-valued over a range of values of b/a .

A small value of $\bar{\beta}$ corresponds to a high impedance, and it is reasonable to suppose that for a wave in the H_{11} mode travelling in the guide, it will be the extreme values of $\bar{\beta}$ that will be preferred in the three-valued range. If

* Parts 1 and 2 of this paper have been published in the October and November issues of the *Journal* (pages 597-612 and 677-690).

† Marconi's Wireless Telegraph Co. Ltd., Baddow Research Laboratories, Chelmsford, Essex.
U.D.C. No. 621.372.852.22

‡ Tables 4-7 are published at the end of Part 2 (pp. 688-90) and Tables 8-14 at the end of this Part.

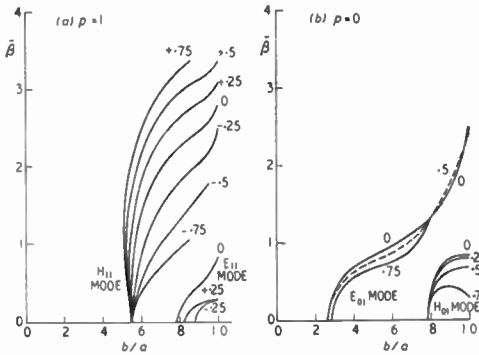


Fig. 17. Curves of normalized phase constant $\bar{\beta}$ against b/a for $a/\lambda_0=0.2$, $\mu=1$, $\epsilon=10$ and stated values of α .

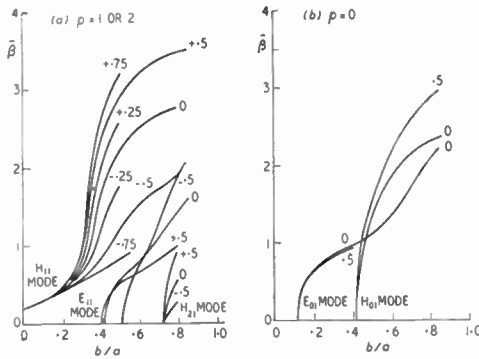


Fig. 18. As Fig. 17 but for $a/\lambda_0=0.3$.

we take a rod of ferrite of steadily decreasing radius, and measure the phase constant, we may expect that this will be found to follow the upper branch as far as A, and the lower branch from B onwards. Between these points, it is difficult to say exactly what will happen, but it may be surmised that for values of b/a nearer C than D a real phase constant will be preferred, and for values of b/a nearer D than C the imaginary value of $\bar{\beta}$ will be preferred. This behaviour is somewhat analogous to that of a van der Waals gas on liquefaction, where the theoretical curve is cubic in form, and the observed PV curve is discontinuous in the neighbourhood of the re-entrant part of the theoretical curve.

Higher H-modes are not likely to be of much practical value, but it is interesting to get some idea of how they behave. The cut-off studies of Section 7 indicate when such modes are able

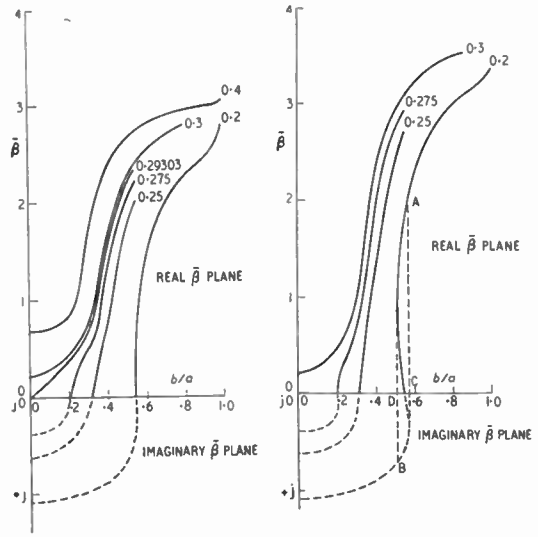


Fig. 19 (above, left). Curves of normalized phase constant $\bar{\beta}$ against b/a for $\epsilon=10$, $\mu=1$, $\alpha=0$ and stated values of a/λ_0 (H_{11} mode). The dashed curves are not accurately computed.

Fig. 20 (above, right). As Fig. 19 but for $\alpha=0.5$.

to propagate; values of $\bar{\beta}$ have also been calculated as a function of b/a in one or two cases for the H_{01} and H_{21} modes, and these are illustrated in Figs. 17 and 18. The curves for the H_{21} mode seem to be of the same general shape as those of the H_{11} mode, except that the effect of α is greater. The curves of Fig. 18(a) (calculated points given in Table 9(l)) may be compared with the values given in Table 6(a); the curves for $\alpha=\pm 0.5$ differ more widely from that for $\alpha=0$ in the case of the H_{21} mode than they do in the case of the H_{11} mode. It seems to be a general trend that the effect of α increases as p increases, for in the case of the H_{11} mode the effect of α is quite small, as can be seen from Fig. 18(b).

It is not unlikely that, for sufficiently large values of ϵ and a/λ_0 , the H_{21} curves will also exhibit the "bulging" effect observed with the H_{11} mode; in the case of the H_{01} mode, a fair number of curves have been obtained, but there is no indication that the bulging effect takes place, and it is not possible to say, on the evidence we have, whether this effect is likely or not.

One interesting point to notice about the H_{01} mode is that for a sufficiently high value of α , the curves of $\bar{\beta}$ against b/a ascend to a maximum and then decrease. An example of this behaviour is given in Fig. 17(b), for the case $\alpha=0.75$.

The phase constant curves for E-modes exhibit considerable differences from those for H-modes. In none of the cases for which we have performed computations has a very steep increase of $\bar{\beta}$ with increasing b/a been observed, and the "bulging" effect found with the H_{11} mode is absent. Another difference is that the curves for different values of α cross in the case of E-modes, while they remain separated in the case of H-modes.

It was pointed out in Section 7.8 that when the cut-off curve is of the form, for example, of that for the E_{01} mode in Fig. 7*, for $\alpha=0.5$, the phase constant curve may be expected to increase from zero, reach a maximum, and fall again, perhaps reaching zero, perhaps a point on the line $b/a=1$. This expectation is justified—examples are provided by Tables 5(d) and 6(e). This kind of behaviour may be expected to occur, for suitable values of the parameters, for all E-modes; it is indicated by the cut-off curves. We have not, however, observed it in the case of the E_{11} mode, although in Fig. 17(a) there is some indication that it would occur for a higher value of α than has been taken.

9. Faraday Rotation

It is apparent on inspection that eqns. (23) and (34) are not symmetrical with respect to a change in sign of α . In this respect they differ from eqns. (24) and (41), which are independent of α . The physical significance of a change of sign of α is that the hand of helical polarization is reversed; if α is negative, there is a right-handed helical wave, while if α is positive, the wave is left-handed. In the isotropic case, the right-handed and left-handed waves travel with the same velocity, i.e. have the same value of $\bar{\beta}$. The composite wave, composed of right- and left-handed waves of equal amplitude, travels with the same velocity as the two components and without change in the field patterns in the transverse plane.

In the anisotropic case, the value of $\bar{\beta}$ depends on the sign of α , so that the right- and left-handed components of the composite wave travel with different velocities. The result is that the field patterns of the composite wave rotate as the wave progresses. This is the phenomenon of Faraday rotation. The angle through which the field patterns rotate may be easily calculated when the values of $\bar{\beta}$ for the two component waves are known. Let these values be $\bar{\beta}_+$ for positive α and $\bar{\beta}_-$ for negative α , in the case of one of the normal modes. Thus if the polarizing field is in the positive z-direction, $\bar{\beta}_-$ corresponds to right-helically polarized waves (with respect to the polarizing field) and $\bar{\beta}_+$ to left-handed waves. Then

$$1/\lambda_+ = \bar{\beta}_+/\lambda_0; \quad 1/\lambda_- = \bar{\beta}_-/\lambda_0$$

The wavelength λ_g of the composite wave is

$$\lambda_g = \frac{1}{2} \cdot (\lambda_+ + \lambda_-) = \frac{\lambda_0}{2} \left[\frac{1}{\bar{\beta}_+} + \frac{1}{\bar{\beta}_-} \right]$$

If the + and - waves start with zero phase, then after travelling a distance λ_g along the guide the phase of the wave is $\pi(1 + \bar{\beta}_+/\bar{\beta}_-)$ and that of the - wave is $\pi(1 + \bar{\beta}_-/\bar{\beta}_+)$. The Faraday rotation in a length λ_g is therefore

$$\varphi_g = \frac{\pi}{2} \left[\frac{\bar{\beta}_+}{\bar{\beta}_-} + \frac{\bar{\beta}_-}{\bar{\beta}_+} \right]$$

the signs being such that if φ_g is positive the rotation is left-handed. To conform with the system adopted throughout this paper, we now express the Faraday rotation in radians per unit length of waveguide, the unit of length being λ_0 . We thus have

$$\varphi_0 = \pi \left(\frac{\bar{\beta}_+}{\bar{\beta}_-} - \frac{\bar{\beta}_-}{\bar{\beta}_+} \right) \dots\dots\dots(69)$$

In practice, it is convenient to think in terms of the rotation in degrees per centimetre, which is

$$\varphi = \frac{180}{\lambda_0} (\bar{\beta}_+ - \bar{\beta}_-) \dots\dots\dots(70)$$

Again the sign convention is such that a positive value of φ_0 or φ represents a left-handed rotation.

It is often desired in practice to obtain the maximum rotation for minimum loss, and it is convenient to express the rotation as so many degrees in the length of guide for which the loss is 1db. Suppose that the propagation

* Reproduced in Part 2.

constant is $\gamma = \delta + j\beta$; alternatively β may be supposed to contain an imaginary part $-j\delta$. The damping factor is thus $e^{-\delta z}$, and the length of guide in which the loss is 1db is

$$l = \frac{1}{\delta} \log_e(\text{antilog}_{10} 0.05)$$

i.e. $l = 0.1151/\delta$

The rotation per unit loss is thus $\varphi_1 = l\varphi$,

i.e.
$$\varphi_1 = \frac{0.1151 \times 180}{\delta \lambda_0} (\bar{\beta}_+ - \bar{\beta}_-), \dots (71)$$

The rotation per unit loss is often called the "specific rotation". This usage is unjustifiable, and we shall use the term "specific rotation" in its proper sense.

9.1. Specific Rotation

A convenient unit in terms of which Faraday rotation may be expressed is a rotation of π in a length of waveguide λ_0 . Thus specific rotation may be defined as the actual rotation per unit length (λ_0 being the unit) expressed as a multiple of this unit. We then have for the specific rotation

$$\varphi_s = \varphi_0/\pi = (\bar{\beta}_+ - \bar{\beta}_-) \dots (72)$$

It will be seen from the results of Section 8 that for the H_{11} mode, in which we are mainly interested, the phase constant curves for positive values of α are always above those for negative values of α , so that $\bar{\beta}_+ > \bar{\beta}_-$, and φ_0 , φ_+ , φ , and φ_s are all positive, corresponding to an anti-clockwise rotation of the field patterns as the wave progresses.

9.2. Non-Reciprocity of Faraday Rotation

Suppose that the polarizing field is directed in the positive z -direction, and consider a forward wave. The specific rotation is

$$\varphi_s = (\bar{\beta}_+ - \bar{\beta}_-)$$

For a backward wave, $\bar{\beta}_+$ and $\bar{\beta}_-$ change sign, so that $(\bar{\beta}_+ - \bar{\beta}_-)$ changes sign. Now, this gives the rotation as observed by an observer looking in the direction of propagation; for an observer looking in the same direction regardless of the direction of travel of the waves, this change of sign does not take place, and the rotation is in the same sense for forward and backward waves. If a wave travels a certain distance along a guide and is rotated through an angle $+\theta$ with respect to the direction of the polarizing field, and if then

the wave is reflected and returns to its starting point, the rotation on return is again $+\theta$, so that at the starting point the returning wave, instead of being rotated back to the orientation of the outgoing wave, has been rotated through an angle $+2\theta$ with respect to the outgoing wave. Thus Faraday rotation is a non-reciprocal effect.

9.3. Results

A large number of results will not be given here, but the general behaviour will be indicated by selecting a few cases. Fig. 21 shows the specific rotation, φ_s , as a function of b/a , for a range of values of a/λ_0 . The value of ϵ is 10, μ is unity, and α is ± 0.5 .

For $a/\lambda_0 = 0.2$, $\bar{\beta}_-$ becomes zero at $b/a = 0.546$, and for values of b/a below this value $\bar{\beta}_-$ is imaginary, so that φ_s is complex. A complex value of Faraday rotation may be interpreted physically by considering the behaviour of the individual helically-polarized waves. The left-helically polarized wave has a real value of $\bar{\beta}_+$, and so can propagate without attenuation. The right-helically polarized wave has $\bar{\beta}_-$ imaginary, and so is evanescent; in an infinitely long system it would not exist, but if it is generated at some point with amplitude equal to that of the left-helically polarized wave, it will have a finite amplitude a finite distance away. The two waves will combine to give a composite wave of the H_{11} type at the point of origin; there will then be linear polarization at the centre of the waveguide. This linear polarization will change progressively as the waves proceed, becoming elliptical with less and less eccentricity. At an infinite distance, the right-helically polarized wave will have died away completely, so that at the centre of the guide there will now be circular polarization. The real part of complex rotation is to be interpreted as a rotation of the axes of the ellipse of polarization in a system which is not infinitely long; the imaginary part represents a progressive change in eccentricity.

For the empty waveguide ($b/a = 0$), when a/λ_0 is sufficiently great for propagation to take place, the Faraday rotation is zero. As b/a increases from zero, φ_s increases, as can be seen in Fig. 21 for the cases $a/\lambda_0 = 0.4$, $a/\lambda_0 = 0.3$. When a/λ_0 decreases below the cut-off value

(0.29303), the curve of φ_s against b/a intersects the b/a axis at the cut-off value of b/a , with finite slope, provided that the bulge has not yet appeared. Below this value of b/a , both $\bar{\beta}_+$ and $\bar{\beta}_-$ are imaginary, so that the Faraday rotation is imaginary. In an infinitely long system, no wave propagates and the situation is trivial. In a finite system, if the two helically-polarized waves are of equal amplitude at $z=0$, then at $z=z$ the amplitudes will in general be different, so that at the centre of the waveguide there will be elliptical polarization of eccentricity varying as z varies, and of amplitude approaching zero as z approaches infinity. As a/λ_0 decreases further, and if ϵ is sufficiently great, the bulge appears and there is a range of values of b/a for which φ_s is complex, as discussed above for the case $a/\lambda_0=0.2$.

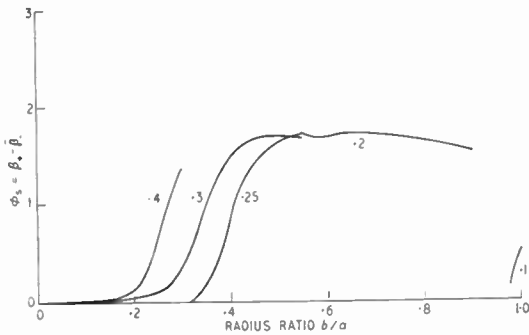


Fig. 21. Curves of specific rotation φ_s against b/a for $\epsilon=10$, $\mu=1$, $\alpha = \pm 0.5$, and stated values of a/λ_0 (H_{11} mode).

It is interesting to notice that φ_s reaches a maximum value for some value of b/a ; for suitable values of a/λ_0 , this occurs at such a value of b/a that the E_{11} mode is cut off. For example, when $a/\lambda_0=0.2$, the maximum value of φ_s occurs when $b/a \cong 0.66$, while the E_{11} mode does not exist for any value of b/a . We also notice that this maximum value of φ_s is not greatly dependent on the value of a/λ_0 , and that the value of b/a is not very critical. For a polarization field well below the value required to give ferromagnetic resonance, we may write, from eqns. (50) and (51),

$$|\alpha| \propto \lambda_0; \mu \cong 1 \quad \dots\dots(73)$$

Examination of Tables 4-13 shows that $\bar{\beta}_+ - \bar{\beta}_-$ is approximately proportional to $|\alpha|$, when all the other parameters are constant. It follows that at the maximum point φ_s is approximately proportional to λ_0 , so that the rotation for a given length of the waveguide-ferrite system, equal to $l\varphi_s/\lambda_0$, is approximately independent of λ_0 , i.e. of frequency. The implications for broadbanding of Faraday rotation devices are obvious.

10. Power Flow

We shall confine our attention here to the case of a waveguide containing a dielectric rod. The power flow across a small area in the transverse plane is given by

$$dP = (\mathbf{E} \times \mathbf{H}^*) \cdot d\mathbf{s} \quad \dots\dots(74)$$

where the asterisk (*) means that $e^{j\omega t}$ is to be replaced by $e^{-j\omega t}$. Equations (42)-(45) give $H_r, H_\theta, E_r,$ and E_θ in terms of H_z and E_z for the ferrite case. Putting $\mu=1$, $\alpha=0$, for the dielectric case, these give

$$\left. \begin{aligned} H_{r1}^* &= \frac{-1}{k_1^2} \left\{ j\beta \cdot \frac{\partial H_{z1}}{\partial r} + \frac{\omega\epsilon_0\rho}{r} \cdot E_{z1} \right\} \\ H_{\theta 1}^* &= \frac{1}{k_1^2} \left\{ \frac{-\beta\rho}{r} \cdot H_{z1} + j\omega\epsilon_0\epsilon \cdot \frac{\partial E_{z1}}{\partial r} \right\} \\ E_{r1} &= \frac{-1}{k_1^2} \left\{ j\beta \cdot \frac{\partial E_{z1}}{\partial r} + \frac{\omega\mu_0\rho}{r} \cdot H_{z1} \right\} \\ E_{\theta 1} &= \frac{1}{k_1^2} \left\{ \frac{-\rho\beta}{r} \cdot E_{z1} + j\omega\mu_0 \cdot \frac{\partial H_{z1}}{\partial r} \right\} \end{aligned} \right\} \dots\dots(75)$$

In the space surrounding the central dielectric, which may contain only air, or another dielectric, the field equations may be obtained from eqns. (75) by putting $\epsilon=1$, when k_1 becomes identical with k_0 . Thus

$$\left. \begin{aligned} H_{rd}^* &= \frac{-1}{k_0^2} \left\{ j\beta \cdot \frac{\partial H_{zd}}{\partial r} + \frac{\omega\epsilon_0\rho}{r} \cdot E_{zd} \right\} \\ H_{\theta d}^* &= \frac{1}{k_0^2} \left\{ \frac{-\rho\beta}{r} \cdot H_{zd} + j\omega\epsilon_0 \cdot \frac{\partial E_{zd}}{\partial r} \right\} \\ E_{rd} &= \frac{-1}{k_0^2} \left\{ j\beta \cdot \frac{\partial E_{zd}}{\partial r} + \frac{\omega\mu_0\rho}{r} \cdot H_{zd} \right\} \\ E_{\theta d} &= \frac{1}{k_0^2} \left\{ \frac{-\rho\beta}{r} \cdot E_{zd} + j\omega\mu_0 \cdot \frac{\partial H_{zd}}{\partial r} \right\} \end{aligned} \right\} \dots\dots(76)$$

Evaluating eqn. (74), we obtain, for the central dielectric, using eqns. (36) and (76)

$$dP_f = \omega\beta k_1^2 \left[\epsilon \epsilon_0 A_p'^2 - \mu_0 B_p'^2 \right] \left[J_{p-1}^2(k_1 r) - \frac{2p}{k_1 r} \cdot J_p(k_1 r) \cdot J_{p-1}(k_1 r) \right] dS - \frac{2jp}{r} \cdot k_1^3 \cdot A_p' B_p' \cdot J_p(k_1 r) \left[J_{p-1}(k_1 r) - \frac{p}{k_1 r} \cdot J_p(k_1 r) \right] dS \dots\dots\dots(77)$$

dP_f being the (complex) power flowing through the element of area dS , lying in the transverse plane. Similarly, using eqns. (20) and (76), the power flow in the medium surrounding the central dielectric is

$$dP_d = \omega\beta k_0^2 dS \left\{ \begin{aligned} & (\epsilon_0 C_p^2 - \mu_0 F_p^2) \left[J_{p-1}^2(k_0 r) - \frac{2p}{k_0 r} \cdot J_p(k_0 r) \cdot J_{p-1}(k_0 r) \right] + \\ & + (\epsilon_0 D_p^2 - \mu_0 G_p^2) \left[Y_{p-1}^2(k_0 r) - \frac{2p}{k_0 r} \cdot Y_p(k_0 r) \cdot Y_{p-1}(k_0 r) \right] + \\ & + 2(\epsilon_0 C_p D_p - \mu_0 G_p F_p) [Y_{p-1}(k_0 r) \cdot J_{p-1}(k_0 r) - \\ & - \frac{p}{k_0 r} (Y_p(k_0 r) \cdot J_{p-1}(k_0 r) + J_p(k_0 r) \cdot Y_{p-1}(k_0 r))] \end{aligned} \right\} - \frac{jp k_0^3 dS}{r} \left\{ \begin{aligned} & 2F_p C_p J_p(k_0 r) \left[J_{p-1}(k_0 r) - \frac{p}{k_0 r} \cdot J_p(k_0 r) \right] + \\ & + 2D_p G_p Y_p(k_0 r) \left[Y_{p-1}(k_0 r) - \frac{p}{k_0 r} \cdot Y_p(k_0 r) \right] + \\ & + (F_p D_p + C_p G_p) \left\{ J_p(k_0 r) \left[Y_{p-1}(k_0 r) - \frac{p}{k_0 r} \cdot Y_p(k_0 r) \right] + \right. \\ & \left. + Y_p(k_0 r) \left[J_{p-1}(k_0 r) - \frac{p}{k_0 r} \cdot J_p(k_0 r) \right] \right\} \end{aligned} \right\} \dots\dots\dots(78)$$

The second terms on the right-hand sides of eqns. (77) and (78) contain j as a factor, but it cannot be concluded that they are imaginary, since the arbitrary constants are, in general, complex. Similarly, the first terms on the right-hand sides are not necessarily real. The right-hand sides must therefore be retained as they stand; when a numerical example is taken, dP_f and dP_d can then be taken to be the real parts of the right-hand sides. This applies also to the expressions which will be obtained below for the total power flow in the guide.

It should be remembered that E_z and H_z both contain the factor $e^{-j\theta}$, so that there is implicit on the right-hand sides of eqns. (77) and (78) a factor $e^{-2j\theta}$, which represents either $\cos^2\theta$ or $\sin^2\theta$. We may thus write

$$\int_{\theta=0}^{2\pi} r \cdot dS = \begin{cases} \pi r \cdot dr & (p \geq 1) \\ 2\pi r \cdot dr & (p = 0) \end{cases}$$

We now require the total power flowing in the waveguide, which may be split into two parts, the total power flowing in the central dielectric and the total power flowing in the medium surrounding it. Integrating eqn. (77), we obtain

$$P_f = \omega\beta k_1^2 \left[\epsilon_0 \epsilon A_p'^2 - \mu_0 B_p'^2 \right] U_p(k_1 b) - jp k_1^2 A_p' B_p' \cdot V_p(k_1 b) \dots\dots\dots(79)$$

where

$$\begin{aligned}
 U_0(k_1b) &= b^2 \left[J_0^2(k_1b) - \frac{2}{k_1b} J_0(k_1b)J_1(k_1b) + J_1^2(k_1b) \right] \\
 U_1(k_1b) &= \frac{b^2}{2} \left[J_0^2(k_1b) + J_1^2(k_1b) \right] + \frac{1}{k_1^2} \left[J_0^2(k_1b) - 1 \right] \\
 U_p(k_1b) &= \frac{b^2}{2} \left[J_{p-2}^2(k_1b) - \frac{2(p-1)}{k_1b} J_{p-2}(k_1b)J_{p-1}(k_1b) + J_{p-1}^2(k_1b) \right] + \\
 (p \geq 2) & \\
 &+ \frac{p}{k_1^2} \left[J_1^2(k_1b) - 1 \right] + \frac{2p}{k_1^2} \sum_{q=1}^{p-1} J_q^2(k_1b)
 \end{aligned}
 \tag{80}$$

and

$$V_p(k_1b) = J_p^2(k_1b) \text{ for } p \geq 1, \quad V_0(k_1b) = 2J_0^2(k_1b)$$

Similarly, for the power in the medium surrounding the central dielectric, on integrating eqn. (78)

$$\begin{aligned}
 P_d &= \omega\beta k_0^2 \left\{ \begin{aligned} &(\epsilon_0 C_p^2 - \mu_0 F_p^2) [U_p(k_0a) - U_p(k_0b)] \\ &+ (\epsilon_0 D_p^2 - \mu_0 G_p^2) [U_p'(k_0a) - U_p'(k_0b)] \\ &+ 2(\epsilon_0 C_p D_p - \mu_0 F_p G_p) [U_p''(k_0a) - U_p''(k_0b)] \end{aligned} \right\} - \\
 &- j p k_0^2 \left\{ \begin{aligned} &F_p C_p [V_p(k_0a) - V_p(k_0b)] \\ &+ D_p G_p [V_p'(k_0a) - V_p'(k_0b)] \\ &+ (F_p D_p + C_p G_p) [V_p''(k_0a) - V_p''(k_0b)] \end{aligned} \right\} \dots\dots\dots(81)
 \end{aligned}$$

where $U'_p, V'_p,$ are obtained from eqns. (80) by replacing J everywhere by Y , and $U''_p, V''_p,$ are obtained from the equations by replacing J^2_n everywhere with $J_n \cdot Y_n,$ and $J_n \cdot J_{n-1}$ everywhere with $0.5(J_{n-1} \cdot Y_n + J_n \cdot Y_{n-1}).$

11. Losses

In Section 8 exact solutions have been given of the characteristic equation for the lossless case, i.e. for real values of the parameters $a/\lambda_0, b/\lambda_0, \epsilon, \mu,$ and $\alpha.$ These results may be extended quite easily to cover the case of small losses by the following method. The characteristic equation may, in principle, be written

$$\bar{\beta} = \bar{\beta}(a/\lambda_0, b/\lambda_0, \epsilon, \mu, \alpha)$$

although it would be very difficult to do this in fact. If a small change in, say, μ takes place, then

$$\bar{\beta} + \delta\bar{\beta} = \bar{\beta}(a/\lambda_0, b/\lambda_0, \epsilon, \mu + \delta\mu, \alpha)$$

where $\delta\bar{\beta} = \frac{\partial \bar{\beta}}{\partial \mu} \cdot \delta\mu.$ It would be very difficult to

calculate $\frac{\partial \bar{\beta}}{\partial \mu}$ by differentiating the characteristic equation; apart from the tedium of the algebra, the result would be an equation for $\partial \bar{\beta} / \partial \mu$ much more complicated and difficult to solve than the characteristic equation itself. However, it is not necessary to go to this trouble; from the results given in Section 8 it is possible to plot rough

graphs of $\bar{\beta}$ against $\mu,$ for constant values of the other parameters. From such graphs values of $\partial \bar{\beta} / \partial \mu$ can be obtained that are sufficiently accurate for practical purposes.

In general, it is found that μ is a complex quantity which may be written $\mu' - j\mu'';$ the imaginary term μ'' represents a magnetic loss. Provided that $\mu'' \ll \mu',$ we may replace $\delta\mu$ by $j\mu''$ in the preceding paragraph, so that $\delta\bar{\beta} = -j\mu'' \frac{\partial \bar{\beta}}{\partial \mu};$ this is imaginary, indicating an exponential decay of the amplitude as the wave progresses along the guide. Losses due to imaginary parts of α and ϵ may be treated in the same way.

There may also be dielectric losses in the medium that surrounds the ferrite in the guide. These may be expressed by an imaginary part in ϵ_0 and by a change in the value of $\epsilon''.$ The characteristic equation (34), can be written in a form such that ϵ_0 does not occur explicitly, only as a product with $\mu_0.$ The imaginary part of ϵ_0 can be thus be expressed as an imaginary part of $\lambda_0,$ hence of $a/\lambda_0,$ and the corresponding

imaginary part of the phase constant can be found in the same way as for imaginary parts of ϵ , μ , and α .

There remains the loss due to the finite conductivity of wave-guide wall. This can be treated in the manner described by Lamont¹², and we shall not discuss it further here. To use Lamont's result, it is necessary to know the magnetic field at the guide wall, which can be obtained from eqns. (46) and (20), once the characteristic equation has been solved and the arbitrary constants evaluated. It is also necessary to know the power flowing in the guide. This is dealt with in Section 10 for the dielectric case; the ferrite case may be treated analogously.

12. Approximate Methods

Because of the difficulty of the exact solution of the characteristic equation, several attempts have been made to obtain approximate solutions. Berk¹⁰ has given a detailed treatment of approximate methods for treating cavities and waveguides containing inhomogeneous and anisotropic media. Suhl and Walker⁷ give two perturbation formulae; one is for a cylindrical guide containing a thin rod of ferrite, regarded as a perturbation of an empty guide, the other for a guide containing a ferrite of arbitrary radius, regarded as a perturbation of a guide containing a dielectric of the same radius and relative permittivity.

These results are of limited value, because in practice the value of radius ratio (b/a) is not small, and the magnetic properties of a ferrite (μ and α) depart considerably from those of a dielectric ($\mu=1, \alpha=0$). However, the case of a thin rod is useful as a check on the exact theory, so a formula will be quoted here. This formula is equivalent to that of Suhl and Walker, but we have repeated the work and give the formula in the notation of the present paper, with μ and α as parameters instead of Suhl's and Walker's σ and p (See Section 1). For the H_{11} mode, the perturbation result is

$$\frac{\delta\bar{\beta}}{\bar{\beta}} = \frac{2.0947}{(1 - 0.08587 \lambda_0^2/a^2)} \left\{ \frac{\epsilon - 1}{\epsilon + 1} + \left[1 - 0.08587 \frac{\lambda_0^2}{a^2} \right] \left(\frac{\mu \pm \alpha - 1}{\mu \pm \alpha + 1} \right) \right\} \dots\dots\dots(82)$$

where $\bar{\beta}$ is the normalized phase constant in the empty guide and $\bar{\beta} + \delta\bar{\beta}$ is the normalized phase constant when the guide contains a thin rod of ferrite.

For the E_{01} mode, there is no contribution due to the magnetic properties of the ferrite, and the result is

$$\frac{\delta\bar{\beta}}{\bar{\beta}} = \frac{0.2718 b^2/a^2 \cdot (\epsilon - 1)}{\left[\frac{a^2}{\lambda_0^2} - 0.1465 \right]} \dots\dots\dots(83)$$

It will be seen that as a/λ_0 approaches the value at which cut-off occurs in the empty guide, $\delta\bar{\beta}/\bar{\beta}$ approaches infinity. Since the derivation of the perturbation formulae depends on the assumption that $\delta\bar{\beta}/\bar{\beta}$ is small, eqns. (82) and (83) are only valid well away from cut-off in the empty guide. This is true of all modes, not only the H_{11} and E_{01} .

Another case we shall find useful is that of a guide containing a dielectric rod of slightly smaller radius, regarded as a perturbation of a guide filled with dielectric. For the H_{11} mode, we obtain

$$\frac{\delta\bar{\beta}}{\bar{\beta}} = \frac{0.4184 \epsilon(\epsilon - 1)(1 - b/a)}{\beta^2} \dots\dots\dots(84)$$

which is again applicable only well away from cut-off.

13. Accuracy and Checks

While there is no way of demonstrating that the values of phase constant that we have calculated are all correct, it is possible to make checks in certain cases. A complete check would require an alternative method of obtaining the results; such a method must be at least as difficult as the one used in the present work. For the case of small ferrite radius, or the nearly filled guide when $\mu=1$ and $\alpha=0$, however, the results obtained may be compared with calculations from the perturbation formulae of Section 12. This has been done, and good agreement has been found; however, the ranges over which perturbation theory is valid are quite small. Another check that we have applied is to calculate the phase constant for the filled guide from Suhl's and Walker's⁷ characteristic equation (eqn. 23 of the present work) and compare

this value with the value obtained from eqn. (34).

We have thus made independent checks of the results for the cases b/a small, $b/a=1$, and b/a slightly less than 1, and we conclude that since the electronic machine has given correct solutions in these cases there is no fault in the programme. It may therefore be assumed that all calculations will be correct, unless there is a machine error or a wrong value of a parameter is supplied to the machine, due to an error in punching cards. Machine errors have occurred due to the extremely complicated behaviour of the determinant of eqn. (34), regarded as a function of $\bar{\beta}$. It has been impossible to foresee all difficulties, but many have been cleared up in the course of the work; however, there have remained some points of difficulty which could not be conveniently allowed for in the programme. Since the machine is not intelligent, it has sometimes been misled in such cases, and has given a spurious result. In some cases we have not been able to discover why this has happened.

Often a spurious point has been detected because it does not lie on a smooth curve drawn through other points; in these cases, a value has been estimated, and the machine set to search for a result in this region. It is possible that some spurious results have been obtained that have not been detected. Every result has been checked graphically against other results, so that there can only be spurious results which differ from the correct result by an amount too small to show up in this way. The error in these cases will usually not be important for most practical purposes—an error sufficiently large to matter would have been detected. We have estimated that less than 5 per cent. of points will have such undetected errors.

There remains the remote possibility that the programme is such as to give correct results for $b/a \sim 0$ and $b/a \sim 1$, but not in between,

although the results it does give lie on a smooth curve. The probability of this has been rendered extremely small by making independent calculations of the phase constant in one or two cases and comparing these results with those given by the machine.

The machine programme was so designed as to give results accurate to ± 1 in the third decimal place; this applies to the phase constant calculations. The values given of b/a for cut-off, or of ϵ or μ for cut-off in the filled guide, are accurate to ± 1 in the last significant figure given. Calculations on the machine have been made either of $\bar{\beta}$ for a given value of b/a , or of b/a for a given value of $\bar{\beta}$. The given values of b/a are always multiples of 0.05 while given values of $\bar{\beta}$ are always odd multiples of 0.125. It is thus easy to see, in the tables, which of a pair of values is the one whose accuracy is ± 0.001 and which is the one to be taken as exact. In the case of the cut-off curves of b/a against ϵ or μ , the given value has always been that of ϵ or μ , and b/a is the calculated value.

14. Acknowledgments

Mr. N. A. Huttly has carried out the programming of the characteristic equation for computation of the phase constant, and has performed the computations of phase constants. The author also wishes to express his gratitude to the Chief Engineer of Marconi's Wireless Telegraph Co., Ltd., for permission to publish this work.

References (Part 3)

7. H. Suhl and L. R. Walker, "Topics in guided wave propagation through gyromagnetic media," *Bell Syst. Tech. J.*, 33, pp. 579-659, 939-86, 1133-94, 1954.
10. A. D. Berk, "Cavities and Waveguides with Inhomogeneous and Anisotropic Media," Massachusetts Institute of Technology Technical Report 284 (February 11, 1955).
12. H. R. L. Lamont, "Waveguides," pp. 44-46 (Methuen, London, 1950).

Table 8 : Phase Constants, $a/\lambda_0=0.3, \mu=0.8$

(a) H_{11} Mode, $\epsilon = 5$

b/a	Values of β				
	a = -0.5	a = -0.25	a = 0	a = +0.25	a = +0.5
0	0.215	0.215	0.215	0.215	0.215
0.1	0.271	0.272	0.273	0.273	0.274
0.2	0.397	0.403	0.408	0.413	0.417
0.3	0.545	0.570	0.594	0.616	0.637
0.4	0.710	0.785	0.873	0.970	1.069
0.5	0.898	1.077	1.280	1.479	1.659
0.6	1.098	1.360	1.612	1.836	2.035
0.7	1.268	1.598	1.820	2.050	2.256

(b) H_{11} Mode, $\epsilon = 10$

b/a	Values of β				
	a = -0.5	a = -0.25	a = 0	a = +0.25	a = +0.5
0	0.215	0.215	0.215	0.215	0.215
0.05	0.233	0.233	0.233	0.233	0.233
0.1	0.283	0.284	0.285	0.286	0.286
0.15	0.352	0.356	0.359	0.361	0.363
0.2	0.434	0.443	0.451	0.459	0.465
0.25	0.527	0.551	0.576	0.601	0.625
0.3	0.641	0.713	0.812	0.936	1.074
0.35	0.809	1.060	1.410	1.739	2.016
0.4	1.100	1.570	1.976	2.309	2.592
0.45	1.439	1.933	2.326	2.654	2.941

(c) H_{11} Mode, $\epsilon = 15$

b/a	Values of β				
	a = -0.5	a = -0.25	a = 0	a = +0.25	a = +0.5
0	0.215	0.215	0.215	0.215	0.215
0.05	0.234	0.234	0.234	0.235	0.235
0.1	0.288	0.289	0.290	0.290	0.291
0.15	0.362	0.366	0.369	0.372	0.374
0.2	0.451	0.464	0.477	0.489	0.500
0.25	0.567	0.622	0.700	0.804	0.925
0.3	0.793	1.242	1.809	2.259	2.615
0.35	1.436	2.114	2.622	3.034	3.387
0.4	1.966	2.574	3.051	3.454	3.810

(d) E_{01} Mode, $\epsilon = 5$

b/a	Values of β	
	a = 0	a = ± 0.5
0.19	0	0
0.20	0	0
0.2	0.178	0
0.3	0.572	0.538
0.4	0.718	0.673
0.5	0.809	0.753
0.6	0.884	0.829
0.7	0.965	0.970

(e) E_{01} Mode, $\epsilon = 10$

b/a	Values of β		
	a = 0	a = ± 0.25	a = ± 0.5
0.12	0	0	0
0.15	0.436	0.431	0.416
0.2	0.645	0.639	0.622
0.25	0.756	0.749	0.728
0.3	0.828	0.819	0.794
0.35	0.882	0.872	0.844
0.4	0.927	0.919	0.894
0.45	0.971	0.996	1.046

Table 9 : Phase Constants, $a/\lambda_0=0.3, \mu=1$

(a) H_{11} Mode, $\epsilon = 0.5$

b/a	Values of β		
	a = -0.5	a = 0	a = +0.5
0	0.215	0.215	0.215
0.10	0.178	0.179	0.180
0.15	0.123	0.125	0.126
0.18	0	0	0

(b) H_{11} Mode, $\epsilon = 1$

b/a	Values of β		
	a = -0.5	a = 0	a = +0.5
0	0.215	0.215	0.215
0.1	0.212	0.215	0.215
0.2	0.208	0.215	0.217
0.3	0.202	0.215	0.222
0.4	0.196	0.215	0.228
0.5	0.188	0.215	0.234
0.6	0.181	0.215	0.241
0.7	0.174	0.215	0.247
0.8	0.168	0.215	0.252
0.9	0.163	0.215	0.254
1	0.158	0.215	0.254

(c) H_{11} Mode, $\epsilon = 3$

b/a	Values of β				
	a = -0.5	a = -0.25	a = 0	a = +0.25	a = +0.5
0	0.215	0.215	0.215	0.215	0.215
0.1	0.257	0.258	0.259	0.259	0.260
0.2	0.351	0.358	0.363	0.367	0.370
0.3	0.437	0.475	0.491	0.506	0.518
0.4	0.537	0.596	0.634	0.670	0.706
0.5	0.648	0.715	0.786	0.860	0.936
0.6	0.730	0.829	0.940	1.056	1.173
0.7	0.807	0.937	1.079	1.224	1.366
0.8	0.883	1.038	1.197	1.355	1.507
0.9	0.966	1.138	1.302	1.460	1.611
1	1.073	1.271	1.430	1.575	1.714

(d) H_{11} Mode, $\epsilon = 5$

b/a	Values of β						
	a = -0.75	a = -0.5	a = -0.25	a = 0	a = +0.25	a = +0.5	a = +0.75
0	0.215	0.215	0.215	0.215	0.215	0.215	0.215
0.05	0.229	0.229	0.229	0.230	0.230	0.230	0.230
0.1	0.269	0.270	0.271	0.272	0.273	0.273	0.274
0.15	0.322	0.327	0.330	0.333	0.335	0.336	0.338
0.2	0.381	0.390	0.398	0.404	0.409	0.414	0.418
0.25	0.440	0.457	0.472	0.485	0.496	0.506	0.515
0.3	0.497	0.524	0.550	0.575	0.598	0.620	0.640
0.35	0.550	0.591	0.633	0.678	0.724	0.770	0.814
0.4	0.599	0.657	0.724	0.801	0.887	0.978	1.068
0.45	0.644	0.723	0.822	0.947	1.091	1.239	1.379
0.5	0.687	0.788	0.929	1.110	1.306	1.493	1.662
0.55	0.727	0.855	1.040	1.268	1.494	1.699	1.883
0.6	0.766	0.920	1.166	1.404	1.645	1.860	2.052
0.65	0.805	0.985	1.242	1.516	1.764	1.984	2.182
0.7	0.845	1.048	1.326	1.607	1.858	2.082	2.284
0.75	0.887	1.108	1.397	1.681	1.934	2.160	2.364
0.8	0.932	1.169	1.458	1.741	1.995	2.222	2.429
0.85		1.231				2.273	

PROPAGATION IN CYLINDRICAL WAVEGUIDES CONTAINING FERRITE

Table 9 (cont.)

(e) H_{11} Mode, $\epsilon = 10$

b/a	Values of β						
	a = -0.75	a = -0.5	a = -0.25	a = 0	a = +0.25	a = +0.5	a = +0.75
0	0.215	0.215	0.215	0.215	0.215	0.215	0.215
0.05	0.232	0.233	0.233	0.233	0.233	0.233	0.233
0.1	0.280	0.282	0.283	0.284	0.285	0.286	0.286
0.15	0.344	0.349	0.353	0.356	0.359	0.361	0.363
0.2	0.414	0.425	0.436	0.445	0.453	0.460	0.466
0.25	0.484	0.508	0.531	0.556	0.580	0.602	0.623
0.250						0.625	0.625
0.255						0.625	0.625
0.263						0.625	0.625
0.273				0.625	0.625	0.625	0.625
0.288						0.875	0.875
0.295						0.875	0.875
0.3	0.553	0.597	0.653	0.726	0.816	0.919	1.019
0.306						1.125	1.125
0.307						0.875	0.875
0.315						1.125	1.125
0.319				0.875	1.125	1.375	1.375
0.325						1.625	1.625
0.329						1.875	1.875
0.330						1.625	1.625
0.331						1.625	1.625
0.344						1.625	1.875
0.345						1.875	1.875
0.347						1.875	1.875
0.35	0.619	0.699	0.842	1.094	1.411	1.705	1.955
0.352				1.125	1.375	1.625	1.625
0.356			0.875				2.125
0.360							2.125
0.361						1.875	1.875
0.365						1.625	1.625
0.375						1.375	1.375
0.380						2.125	2.125
0.381						2.125	2.125
0.387						1.875	1.875
0.393			1.125	1.617	1.994	2.309	2.579
0.4	0.684	0.828	1.172	1.617	1.994	2.309	2.579
0.400				1.625			2.625
0.404						2.125	2.125
0.407						2.125	2.125
0.415						2.125	2.125
0.427						1.375	1.375
0.432						1.875	1.875
0.437						1.875	1.875
0.441						2.625	2.625
0.45	0.749	1.004	1.524	1.985	2.357	2.674	2.953
0.453						2.375	2.375
0.467						1.625	1.625
0.476						2.125	2.125
0.482						3.125	3.125
0.490						2.875	2.875
0.5	0.816	1.208	1.780	2.229	2.597	2.916	3.201
0.55	0.888	1.392	2.099	2.399	2.607	2.875	3.125
0.6		1.536	2.524	2.619	3.312		
0.65		1.648	2.639	2.692	3.388		
0.7		1.737	2.692		3.448		
0.75		1.811	2.750		3.496		
0.8		1.90	2.795		3.535		
0.85							

(f) H_{11} Mode, $\epsilon = 15$

b/a	Values of β						
	a = -0.75	a = -0.5	a = -0.25	a = 0	a = +0.25	a = +0.5	a = +0.75
0	0.215	0.215	0.215	0.215	0.215	0.215	0.215
0.05	0.234	0.234	0.234	0.234	0.235	0.235	0.235
0.1	0.285	0.286	0.288	0.289	0.290	0.290	0.290
0.15	0.352	0.358	0.362	0.366	0.370	0.372	0.375
0.2	0.426	0.440	0.454	0.467	0.479	0.489	0.499
0.228						0.625	0.625
0.232						0.625	0.625
0.238						0.625	0.625
0.248						0.625	0.625
0.25	0.502	0.534	0.575	0.625	0.670	0.774	0.842
0.251						0.875	0.875
0.256						0.875	0.875
0.261						0.875	0.875
0.264			0.625			0.875	0.875
0.265						0.875	0.875
0.267						1.125	1.125
0.268						1.125	1.125
0.273						1.375	1.375
0.274						1.375	1.375
0.276						1.125	1.125
0.279					0.875	1.125	1.125
0.281						1.625	1.625
0.285						1.375	1.375
0.286						1.875	1.875
0.288						1.875	1.875
0.293					1.125	1.625	1.625
0.294						1.625	1.625
0.297						2.125	2.125
0.3	0.579	0.654	0.836	1.275	1.783	2.193	2.524
0.303			0.875	1.375	1.875	2.125	2.524
0.304						2.375	2.625
0.307						2.375	2.375
0.315						1.625	1.625
0.316						2.125	2.125
0.320						2.625	2.625
0.322				1.125	1.875	2.375	2.375
0.329						2.875	2.875
0.330						2.875	2.875
0.337						2.875	2.875
0.338				1.375			
0.345					2.125	2.625	
0.348						2.625	
0.349						3.077	3.378
0.35	0.657	0.867	1.543	2.166	2.644	3.077	3.378
0.351		0.875					
0.356				1.625			
0.357						2.375	3.125
0.368						2.875	
0.372						2.875	
0.373						3.625	
0.378				1.875			
0.382					1.125	1.875	
0.398					1.281	2.066	2.625
0.4	0.743	1.281	2.066	2.625	3.092	3.484	3.833
0.404					3.125		
0.407				2.125			
0.410				1.375			
0.440					1.625		
0.445					2.375		
0.449					2.378		
0.45	0.845	1.651	2.378	2.920	3.370	3.764	4.120
0.493		1.875					
0.5	0.970	1.903	2.584	3.111	3.559	3.956	4.317
0.504				3.125			

(g) E_{01} Mode, $\epsilon = 5$

b/a	Values of β		
	a = 0	a = ±0.25	a = ±0.5
0.189	0	0	0
0.190			
0.192			
0.2	0.206	0.197	0.170
0.3	0.595	0.598	0.567
0.4	0.751	0.741	0.713
0.5	0.858	0.846	0.809
0.6	0.958	0.946	0.908
0.7	1.077	1.079	1.079
0.8	1.235	1.264	1.333

(h) E_{01} Mode, $\epsilon = 10$

b/a	Values of β		
	a = 0	a = ±0.25	a = ±0.5
0.118	0	0	0
0.119			
0.15	0.449	0.445	0.433
0.2	0.661	0.656	0.642
0.25	0.776	0.770	0.752
0.3	0.853	0.846	0.824
0.35	0.915	0.906	0.880
0.4	0.971	0.962	0.937
0.45	1.029	1.054	
0.5	1.100	1.199	
0.55	1.193	1.712	
0.6	1.324		
0.65	1.502		
0.7	1.705		
0.75	1.901		
0.8	2.074		
0.85	2.222		

(i) E_{01} Mode, $\epsilon = 15$

b/a	Values of β		
	a = 0	a = ±0.25	a = ±0.5
0.092	0	0	0
0.093			
0.094			
0.15	0.649	0.645	0.633
0.2	0.797	0.792	0.777
0.25	0.885	0.878	0.858
0.3	0.950	0.942	0.918
0.35	1.011	1.032	
0.4	1.082	1.048	0.978
0.45	1.187	1.133	1.029
0.5	1.382	1.267	1.087

(j) E_{11} Mode, $\epsilon = 10$

b/a	Values of β		
	a = -0.5	a = 0	a = +0.5
0.400	0	0	0
0.413			
0.505	0	0	0
0.45			0.405
0.5			0.561
0.55	0.520		0.575
0.6	0.736		0.786
0.65	0.968		0.921
0.7	1.267		1.075
0.75	1.572		1.256
0.8	1.90		1.432
0.85	2.061		1.590

(k) H_{02} Mode, $\epsilon = 10$

b/a	Values of β	
	a = 0	a = ±0.5
0.413	0	0
0.45	0.893	1.102
0.5	1.335	1.515
0.55	1.630	1.871
0.6	1.848	2.159
0.65	2.015	2.395
0.7	2.145	2.587
0.75	2.245	2.743
0.8	2.321	2.869
0.85	2.374	2.971

(l) H_{21} Mode, $\epsilon = 10$

b/a	Values of β		
	a = -0.5	a = 0	a = +0.5
0.72	0	0	0
0.75	0.587	0.293	0.141
0.8	0.938	0.546	0.272

Table 10 : Phase Constants, $a/\lambda_0=0.3, \mu=1.2$

(a) H_{11} Mode, $\epsilon = 5$

b/a	Values of β				
	a = -0.5	a = -0.25	a = 0	a = +0.25	a = +0.5
0	0.215	0.215	0.215	0.215	0.215
0.05	0.269	0.270	0.271	0.272	0.273
0.1	0.383	0.392	0.399	0.405	0.410
0.2	0.503	0.530	0.555	0.579	0.602
0.3	0.610	0.669	0.738	0.815	0.897
0.4	0.704	0.813	0.961	1.139	1.324
0.5	0.791	0.960	1.194	1.443	1.673
0.6	0.876	1.099	1.381	1.652	1.995
0.7					

(b) H_{11} Mode, $\epsilon = 10$

b/a	Values of β				
	a = -0.5	a = -0.25	a = 0	a = +0.25	a = +0.5
0	0.215	0.215	0.215	0.215	0.215
0.05	0.232	0.233	0.233	0.233	0.233
0.1	0.281	0.282	0.284	0.284	0.285
0.15	0.345	0.350	0.354	0.357	0.360
0.2	0.416	0.428	0.438	0.446	0.454
0.25	0.489	0.512	0.536	0.559	0.582
0.3	0.561	0.607	0.664	0.734	0.812
0.35	0.632	0.720	0.871	1.106	1.378
0.4	0.704	0.874	1.230	1.640	1.990
0.45	0.779	1.087	1.591	2.021	2.377

(c) H_{11} Mode, $\epsilon = 15$

b/a	Values of β				
	a = -0.5	a = -0.25	a = 0	a = +0.25	a = +0.5
0	0.215	0.215	0.215	0.215	0.215
0.05	0.234	0.234	0.234	0.234	0.235
0.1	0.285	0.287	0.288	0.289	0.290
0.15	0.353	0.359	0.363	0.366	0.370
0.2	0.429	0.443	0.456	0.468	0.480
0.25	0.508	0.541	0.583	0.633	0.688
0.3	0.590	0.676	0.869	1.021	1.474
0.35	0.679	0.949	1.615	2.187	2.638
0.4	0.786	1.426	2.144	2.680	3.121

(d) E_{01} Mode, $\epsilon = 5$

b/a	Values of β	
	a = 0	a = ± 0.5
0.19	0	0
0.2	0.231	0.205
0.3	0.618	0.592
0.4	0.786	0.752
0.5	0.911	0.866
0.6	1.040	0.992
0.7	1.202	1.200

(e) E_{01} Mode, $\epsilon = 10$

b/a	Values of β		
	a = 0	a = ± 0.25	a = ± 0.5
0.12	0	0	0
0.1	0.449	0.459	0.463
0.2	0.660	0.673	0.677
0.25	0.775	0.791	0.796
0.3	0.854	0.874	0.881
0.35	0.918	0.943	0.951
0.4	0.987	1.013	1.022
0.45	1.1(0)	1.125	1.104

Table 11 : Phase Constants, $a/\lambda_0=0.4, \mu=0.8$

(a) H_{11} Mode, $\epsilon = 5$

b/a	Values of β				
	a = -0.5	a = -0.25	a = 0	a = +0.25	a = +0.5
0	0.681	0.681	0.681	0.681	0.681
0.05	0.685	0.685	0.686	0.686	0.686
0.1	0.699	0.703	0.703	0.705	0.707
0.15	0.722	0.729	0.735	0.740	0.745
0.2	0.754	0.772	0.786	0.800	0.811
0.25	0.801	0.834	0.867	0.901	0.934
0.3	0.860	0.926	1.002	1.087	1.174
0.35	0.935	1.060	1.213	1.374	1.527
0.4	1.030	1.232	1.449	1.651	1.893
0.45	1.139	1.399	1.644	1.861	2.054

(b) H_{11} Mode, $\epsilon = 10$

b/a	Values of β				
	a = -0.5	a = -0.25	a = 0	a = +0.25	a = +0.5
0	0.681	0.681	0.681	0.681	0.681
0.05	0.686	0.687	0.687	0.687	0.688
0.1	0.704	0.707	0.709	0.711	0.713
0.15	0.737	0.747	0.755	0.763	0.770
0.2	0.782	0.823	0.877	0.893	0.929
0.25	0.896	1.035	1.253	1.512	1.758
0.3	1.162	1.593	1.995	2.313	2.594

(c) H_{11} Mode, $\epsilon = 15$

b/a	Values of β				
	a = -0.5	a = -0.25	a = 0	a = +0.25	a = +0.5
0	0.681	0.681	0.681	0.681	0.681
0.05	0.686	0.687	0.687	0.688	0.688
0.1	0.707	0.710	0.713	0.715	0.717
0.15	0.746	0.759	0.772	0.784	0.795
0.2	0.833	0.921	1.078	1.322	1.601
0.25	1.127	1.896	2.417	2.835	3.187

(d) E_{01} Mode, $\epsilon = 5$

b/a	Values of β	
	a = 0	a = ± 0.5
0	0.290	0.290
0.05	0.344	0.344
0.1	0.466	0.464
0.15	0.588	0.582
0.2	0.685	0.673
0.25	0.756	0.738
0.3	0.811	0.787
0.35	0.854	0.826
0.4	0.891	0.864
0.45	0.926	0.918

(e) E_{01} Mode, $\epsilon = 10$

b/a	Values of β		
	a = 0	a = ± 0.25	a = ± 0.5
0	0.290	0.290	0.290
0.05	0.405	0.405	0.405
0.1	0.613	0.612	0.609
0.15	0.768	0.765	0.758
0.2	0.869	0.865	0.853
0.25	0.945	0.939	0.922
0.3	1.005	1.011	0.995

Table 12 : Phase Constants, $a/\lambda_0=0.4, \mu=1$

(a) H_{11} Mode, $\epsilon = 0.5$

b/a	Values of β			
	a = -0.5	a = 0	a = +0.5	a = 0
0	0.681	0.681	0.681	0.681
0.1	0.666	0.670	0.673	0.673
0.15	0.650	0.658	0.664	0.664
0.2	0.628	0.642	0.651	0.651
0.25	0.603	0.622	0.635	0.635
0.3	0.573	0.597	0.614	0.614
0.35	0.539	0.569	0.589	0.589
0.4	0.537	0.537	0.539	0.539
0.45	0.460	0.501	0.524	0.524
0.5	0.416	0.460	0.497	0.497
0.55	0.369	0.417	0.456	0.456
0.6	0.321	0.370	0.411	0.411
0.65	0.271	0.320	0.361	0.361
0.7	0.222	0.268	0.306	0.306
0.75	0.171	0.212	0.245	0.245
0.8	0.117	0.148	0.173	0.173
0.85	0.043	0.053	0.065	0.065
0.86	0	0	0	0

(b) H_{11} Mode, $\epsilon = 1$

b/a	Values of β		
	a = -0.5	a = 0	a = +0.5
0	0.681	0.681	0.681
0.1	0.676	0.681	0.683
0.2	0.663	0.681	0.692
0.3	0.646	0.681	0.706
0.4	0.626	0.681	0.723
0.5	0.604	0.681	0.741
0.6	0.581	0.681	0.756
0.7	0.559	0.681	0.761
0.8	0.539	0.681	0.751
0.9	0.521	0.681	0.717
1	0.506	0.681	

(c) H_{11} Mode, $\epsilon = 5$

b/a	Values of β						
	a = -0.75	a = -0.5	a = -0.25	a = 0	a = +0.25	a = +0.5	a = +0.75
0	0.681	0.681	0.681	0.681	0.681	0.681	0.681
0.05	0.683	0.684	0.685	0.685	0.686	0.686	0.686
0.1	0.692	0.696	0.699	0.702	0.704	0.705	0.707
0.15	0.706	0.716	0.724	0.731	0.736	0.741	0.746
0.2	0.724	0.743	0.760	0.775	0.789	0.802	0.813
0.25	0.744	0.776	0.808	0.840	0.873	0.905	0.936
0.3	0.766	0.815	0.872	0.939	1.014	1.094	1.174
0.35	0.789	0.859	0.957	1.085	1.233	1.383	1.523
0.4	0.812	0.910	1.064	1.266	1.474	1.666	1.840
0.45	0.835	0.966	1.183	1.439	1.673	1.882	2.069

PROPAGATION IN CYLINDRICAL WAVEGUIDES CONTAINING FERRITE

Table 12 (cont.)

(d) H_{11} Mode, $\epsilon = 10$

b/a	Values of $r\beta$						
	a = -0.75	a = -0.5	a = -0.25	a = 0	a = +0.25	a = +0.5	a = +0.75
0	0.681	0.681	0.681	0.681	0.681	0.681	0.681
0.05	0.684	0.685	0.686	0.687	0.687	0.687	0.688
0.1	0.697	0.701	0.705	0.708	0.710	0.712	0.713
0.15	0.717	0.729	0.739	0.748	0.757	0.764	0.770
0.189							0.875
0.195							0.875
0.2	0.743	0.769	0.797	0.828	0.861	0.893	0.923
0.2				0.875	0.875		
0.203							1.125
0.216							1.125
0.222							1.125
0.229							1.125
0.236							1.375
0.237			0.875				1.375
0.240					1.125		1.375
0.244							1.375
0.247							1.625
0.25	0.774	0.829	0.916	1.056	1.255	1.476	1.683
0.257				1.125	1.375	1.625	1.875
0.258							1.875
0.270							2.125
0.272							1.625
0.278					1.375		2.375
0.284							2.125
0.285							2.375
0.287			1.125				2.375
0.289							1.875
0.298							2.004
0.3	0.810	0.929	1.225	1.625	2.004	2.303	2.582
0.323				1.625	2.004		2.582
0.35				2.084			2.582
0.356							2.125
0.4							2.354
0.404							2.375
0.45							2.375
0.5							2.625
0.55							2.740
0.6							2.807
0.65							2.858
0.7							2.899
0.75							2.931
0.8							2.997
0.85							2.978
0.9							2.995
0.95							3.009
1.0							3.018
1.0							3.076

(e) H_{11} Mode, $\epsilon = 15$

b/a	Values of β						
	a = -0.75	a = -0.5	a = -0.25	a = 0	a = +0.25	a = +0.5	a = +0.75
0	0.681	0.681	0.681	0.681	0.681	0.681	0.681
0.05	0.685	0.686	0.687	0.687	0.688	0.688	0.688
0.1	0.699	0.703	0.707	0.710	0.713	0.715	0.717
0.15	0.721	0.735	0.749	0.762	0.774	0.785	0.794
0.170							0.875
0.174							0.875
0.180							0.875
0.190				0.875			0.875
0.191							1.125
0.195							1.125
0.199							1.125
0.2	0.752	0.789	0.844	0.932	1.065	1.236	1.410
0.2							1.125
0.203							1.375
0.204							1.625
0.207							1.375
0.209							1.625
0.210							1.375
0.212							1.625
0.214							2.125
0.215							1.125
0.216							1.625
0.219							1.625
0.220							2.125
0.222							2.125
0.226							1.375
0.227							1.875
0.228							2.625
0.228							2.375
0.230							2.375
0.236							1.625
0.236							2.125
0.237							2.625
0.240							2.625
0.246							1.875
0.248							2.625
0.25	0.792	0.910	1.239	1.543	2.208	2.843	3.125
0.25							1.125
0.251							1.375
0.266							1.625
0.281							1.375
0.3	0.845	1.125	1.313	1.4625			1.375
0.305							2.072
0.305							3.484

(i) H_{01} Mode, $\epsilon = 10$

b/a	Values of β	
	a = 0	a = ±0.5
0.288	0	0
0.3	0.511	0.515
0.35	1.200	1.239
0.4	1.615	1.806
0.45	1.905	2.189

(f) E_{01} Mode, $\epsilon = 5$

b/a	Values of β		
	a = 0	a = ±0.25	a = ±0.5
0	0.290	0.290	0.290
0.05	0.345	0.345	0.344
0.1	0.467	0.467	0.465
0.15	0.593	0.591	0.587
0.2	0.693	0.691	0.683
0.25	0.770	0.766	0.754
0.3	0.830	0.824	0.808
0.35	0.880	0.873	0.854
0.4	0.926	0.919	0.899
0.45	0.972	0.969	0.961

(g) E_{01} Mode, $\epsilon = 10$

b/a	Values of β		
	a = 0	a = ±0.25	a = ±0.5
0	0.290	0.290	0.290
0.05	0.405	0.405	0.404
0.1	0.609	0.608	0.605
0.15	0.739	0.736	0.748
0.2	0.853	0.849	0.836
0.25	0.920	0.914	0.897
0.3	0.978	0.973	0.959
0.4			0.995
0.45	1.260		1.041

(h) E_{01} Mode, $\epsilon = 15$

b/a	Values of β		
	a = 0	a = ±0.25	a = ±0.5
0	0.290	0.290	0.290
0.05	0.439	0.439	0.457
0.1	0.703	0.701	0.696
0.15	0.844	0.840	0.830
0.2	0.927	0.922	0.906
0.25	0.992	0.990	0.983
0.3	1.065	1.040	

(j) E_{11} Mode, $\epsilon = 10$

b/a	Values of β		
	a = -0.5	a = 0	a = +0.5
0.27			0
0.288		0	
0.3		0.373	0.464
0.35	0	0.634	0.618
0.4	0.995	0.735	0.692
0.45	0.802	0.823	0.748

Table 13: Phase Constants, $a/\lambda_0 = 0.4$, $\mu = 1.2$

(a) H_{11} Mode, $\epsilon = 5$

b/a	Values of β				
	a = -0.5	a = -0.25	a = 0	a = +0.25	a = +0.5
0	0.681	0.681	0.681	0.681	0.681
0.05	0.683	0.684	0.685	0.685	0.685
0.1	0.693	0.697	0.700	0.702	0.704
0.15	0.708	0.717	0.725	0.732	0.737
0.2	0.728	0.746	0.763	0.778	0.791
0.25	0.750	0.782	0.814	0.846	0.878
0.3	0.775	0.825	0.884	0.951	1.023
0.35	0.801	0.876	0.978	1.105	1.245
0.4	0.828	0.936	1.098	1.295	1.492
0.45	0.855	1.002	1.229	1.473	1.697

(b) H_{11} Mode, $\epsilon = 10$

b/a	Values of β				
	a = -0.5	a = -0.25	a = 0	a = +0.25	a = +0.5
0	0.681	0.681	0.681	0.681	0.681
0.05	0.685	0.686	0.686	0.687	0.687
0.1	0.598	0.702	0.705	0.708	0.710
0.15	0.719	0.731	0.741	0.750	0.758
0.2	0.748	0.774	0.803	0.833	0.863
0.25	0.784	0.843	0.933	1.067	1.234
0.3	0.826	0.967	1.277	1.532	1.999

(c) H_{11} Mode, $\epsilon = 15$

b/a	Values of β				
	a = -0.5	a = -0.25	a = 0	a = +0.25	a = +0.5
0	0.681	0.681	0.681	0.681	0.681
0.05	0.685	0.686	0.687	0.687	0.688
0.1	0.700	0.704	0.708	0.711	0.713
0.15	0.724	0.738	0.751	0.763	0.775
0.2	0.758	0.798	0.855	0.935	1.033
0.25	0.806	0.952	1.399	1.950	2.401

Table 13 (cont.)

b/a	Values of β	
	$\alpha = 0$	$\alpha = \pm 0.5$
0.0	0.290	0.290
0.05	0.345	0.345
0.1	0.469	0.467
0.15	0.597	0.593
0.2	0.702	0.693
0.25	0.784	0.770
0.3	0.850	0.831
0.35	0.909	0.884
0.4	0.966	0.938
0.45	1.027	1.013

b/a	Values of β		
	$\alpha = 0$	$\alpha = \pm 0.25$	$\alpha = \pm 0.5$
0	0.290	0.290	0.290
0.05	0.404	0.404	0.404
0.1	0.605	0.604	0.600
0.15	0.750	0.747	0.738
0.2	0.839	0.834	0.820
0.25	0.899	0.893	0.875
0.3	0.946	0.941	0.929

Table 14: Phase Constants, $\epsilon = 10$, $\mu = 1$, H_{11} Mode

b/a	Values of β		
	$\alpha = -0.5$	$\alpha = 0$	$\alpha = +0.5$
0.546	0	0	0
0.6	0.529	1.425	2.219
0.65	0.777	1.758	2.903
0.7	0.989	1.980	2.706
0.75	1.169	2.142	2.858
0.8	1.324	2.266	2.975
0.85	1.463	2.365	3.068
0.9	1.603	2.452	3.144

b/a	Values of β		
	$\alpha = -0.5$	$\alpha = 0$	$\alpha = +0.5$
0.32	0	0	0
0.35	0.260	0.326	0.430
0.4	0.451	0.718	1.311
0.45	0.617	1.289	
0.5	0.793	1.724	2.437
0.55	0.987	2.011	2.712

b/a	Values of β		
	$\alpha = -0.5$	$\alpha = 0$	$\alpha = +0.5$
0.20	0	0	0
0.25	0.291	0.314	0.335
0.3	0.423	0.492	0.574
0.35	0.545	0.750	1.144
0.4	0.674	1.240	1.933
0.45	0.828	1.711	2.432
0.5	1.015	2.025	2.718
0.55	1.211	2.239	2.930

b/a	Values of β		
	$\alpha = -0.5$	$\alpha = 0$	$\alpha = +0.5$
0	0	0	0
0.05	0.092	0.092	0.092
0.1	0.185	0.187	0.188
0.15	0.278	0.284	0.288
0.2	0.370	0.386	0.399
0.25	0.462	0.504	0.543
0.3	0.557	0.668	0.823
0.35	0.662	0.997	1.567
0.4	0.789	1.524	2.218
0.45	0.956	1.918	2.609
0.5	1.157	2.179	2.86
0.55	1.345	2.360	

b/a	Values of β		
	$\alpha = -0.5$	$\alpha = 0$	$\alpha = +0.5$
0	0.115	0.115	0.115
0.05	0.147	0.148	0.148
0.1	0.218	0.219	0.221
0.15	0.300	0.306	0.311
0.2	0.387	0.404	0.417
0.25	0.476	0.519	0.561
0.3	0.569	0.684	0.849
0.35	0.672	1.024	1.607
0.4	0.800	1.551	2.245
0.45	0.970	1.998	2.628
0.5	1.172	2.193	2.88
0.55	1.399	2.371	

b/a	Values of β		
	$\alpha = -0.5$	$\alpha = 0$	$\alpha = +0.5$
0	0.215	0.215	0.215
0.05	0.233	0.233	0.233
0.1	0.282	0.284	0.286
0.15	0.349	0.356	0.361
0.2	0.425	0.443	0.460
0.25	0.508	0.556	0.602
0.3	0.597	0.726	0.919
0.35	0.699	1.094	1.705
0.4	0.828	1.617	2.309
0.45	1.004	1.985	2.674
0.5	1.208	2.229	2.916
0.55	1.392	2.399	3.087

b/a	Values of β			b/a	Values of β		
	$\alpha = -0.5$	$\alpha = 0$	$\alpha = +0.5$		$\alpha = -0.5$	$\alpha = 0$	$\alpha = +0.5$
0	0.681	0.681	0.681	0.3	0.929	1.637	2.313
0.05	0.685	0.687	0.687	0.35	2.084		
0.1	0.701	0.708	0.712	0.4	2.354		
0.15	0.729	0.748	0.764	0.45	2.529		
0.2	0.769	0.828	0.899	0.5	2.631		
0.25	0.829	1.056	1.476	0.55	2.740		

ERRATA :

Part 1 :

Page 603, right hand column, 3rd line from bottom—

For $(uE_{ta})_0$ read $(u'E_{ta})_0$

Page 605, equation (41), the determinant, bottom row—

Column 2 For $j\psi \sqrt{\frac{\mu_0}{\epsilon_0}} J_p'(k_0b)$ read $j\psi \sqrt{\frac{\mu_0}{\epsilon_0}} J_p(k_1b)$.

Column 3 For $-Y_p'(k_0b)$ read $-J_p'(k_0b)$.

Column 4 For $-Y_p(k_0b)$ read $-Y_p'(k_0b)$.

Part 2 :

Page 679, Section 7.4, fourth line—

Reference 11 should be indicated.

Page 686, caption to Fig. 16—

For E_{0q} read E_{pq}

APPLICANTS FOR ELECTION AND TRANSFER

As a result of its November meeting the Membership Committee recommended to the Council the following elections and transfers.

In accordance with a resolution of Council, and in the absence of any objections, the election and transfer of the candidates to the class indicated will be confined fourteen days after the date of circulation of this list. Any objections or communications concerning these elections should be addressed to the General Secretary for submission to the Council.

Direct Election to Member

BUCKLEY, Rear Admiral Kenneth Robertson, R.N. *Lee-on-the-Solent*.
LEWIS, John Henry Walter. *Jersey*.
STANLEY, John Orr, M.A. *Newmarket*.

Transfer from Associate Member to Member

GARNER, Raymond Hubert, B.Sc.(Eng.). *Cambuslang*.
LOWE, Wing Cdr. Francis Cyril, R.A.F. *Buckhurst Hill*.

Transfer from Associate to Member

RENWICK, William, B.Sc. *Romsey*.

Direct Election to Associate Member

COLLIER, Commander Thomas Anthony, R.N. *Bournemouth*.
DENBY, William. *Hinchley Wood*.
GAMBLING, William Alexander, B.Sc., Ph.D. *Chandler's Ford*.
HARMSWORTH, Allan, B.Sc.(Eng.). *Bolton*.
HUNTER, Arthur James, B.Sc. *Hatfield*.
MACKERETH, Commander William Winter, R.N. *Singapore*.
MEDCALF, Charles Leonard Hume, B.Sc. *St. Albans*.
PIKE, Commander William James, R.N. *Belfast*.
PUGSLEY, Donald John Davey. *Cambridge*.
TRANTER, Anthony, B.Sc.(Eng.). *Cheltenham*.

Transfer from Associate to Associate Member

CALCROFT, Norman. *Welling*.
HAWORTH, John. *Salisbury, Southern Rhodesia*.
LIPSCHITZ, Gerhard Gad. *Haija*.
ROGERS, Major Donald Thomas Chaplin, R.E.M.E. *Anglesey*.
STANTON, Donald. *Coventry*.

Transfer from Graduate to Associate Member

BANERJI, Ranan Behari, M.Sc. *Cleveland, Ohio*.
BECKLEY, Norman James. *Wembley*.
CLARKE, Peter. *London, W.3*.
DANCE, Philip Ernest. *Crawley*.
HENOCO, Cecil. *Haywards Heath*.
LOWRY, Peter. *London, S.E.27*.
MELINN, Capt. Michael Gerard, Eireann Army. *Balbriggan, Co. Dublin*.

Transfer from Student to Associate Member

HUDSON, Harry. *Bishop's Stortford*.
STEVENS, Lionel. *Manchester*.

Direct Election to Associate

BURTON, Ernest Douglas. *Reading*.
CUNNINGHAM, John. *London, W.1*.
LAUGHTON, Commander John Knox, R.N. *Haslemere*.
MULLAN, John. *Carnwath*.
NURAL HAQUE, A.B.M. *Shonaimuri, East Pakistan*.
PAIN, Clifford Henry. *Port of Spain, Trinidad*.
RAMBERT, Noel. *Mauritius*.
RUTHERFORD, Thomas Graham. *Whitley Bay*.
WILKINS, Derek James. *Barnehurst*.

Transfer from Student to Associate

HERRING, Donald Peter. *B.F.P.O.6*.
PLANT, Victor Ernest. *London, E.17*.

Direct Election to Graduate

BODY, Malcolm Smith. *London, S.W.19*.
BUCKE, David Anthony. *Bradford, Yorks*.
BULGIN, Ronald Arthur, B.A. *Chigwell*.
CHAMBERS, John Albert. *London, N.W.9*.
CHAMPION, Robert John Bruce. *Slough*.
CROSSLEY, Sub. Licut. William James, R.A.N. *Sydney, Australia*.

DALTON, Walter James. *London, W.4*.
DREWITT, Andrew Bruce. *Woking*.
FERRIS, Sub. Licut. Philip Anthony, R.N. *Fareham*.
HIGGS, Brian Patrick. *Watford*.
ISAACS, Eliot Ephraim, D.L.C. *St. Albans*.
JONES, Raymond, B.Sc. *Port Talbot*.
KIRBY, Alan. *London, N.15*.
LANGTON, Victor Rae Musk. *Bexley*.
MORRIS, David Joseph, B.Sc. *Boston*.
MUNIM, 2nd Lt. Muhammad Abdul, B.Sc., Pakistan E.M.E. *Dacca*.

NETHERSOLE, Michael John. *Johannesburg*.
PATERSON, James Hugh, B.Sc.(Eng.). *Shortlands*.
PAYNE, Michael Roy. *Hayes, Middlesex*.
POOL, William John. *Hayes, Middlesex*.
RICH, Edmund Patrick. *Arborfield*.
ROBERTS, Allan John. *Welwyn*.
SHAH, Lt. Munawar, B.Sc. Pakistan E.M.E. *Rawalpindi*.
STATT, Stanley. *Rutherglen*.
THOMPSON, Raymond. *Cheltenham*.
WALFORD, John Robin. *Malvern*.

The following Direct Elections to Graduate were incorrectly listed as Transfers from Student to Associate in the October Journal.

BRIGHT, John Alexander Sydney. *Surbiton*.
DAVIES, Roy Patrick. *Egham*.
GIDDENS, Leonard. *Hayes, Middlesex*.
GREENWOOD, John Dewhurst. *Basingstoke*.
HALL, Michael William George. *Watford*.
HODGSON, John Ernest, B.Sc.(Eng.). *Cowes*.
KHANU, Abdul Hakim. *London, S.W.4*.
MEARNS, James Robert. *Hayes, Middlesex*.
MORRISON, John Gordon. *Glasgow*.
MURPHY, Brian. *Harrow Weald*.
NEAL, Geoffrey Frederick. *Brighton*.
PHILADELPHIA, James Lambert. *Kitty, British Guiana*.
TRAVIS, Flt. Lt. Robert Charles, B.Sc., R.A.F. *Henlow*.
WINDSOR, Trevor Charles, B.Sc. *London, S.E.13*.

Transfer from Student to Graduate

BHATTACHARYA, Dilip Kumar. *Barrackpore*.
BONNER, John Stafford. *Croydon*.
CUNNINGHAM, Anthony John. *Leicester*.
GREENWOOD, Frank. *Adelaide*.
HOWARTH, Edwin. *Torpoint*.
KUDDYADY, Chandrashekhar Raghunath, B.Sc. *Bombay*.
MURTY, Suryanarayana Yedavilli, M.Sc. *Ganjam*.
PARSONS, Ronald. *Bexleyheath*.
SIVASANKARA PILLAI, A. *Sonari*.
TSANG HIN-WA, Albert. *London, N.19*.

STUDENTSHIP REGISTRATIONS

Seventy-seven applications for Studentship Registration were approved at the meeting. Details will be published in the next issue of the *Journal*.

. . . Radio Engineering Overseas

621.317.083.3:621.396.96

Radar data transmission. T. E. SCHILIZZI. *Proceedings of the Institution of Radio Engineers, Australia*, 19, pp. 467-480, September 1958.

Information generated by a radar station is often required to be used at a distance. A R.A.A.F. specification has led to a joint engineering developmental project with industry on this problem. This paper presents an estimate of the theoretical information required to be transmitted in a typical case. Practical methods of achieving a remote display over wide- and narrow-bandwidth circuits are reviewed. An experimental system is described which uses commercially available wideband radio links. A description is given of high-brightness display tubes which can be used in large screen projection equipment.

621.372.832.43

A directional coupler for the generation of the H_{01} mode in circular waveguides. A. JAUMANN. *Archiv der Elektrischen Übertragung*, 12, pp. 440-446, October 1958.

The H_{01} mode in a circular waveguide can be generated with a directional coupler that effects a preferred conversion of, for instance, the H_{01} mode in the rectangular waveguide into the desired H_{01} mode in the circular waveguide. The appearance of additional undesired modes cannot be fully eliminated, however. The present paper calculates the mode selectivity of a long-slot directional coupler; it depends on the cross-sectional dimensions of the waveguides. As is known, the function of a directional coupler can be explained to a first approximation by the superposition of two normal modes (called K_I and K_{II} modes). The appearance of undesired modes is primarily due to the K_{II} mode. The field distribution of this mode is represented as a series. As a measure of mode purity serves the ratio of the energy flows, which are calculated in dependence on a design parameter x . The results of the calculation agree sufficiently well with measurements on a practically made directional coupler for 35 kMc/s.

621.382.2/3

On the characteristic curves and noise of silicon p-n diodes and silicon transistors. B. SCHNEIDER and M. J. O. STRUTT. *Archiv der Elektrischen Übertragung*, 12, pp. 429-440, October 1958.

The characteristic curves of silicon diodes show marked deviations from those of germanium diodes. One of the causes of these deviations resides in recombination and generation of carriers within the depletion layer. This cause is considered here and a formula is given for the rate of recombination as dependent on carrier densities, life times, situation within the depletion layer and applied voltage. From this formula the characteristic curves and the differential admittances of silicon diodes are derived, taking into account recombination as well as diffusion. The recombination part of diode noise is calculated using simplifying assumptions (the influence of the simplifications is also evaluated) and is then added to the diffusion part so as to obtain the total diode noise. The equivalent noise resistance is approximately equal to one-half of the total differential resistance in the forward direction. The influence of series resistances is evaluated. Noise measurements have been carried out for the forward direction, using a method, which is described. The calculated values of differential admittances and of noise are compared

A selection of abstracts from European and Commonwealth journals received in the Library of the Institution. Members who wish to borrow any of these journals should apply to the Librarian, stating full bibliographical details, i.e. title, author, journal and date, of the paper required. All papers are in the language of the country of origin of the Journal unless otherwise stated. The Institution regrets that translations cannot be supplied.

with experimental values and a satisfactory coincidence is obtained. Noise figure formulae are derived for silicon transistors, taking into account recombination in the emitter depletion layer. These formulae are compared with experimental values. If we consider regions, where high level injection and flicker noise are of minor importance, a satisfactory coincidence between theoretical and experimental values is obtained.

621.385.621.376.5:632.5

Pulse modulated beam current improves operation of mixer series klystrons. A. K. SCRIVENS. *Canadian Electronics Engineering*, October 1958.

A pulsed modulator is described which is capable of driving klystrons of the low power mixer type to relatively high power output. The klystron is beam-modulated by applying pulses derived from a blocking oscillator and pulse amplifier to both the cathode and reflector elements. A peak power output of 3 to 4 watts was obtained from a number of 2K25 klystrons while operating under low average beam current and low operating temperature conditions. The total input from the line is approximately 80 watts.

621.394:621.371

Optimum conditions for radiotelegraphy system with double diversity and threshold limitation. K. POSTHUMUS. *Tijdschrift van het Nederlands Radio-nootschap*, 23, pp. 155-176, No. 4, 1958.

A radiotelegraphy system under fading conditions is analysed. It is shown that if only signals above a certain threshold value are passed, these threshold limits should vary in inverse proportionality to the signal level. Numerical results are given for the ratio of non-rejected errors to the useful signals, under different noise-conditions. The effect of double diversity is also calculated.

621.396.822

Some aspects of noise in communications and servo systems. R. M. HUEY. *Proceedings of the Institution of Radio Engineers, Australia*, 19, pp. 486-493, September 1958.

For many years conventional methods of designing communications systems and automatic control systems have been based on considering the steady state response to an input comprised of a single pure sinusoid over an appropriate range of frequency. In marginal systems where the designer is confronted with performance limitations these methods are not wholly adequate. Consideration of matters such as non-periodic (random) signals and the response of non-linear systems is necessary. The present paper reviews some necessary background material for treating these topics, and outlines a few examples.

SUBJECT INDEX

Papers and major articles are denoted by printing the page number in bold type.

	Page		Page
Abstracts (<i>see</i> Radio Engineering Overseas and International Symposium on Electronic Components).			
AERIALS:			
Telemetry Aerials for high-speed test vehicles	497	Magnetic Recording of Television Programmes	273
Airborne Doppler Navigation Equipment ...	425	Colour Television Tests	446
Aircraft Industry, and Electronics	539	British Centre for Rocket and Satellite Data	676
Amplitude-modulated or frequency-modulated Signal Generators—Expression of Characteristics	7	British National Committee on Non-Destructive Testing	262
Analogue Computer for Fourier Transforms	233	British Standards	644
Analogue Computers and their use in Nuclear Reactor Safety Studies	95	British Standards Institution:	
Annual General Meeting of the Institution:		Institution representatives on committees ...	570
Notice and Agenda	509	Broadcasting in Rhodesia and Nyassaland ...	236
Report	693	Building Appeal	567, 577
Apparatus for the Measurement of the Velocities of Sonic Pulses in Flawed Materials	371	Calculation of Characteristic Impedance by Conformal Transformation	49
Applicants for Election and Transfer		Canadian Trials of Decca Navigator	676
48, 115, 150, 232, 358, 445, 492, 524, 582, 747		Cathode-Ray Tubes, Optimum design of electrostatically deflected	485
Applications of Gas Discharge Tubes as Noise Sources in the 1700-2300 Mc/s Band ...	541	C.E.R.N., Appointment of United Kingdom Delegate	94
Appointments Register	576	Characteristic Impedance and Phase Velocity of High-Q Triplate Line	715
Approval of Courses	572	CIRCUIT TECHNIQUES:	
Approximate Relations between Transient and Frequency Response	57	Automatic Gain Control in Television Receivers for Negative Modulation Systems	307
ATV and the Institution	386	Design of Detector Stages for Signals with Symmetrical or Asymmetrical Sidebands	525
Australia, Emigration	174	Frequency Modulation by Inductance Variation: A Magnetically-stable Ferrite Modulator	189
Automatic Control in Steel Strip Manufacture	117	Probability of Specified Losses at Mismatched Junctions	293
Automatic Gain Control Circuits in Television Receivers for Negative Modulation Systems	307	Thermally Compensated Crystal Oscillators	613
Automatic Methods in Radio Component Manufacture	227	Circulation of the <i>Journal</i>	496
Awards by the Institution of Radio Engineers, Australia	714	City and Guilds of London Institute:	
Awards and Prizes by City & Guilds of London Institute	58	Annual Report	496
Balance Sheet and Accounts, Institution's General Account	576, 578, 580, 695	Insignia Awards	446
Beam Valves, Design of the transition region of axisymmetric, magnetically focused ...	696	Institution co-operation	573
Benevolent Fund:		Awards and Prizes	581
Trustees	2	Coil winding, Electronic control	227
Report of the Annual General Meeting of Subscribers, 1957	66	Colour television:	
Notice and Agenda of General Meeting of Subscribers	640	Courses	386
Report of the Trustees for 1957-58	641	B.B.C. Tests	446
Report of the Annual General Meeting of Subscribers, 1958	724	COMMUNICATIONS:	
Binding of the Institution's <i>Journal</i>	262	"Evolution of Radio Communication," 1957 Students' Essay Competition	363
Birth Centenary of Sir Jagadish Chandra Bose	661	Recent Developments in Communications	
Birthday Honours List	329, 496	Measuring Instruments	387
British Broadcasting Corporation:		Selective Calling Systems for Mobile Radio-telephony	297
Extension of B.B.C. Television Coverage ...	174	Comparison of Turret-Type and Switch-Type Television Tuners	346
Television Stations for South-East of England	236	Competitions:	
		Students' Essay	362
		Variety Reduction Essay	630
		Waverley Essay	226
		Components, Automatic methods in radio manufacture	227

SUBJECT INDEX

COMPUTERS:

- Analogue Computer for Fourier Transforms 233
 Analogue Computers and their use in Nuclear Reactor Safety Studies 95
 Computer Exhibition and Symposium ... 236
 Decimal Product Accumulator 125
 Electronic Synthesis of Flexible Beam Behaviour 151
 Nuclear Power Plant Training Simulator for Use at Calder Hall 85
 Radar Simulators 17
 Radar Simulators in the Royal Navy, The use of 33
 Conference on Reactor Technology 94
 Congress on U.H.F. Circuits and Antennas ... 6
 Controlled Thermo-nuclear Research ... 398
 Convention on Television Engineering ... 629
 Cooling high-power valves by vaporization of water 621
 Co-operation between engineering Institutions 572
 Corrections 142, 581, 714, 746
 Correlation between the Transient and Frequency Responses in Servomechanisms 101
 Council:
 1958 1
 Election of new members 509, 694
 Courses:
 Colour Television 386
 Reactor Technology 94
 Current Interest 94, 174, 236, 446
 Decca Navigator, Canadian trials 676
 Decimal Product Accumulator 125
 Dectra: A Long-range Radio-navigation Aid 277
 Design and Performance of Magnetic Tape Recording Heads 551
 Design of Detector Stages for Signals with Symmetrical of Asymmetrical Sidebands 525
 Design of Inductive Post-Type Microwave Filters 263
 Dinner of the Institution 70, 142, 206, 321
 Design of the Transition Region of Axisymmetric Magnetically Focused Beam Valves 696
 Diplomas in Technology 65
 Discussions on papers:
 Automatic Control in Steel Strip Manufacture 124
 Decimal Product Accumulator 133
 Machine Tool Control 248
 Dectra: A Long-Range Radio-Navigation Aid 291
 Detection of Pulse Signals in Noise ... 317
 Mass Production of Television Tuners ... 349
 Radio Studies during the I.G.Y. 412
 Factors in the Design of Airborne Doppler Navigation Equipment 442
 New Developments in Silicon Photovoltaic Devices 594
 Editorials:
 Looking Ahead 5
 Wastage of Students 69
 Science in Parliament 141
 Contributions to the Journal 205
 Technicians, Engineers, Scientists 261
 A Guide to Radio Engineering Literature 385
 Television Engineering in Science, Industry and Broadcasting 629
 Education and Examinations Committee:
 Membership 2
 Annual Report 571
 Visit to R.A.F. Technical College 630
 Election of Officers and ordinary members of Council 694
ELECTRO-ACOUSTICS:
 Design and Performance of Magnetic Tape Recording Heads 551
 Electronic Sector Scanning (Acoustic Beams) 465
 Electromagnetic Wave Propagation in Cylindrical Waveguides, containing Gyromagnetic Media (Parts 1, 2, 3) ... 597, 677, 733
 Electromagnetic Protective Device for Automatically-fed Power Presses 229
 Electronic Engineering Association 174
 Electronic Control applied to Coil Winding 227
 Electronic Sector Scanning and Radar Systems 709
 Electronic Sector Scanning (Acoustic Beams) 465
 Electronic Synthesis of Flexible Beam Behaviour 151
 Electronics and the Aircraft Industry ... 539
 E.M.I. College of Electronics 676
 European Organization for Nuclear Research, Appointment of United Kingdom Delegate 94
 "Evolution of Radio Communication," 1957 Students' Essay Competition 363
 Exhibitions:
 Physical Society's Exhibition 70, 581, 714
 Electrical Engineers Exhibition 70
 Radio and Electronic Component Show ... 142
 Computer Exhibition and Symposium ... 236
 Indian Radio & Electronics Exhibition ... 510
 S.B.A.C. Flying Display and Exhibition ... 539
 National Radio Show 561
 Experimental Determination of System Transfer Functions from Normal Operating Data 179
 Factors in the Design of Airborne Doppler Navigation Equipment 425
 Ferrites, in cylindrical waveguides ... 597, 677, 733
 Ferrite modulator 189
 Films, Technical 382
 Filters, Design of inductive post-type microwave 263
 Finance Committee:
 Members 2
 Annual Report 576
 Fourier Transforms, An Analogue Computer for 233
 Frequency Allocation Committee 6, 94
 Frequency Modulation by Inductance Variation: A Magnetically-stable Ferrite Modulator ... 189
 Gas discharge tubes as noise sources in 1700-2300 Mc/s band 541
 Graduateship Examination:
 Pass list, November 1957 134

Dates	142	Binding	262
Pass list, May 1958	506	Circulation	496
Entries and results	571	Contributions	205
Exemption	57	Report for year	568
Group Provident Scheme	142, 329	Library Committee:	
Helical Waveguides—Closed, Open and Coaxial	359	Members	2
Honours List 1958	6, 329, 496	Annual Report	570
Hook transistors, Properties in switching and amplifying circuits	725	"Library Services and Technical Information for the Radio and Electronics Engineer" 385,	571
Impedance, Characteristic, by conformal transformation, Calculation	49	Local Section Committees	3
Independent Television Authority:		Machine Tool Control:	
Station in Isle of Wight	549	Discussion	248
The Institution and programme companies	386	Magnetic Materials:	
INDUSTRIAL APPLICATIONS OF ELECTRONICS:		Technical Committee Survey	449
Analogue Computers and their use in Nuclear Reactor Safety Studies	95	Magnetic Recording of Television Programmes	273
Apparatus for the Measurement of the Velocities of Sonic Pulses in Flawed Materials	371	Magnetic tape recording heads, Design and performance	551
Approximate Relations between Transient and Frequency Response	57	Magneto-ionic Fading in Pulsed Radio Waves reflected at Vertical Incidence from the Ionosphere	669
Automatic Methods in Radio Component Manufacture	227	Mass Production Techniques for Television Tuners	331
Correlation between the Transient and Frequency Responses in Servomechanisms	101	Materials used in Radio and Electronic Engineering:	
Experimental Determination of System Transfer Functions from Normal Operating Data	179	5. Magnetic Materials (Technical Committee survey)	449
Industrial Application of A.C. Polarography	143	MEASUREMENTS:	
Industrial Support for the Institution	84, 386, 577	Apparatus for the Measurement of the Velocities of Sonic Pulses in Flawed Materials	371
Insignia Awards	446	Applications of Gas Discharge Tubes as Noise Sources in the 1700-2300 Mc/s Band	541
Institution:		Calculation of Characteristic Impedance by Conformal Transformation	49
Dinner	70, 142, 206, 321	Communications measuring instruments. Recent developments	387
Meeting in Cambridge	6	Medical Electronics:	
Visits	496, 630	International Conference	505
Representation on other bodies	566, 574	Institution Group Committee	630
Convention	629	Membership Committee:	
Premiums and Prizes	510, 568, 695	Members	2
Institution of Production Engineers	630	Annual Report	574
Institution of Radio Engineers, Australia:		Merseyside Section Committee	3
Silver Jubilee	94	Microwave filters, Design of inductive post-type	263
Awards	714	Mismatched junctions. Probability of specified losses	293
International Conference on Medical Electronics	505, 566	National Radio Show	561
International Geophysical Year:		NAVIGATION AIDS:	
Radio Studies	401	Canadian Trials of Decca Navigator	676
Rocket Experiments	416	Decca: A Long-range Radio-navigation Aid	277
International Radio Organizations:		Factors in the Design of Airborne Doppler Navigation Equipment	425
Some Aspects of their work	631	New Developments in Silicon Photovoltaic Devices	583
International Symposium on Electronic Components	262	New Method of Cooling High-Power Valves by Vaporization of Water	621
Summaries of papers 55, 135, 175, 253, 304,	381	New Year Honours List	6
(<i>Note.</i> —The papers are classified in the Index of Abstracts)		New Zealand Department of Education	226
Investigation of Horizontal Drifts in the E Region of the Ionosphere in Relation to Random Fading of Radio Waves	493	New Zealand Section:	
<i>Journal:</i>		Meetings	662
Back copies	6		

SUBJECT INDEX

Noise Sources in the 1700-2300 Mc/s band			
Application of gas discharge tubes ...	541		
Noise, Transistor; its origin, measurement and behaviour ...	207		
Non-Destructive Testing:			
British National Committee ...	262		
Summer school ...	386		
North Eastern Section:			
Committee ...	3		
Dinner ...	226		
North Western Section Committee ...	3		
Note on The Radio-Frequency Heating of Rubber Compounds ...	663		
Nuclear Power Plant Training Simulator for Use at Calder Hall ...	85		
Obituary Notices:			
Robinson, F. H. ...	70		
Hytch, John ...	70		
Lanchester, R. A. ...	142		
Wiegernick, H. T. J. ...	142		
MacIntosh, A. E. ...	226		
Silver, H. G. ...	226		
Wilkinson, H. ...	262		
Evans, R. B. ...	262		
Mahendru, P. D. ...	262		
Sterling, Sir Louis ...	329, 330		
Hosburn, J. C. ...	329		
Hasson, J. ...	510		
Hawkins, W. E. ...	581		
Of current interest (<i>see</i> Current interest)			
Optimum Design of Electrostatically Deflected Cathode-Ray Tubes ...	485		
Oscillators, Thermally compensated crystal ...	613		
Oscilloscope Tube with Travelling Wave, Deflection System and Large Field of View ...	653		
Overseas Representatives ...	4		
Overseas Sections ...	4		
Photovoltaic devices, Silicon ...	583		
Polarography, A.C., Industrial applications ...	143		
Premiums and Prizes ...	510, 568, 695		
President of the Institution (Mr. G. A. Marriott)			
New Year Message ...	5		
Invitation to Royal Garden Party ...	386		
Visit to Reed's School ...	386		
Annual General Meeting ...	693		
President for 1959 (Professor E. E. Zeppler) elected ...	694		
Probability of Specified Losses at Mismatched Junctions ...	293		
Product accumulator, Decimal ...	125		
Professional Purposes Committee:			
Members ...	2		
Annual Report ...	566		
Programme and Papers Committee:			
Members ...	2		
Annual Report ...	567		
PROPAGATION:			
Radio Studies during the International Geophysical Year 1957-58 ...	401		
Investigation of Horizontal Drifts in the E Region of the Ionosphere in Relation to Random Fading of Radio Waves ...	493		
Magneto-ionic Fading in Pulsed Radio Waves reflected at Vertical Incidence from the Ionosphere ...	669		
Properties of Hook Transistors in Switching and Amplifying Circuits ...	725		
RADAR:			
Radar Simulators ...	17		
Radar Simulators in the Royal Navy, The use of ...	33		
Radar Systems with Electronic Sector Scanning ...	709		
Radar, Type 984 ...	323		
Radio Communication, The Evolution of: 1957 Students' Essay Competition ...	363		
Radio Engineering Overseas (Abstracts) 67, 139, 187, 259, 319, 383, 447, 507, 563, 627, 691, 748			
(<i>Note.</i> —These abstracts are listed in the Index of Abstracts)			
Radio-frequency Heating of Rubber Compounds ...	663		
Radio Industry Council:			
Dinner ...	630		
Retirement of Director ...	6		
Radio-navigation aid, Long-range, Dectra ...	277		
Radio Studies During the International Geophysical Year 1957-8 ...	401		
Radio-telephony, Selective Calling Systems for Mobile ...	297		
Radio Trades Examination Board:			
Annual Report of the Board ...	32		
Annual Report of Institution's Education and Examinations Committee ...	574		
Radio Waves, Investigation of horizontal drifts in the E region of the ionosphere in relation to random fading ...	493		
Recent Developments in Communications Measuring Instruments ...	387		
Recording heads, Design and performance of magnetic tape ...	551		
Reed's School ...	386, 643, 724		
Representation of the Institution on other bodies ...	566, 574		
Rhodesia and Nyasaland. Broadcasting in ...	236		
Rockets and Satellites:			
Radio observations on Russian Satellites ...	362		
I.G.Y. Rocket Experiments ...	416		
British Centre for Data ...	676		
R.A.F. Technical College, Education Committee visit ...	630		
Royal Garden Party ...	386		
Royal Military College of Science, Civilian studentships ...	714		
Royal Society Conversazione ...	362		
Rutherford High Energy Laboratory, Appointment of first director ...	174		
"Sandwich Courses" Grants for students ...	262		
Steady spread of ...	446		
Scatter tropospheric system evaluation ...	511		
Sceptre III ...	362, 400		
Science in Parliament ...	141		
Scottish Section:			
Committee ...	3		

Annual Dinner	82	Some Aspects of the Production of Television Tuners	341
Section Activities	82, 226, 569, 662	Television Engineering in Science, Industry and Broadcasting (1959 Convention)	629
Section Committees	3	Television Links on Cable	116
Selective Calling Systems for Mobile Radiotelephony	297	VERA (Magnetic recording of television programmes)	273
SEMI-CONDUCTORS (<i>see also</i> Transistors):		Thermally Compensated Crystal Oscillators	613
New Developments in Silicon Photovoltaic Devices	583	Thermo-nuclear research, Controlled	398
The use of Semi-conductor Devices	676	Toroidal Transformers for an Analogue System of Machine Tool Control	71
Servomechanisms, Correlation between transient and frequency response	101	TRANSISTORS:	
Servo systems, Closed loop, Applications to machine tool control	237	Properties of Hook Transistors in Switching and Amplifying Circuits	725
Signal Generators, Amplitude-modulated or frequency - modulated, Recommended method of expressing characteristics	7	The Use of Semi-conductor Devices	676
Simulators	17, 33, 85	Transistor Noise: Its Origin, Measurement and Behaviour	207
Solar cells	583	Transistor with Thyatron Characteristics and Related Devices	645
Some Aspects of Television Tuner Production	341	Travelling wave deflection system oscilloscope tube	653
South Wales Section:		Tropospheric Scatter System Evaluation	511
Committee	3	Turret tuner, Construction for mass-production	348
Activities	662	University Extension Lectures	94
South Western Section:		VALVES AND TUBES:	
Inaugural meeting	662	Design of the Transition Region of Axisymmetric Magnetically Focused Beam Valves	696
Specialized Groups	566	New Method of Cooling High-Power Valves by Vaporization of Water	621
Standardization Techniques In Radio (<i>See also</i> British Standards)	596	Optimum Design of Electrostatically Deflected Cathode-Ray Tubes	485
Standing Committees	2	Oscilloscope Tube with Travelling Wave Deflection System and Large Field of View	653
Students' Essay Competition 1957	363	Variety Reduction Essay Prize Competition	630
Students, Wastage of	69	VERA (Magnetic recording of television programmes)	273
Studentships, Civilian, at Royal Military College of Science	714	Visits:	
System transfer functions, The experimental determination from normal operating data	179	Western Germany	70
Tatsfield Receiving Station, Institution visit	496	London Airport	329
Tax relief on Institution subscriptions	581, 695	Tatsfield Receiving Station	496
Technical Authors, Examinations for	386	Vauxhall Motors	630
Technical Committee:		WAVEGUIDES:	
Members	2	Characteristic Impedance and Phase Velocity of High-Q Triplate Line	715
Report of Recommended Methods of Expressing A.M. or F.M. Signal Generator Characteristics)	7	Closed, Open and Coaxial	359
Survey on Magnetic Materials	449	Design of Inductive Post-Type Microwave Filters	263
Annual Report	569	Electromagnetic Wave Propagation in Cylindrical Waveguides containing Gyromagnetic Media	597, 677, 733
Visits	329, 496, 630	Waverley Gold Medal Essay Competition	226
Technical Films	382	West Midlands Section:	
Technical Writing Premium	174	Committee	3
Technology, Diplomas in	65	Activities	662
Telemetry Aerials for High-Speed Test Vehicles	497	ZETA	398
TELEVISION:			
Automatic Gain Control Circuits in Television Receivers for Negative Modulation Systems	307		
Comparison of Turret-Type and Switch-Type Television Tuners	346		
Design of Detector Stages for Signals with Symmetrical or Asymmetrical Sidebands	525		
Magnetic Recording of Television Programmes	273		
Mass Production Techniques for Television Tuners	331		

INDEX OF ABSTRACTS

This index lists the abstracts published under the heading of "Radio Engineering Overseas" and the summaries of papers read at the International Symposium on Electronic Components held in Malvern in 1957.

	<i>Page</i>		<i>Page</i>
Radio Astronomy (523.164)			
Site survey for a national radio astronomy observatory. C. F. Pattenson.	627	The electrical breakdown of small gaps in vacuum. A. S. Denholm.	383
Analysis of meteoric body doppler radar records taken during a Geminid shower period. M. Sriramo Rao.	627	A comparison of wool wax and petroleum jelly as impregnants for paper capacitors. J. S. Dryden and R. J. Meakings.	691
The polarization of solar radio emission at a frequency of 200 Mc/s. F. R. Neubauer and A. D. Fokker.	691	Resistors (621.316)	
Impulsive and long-enduring sudden enhancements of solar radio emission at 10 centimetre wavelength. A. E. Covington and G. A. Harvey.	691	Recent developments in fixed resistors. R. W. Burkett.	175
Temperature Measurement (536.6)			
Use of thermo-sensitive attenuation-coils and transformers. O. Hora.	507	Metal oxide film potentiometers. G. V. Planer.	177
An experimental pyrometer using a photo-transistor and designed for radio-tube inspection. F. H. R. Almer and P. G. Van Zanten.	691	An electronic ground detector. D. W. R. McKinley.	447
Electricity (537.7)			
Research on the high-frequency surface discharge. Toshio Honda.	139	Measurements (621.317)	
Electromagnetism (538)			
The magnetic fields of a ferrite ellipsoid. R. A. Hurd.	691	Noise voltage measurements on low impedance circuit elements with the aid of a valve voltmeter with a preceding transformer. W. Nonnenmacher.	67
Scattering from a small anisotropic ellipsoid. R. A. Hurd.	691	The measurement of the reflection coefficient in television transmission lines and equipment. E. Thinius.	67
The use of Hall-current generators in analogue multipliers. J. Oxenius.	383	A recurrent surge oscillograph for surge-voltage distribution measurements on transformers. F. C. Hawes.	139
Ionospheric Phenomena (551.510)			
The CARDE I.G.Y. upper air research program. R. F. Chinnick.	563	An accurate phasemeter for four-terminal networks. B. Chatterjee.	139
Transformers (621.314.2)			
Transformer miniaturization using fluoro-chemical liquids and conduction techniques. L. F. Kilham.	253	Wave-form observation of electron current using travelling-wave cathode-ray tubes. H. Maida.	187
The development of high temperature transformers. A. G. Gilmour.	254	A measuring device for transmitting tube characteristics. J. W. A. van der Scheer.	187
The differential transformer and its use in the automatic control of machine tools. J. Zeleny.	507	Automation in component testing. J. A. Sargrave.	257
Cables (621.315.2)			
Design, development and standardization of r.f. cables. W. T. Blackband.	255	Correlation measurements in the short-wave range. J. Grosskopf, J. Scholz and K. Vogt. Experimental wide-band thermistor mounts. J. Swift.	447
Insulating Materials. Dielectrics (621.315.6)			
Dielectric walls with a small reflection coefficient at microwaves. H. Meinke.	67	A 2,100 Mc/s microwave propagation test set. F. Ivanek.	447
A survey of dielectric materials. G. C. Gar-ton.	138	Radar data transmission. T. E. Schilizzi.	748
Magnetic Materials (621.318)			
Some recent developments in magnetic alloys. C. E. Richards.			
A survey of ferrites and their applications. A. A. Th. M. van Trier.			
Technology of manufacturing barium ferrite. R. Lappa.			
Microwave ferrites. B. Josephson and P. E. Ljung.			
Square loop ferrites and tests of their storage properties. C. Heck and H. Reiner.			
Studies of ferrite behaviour at radio frequencies.			

Relays (621.318.5)	
Some recent developments in miniature relays. J. H. Mitchell.	304
Capacitors (621.319.4)	
Recent developments in electrolytic capacitor design. G. C. Gaunt.	137
Development of plastic dielectric capacitors. J. H. Cozens.	137
The design of high performance multi-gang variable capacitors. L. W. D. Sharp. ...	175
Life-failure statistics of short rated oil-paper capacitor elements. R. J. Peterson. ...	176
Recent high- <i>k</i> capacitor developments in France. J. Peyssou.	178
Coaxial trimmer capacitor with glass or quartz dielectrics. L. Klauz, M. Schmiedhamer and J. Smetana.	319
Batteries (621.353.5)	
The choice of batteries for use in electronic equipment. F. M. Booth.	253
R.F. Heating (621.365)	
Experimental electronic generator for dielectric heating, with automatic load matching. C. Vazaca.	383
Transmission Lines, Networks and Waveguides (621.372)	
Wave diagrams in waveguides with diaphragms or corrugations. G. Piefke. ...	139
The frequency response of cut-off attenuators with coaxial launching and pick-up probes. A. Sander.	187
On the synthesis of three-terminal networks composed of two kinds of elements. K. M. Adams.	187
Mode conversion losses in transmission of TE ₀₁ modes through conically tapered waveguides. S. Kumagai.	187
Matching elements for a waveguide directional coupler with periodic structure. I. Lucas.	259
A waveguide load made from commercial film resistors. U. V. Kienlin and A. Kurzl. ...	319
The effect of surface resistance of attenuators in travelling wave tubes on gain and stability. W. Eichin and G. Landauer. ...	319
Ferrites for magnetostrictive filters. S. Schweizerhof.	383
The uniform rectangular waveguide with damping foil. H. Buseck and G. Klages. ...	383
Characteristics and properties of long-slot directional couplers. E. Schoun.	447
Operating stability of electronic equipment. M. Saveacu.	507
The design of a triple tuned band-pass filter. R. J. L. Bosselaers and J. Roorda.	507
A new circle diagram for transformations in transmission line technique. G. W. Epprecht.	507
Theory of the helical line of finite wire thickness and applications to the rotation of the plane of polarization of guides waves. G. Piefke.	563
Irises for bandpass waveguide filters. J. Horna.	563
The properties of lossy inhomogeneous transmission lines under matched conditions. H. Meinke.	627
A directional coupler for the generation of the H ₀₁ mode in circular waveguides. A. Jauermann.	748
Oscillators (621.373)	
The generalization of the Barkhausen formula for electronic oscillators. M. Draganescu. ...	67
Transistor oscillators and their sensitivity to load impedance. W. Herzog.	67
Experimental and theoretical investigation into frequency stabilized transistors for 8 Mc/s. H. Schaffhauser.	67
Magnetic pulse generators. D. W. R. Sewell. ...	135
Construction and characteristics of high quality quartz crystals. G. Becker. ...	139
A warble tone generator. R. R. Dutta Gupta. ...	319
The production of extremely steep pulse edges in multi-stage non-linear amplifiers. G. Kohn.	319
Stable flip-flop circuit for measuring instruments. K. Kostal.	320
Studies on thyatron pulse generator. S. C. Mukerjee.	383
Three-phase pulse generator. V. Chlouba. ...	627
Investigation into two-valve oscillators with pi network feedback. E. Frisch.	691
Pulse Processes (621.374)	
Non-saturating junction transistor flip-flop circuits. K. Aoyagi, K. Miyawaki and J. Sasaki.	187
The efficiency of microwave frequency multiplier using a crystal diode. S. Okamura and T. Ohkoshi.	187
The generation and amplification of millimetric waves. W. Kleen and K. Poschl. ...	187
A double cathode-follower. A. Segal.	384
Noise figure for transistor amplifier with high input impedance. A. E. Bachmann.	563
Fast transistor circuits. M. Combier and J. Mey.	692
Delay line frequency dividers and their application to arithmetic. Y. Amran, H. Gullon and B. Ollivier.	692
Amplifiers (621.375)	
A 4,000 Mc/s wide-band amplifier using a disc-seal triode. J. P. M. Gieles.	67
An analysis of transient response of junction transistor amplifiers. J. C. Bhattacharyya. ...	68
Design of magnetic amplifying circuits. B. W. Glover and D. A. Ramsay.	136
A transformerless class B Power amplifier with identical transistors. M. Fedorowski. ...	139
A summary of the theoretical basis for broadband distributed amplifiers suitable for very short pulses. D. Dosse.	259

INDEX OF ABSTRACTS

Transistors for medium frequency—a detector circuit for radio-communication apparatus. G. Rosier.	259	Electronic Valves (621.385)	
Band-pass amplifiers, their synthesis and gain-bandwidth factor. Fuad Surial Atiya. ...	507	The focal length of a diaphragm of finite aperture for electron fields with finite space charge. K. Poschl and W. Veith.	140
A new logarithmic amplifier. T. M. Bajenescu.	508	Automatic tracing of electron trajectories. O. Cahen.	188
A transistorized i.f. amplifier for communication receivers. A. S. Pett.	508	Noise in space charge diodes. K. H. Locherer.	448
Measuring stability of feedback amplifiers. S. Vojtasek and V. Ilsberg.	627	Pulse modulated beam current improves operation of mixer series klystrons. A. K. Scrivens.	748
On the low-frequency behaviour of video-amplifiers. A. P. Bolle.	692		
An experimental induction-heating generator using hydrogen thyratrons. H. L. van der Horst and P. H. G. van Vlodrop.	692	Valves for U.H.F. (621.385.6)	
A very short light pulse generator used for testing photomultipliers. P. Cachon and A. Sarazin.	692	The linearization of frequency modulated reflex klystrons. E. Schuon and H. J. Butterweck.	320
		The Townsend discharge in a coaxial diode with axial magnetic field.	320
		Analogue multiplier and function generator with cathode ray tube. A. K. Choudhury and B. R. Nag.	384
		On the theory of the electron wave tube with elliptic cross-section. P. Mattila.	508
Modulation and Demodulation (621.376)			
Theoretical considerations concerning the frequency compression of periodically recurring processes. R. A. Kaenel.	139	Cathode-ray Tubes (621.385.832)	
Frequency modulation by gas-discharge tubes P. Stiubel.	447	Low-voltage oscilloscope tubes. F. de Boer and W. F. Nienhuis.	67
Semi-conductor Devices (including Transistors) (621.382)		Radiation Counters (621.387.4)	
A short time-constant switching mechanism and its application to component techniques. H. Salow and W. von Münch.	136	Photoionization versus photoelectric effect for discharge spread and output pulse measurements in G-M counters. P. S. Gill and S. P. Puri.	140
Semi-conductor rectifier developments for power supplies to electronic equipment. A. H. B. Walker and K. G. King.	257		
Manufacturing principles of transistors. J. Lantieri.	259	X-ray Equipment (621.386)	
High frequency germanium and silicon transistors. J. Dezoteux.	259	Dosimetry of the very weak X-radiation generated in television receivers and X-ray diffraction apparatus. W. J. Oosterkamp.	260
Stabilization of the operating point of transistors. E. E. P. Poelman.	259		
Experimental and theoretical investigation of the equivalent circuits of new h.f. transistors with special reference to drift transistors. W. Guggenbuhl and W. Wunderlin.	384	Communication Theory (621.391)	
Analogous transistor system design and nodal methods of construction with applications to research equipment and prototype evaluation. R. F. Treharne.	507	Phenomenological model of stochastic signals in measurement techniques. H. R. Loos.	384
An oscilloscope accessory for the display of transistor characteristic curves. R. E. Aitchison.	508	Automatic detection of signs. K. Steinbuch.	384
Transistor monostable multivibrator for use with counting registers. R. E. Aitchison.	508	The reliability of binary code transmission by means of various types of modulation.	508
A storing and switching transistor. W. v. Münch and H. Salow.	508	Transmission of speech with quantizing in only a few stages. K. Kupfmuller and W. Andrich.	627
On the characteristic curves and noise of silicon p-n diodes and silicon transistors. B. Schneider and M. J. O. Strutt.	748	A contribution to the theorem for adding noise voltages in long distance communication systems using amplitude modulation. H. Zuhrt.	628
		Optimum conditions for radiotelegraphy system with double diversity and threshold limitation. K. Posthumus.	748
		Electro-acoustic Devices (621.395)	
		Condenser (earphone) receiver. T. Hayasaka and M. Suzuki.	188
		Advances in the design of loudspeakers. F. K. Schroder.	384
		The operation of corona loudspeakers. G. Bolle.	384
Photocells (621.383)			
A survey of picture storage tubes with reproduction of gradations. H. G. Lubszynski.	320		

Propagation (621.396.11)

- Observations on back scatter echoes for short-wave transmission. Hans-Ulrich Widdel. ... 68
- Determination of a value for the absorption of the ionosphere by an automatic statistical analysis of field strength records. ... 628
- Observations of multi-path propagation on the short-wave link Osaka-Frankfurt-on-Main. B. Beckmann. ... 691

Radio-communication Systems (621.396.6)

- Multichannel u.h.f. radio telephone equipment. J. Fieguth. ... 320
- Radio frequency powers and noise levels in multichannel radiotelephone systems using angular modulation. T. D. Thomson. ... 448

Receivers (621.396.61)

- A high-quality transistor receiver. A. E. Peppercorn. ... 140
- Neutralization of additive mixers. J. Novak. ... 563

Aerials (621.396.67)

- Polarization d/f system. J. Grosskopf and K. Vogt. ... 68
- Some investigations of dielectric aerials. (Mrs.) R. Chatterjee and S. K. Chatterjee. ... 68
- Microwave antenna characteristics in the presence of an intervening ridge. R. Vikramsingh, M. N. Rao and S. Uda. ... 68
- A new way to the solution of the problem of wideband aerials. H. Meinke. ... 188
- The influence of multipath propagation on the spectrum of a received television signal. K. Bernath and H. Brand. ... 260
- On 3- and 4-element antennas. E. Nicolau and A. Dobrescu. ... 448
- The preparation of radiation patterns of Australian army rhombic aerials by an electronic computer and their applications. A. Jacoby and G. Gay. ... 563
- The reduction of bearing errors during multiple incidence in Adcock d.f. systems with a large base. H. Steiner and H. Stittgen. ... 564
- Investigations into diversity reception using the method of aerial selection. ... 628
- Measured self-impedance of a dipole antenna near a conducting cylinder of elliptical cross-section. J. Y. Wong. ... 628
- The theory of helical antennas. W. Peters. ... 628
- Disc antenna. J. Vokurka. ... 628
- Studies on a rhombic antenna with cylindrical helices as the arms. Ashoke Kumar. ... 692

Radio Components (621.396.69)

- Problems affecting the design of service components and a survey of present and future United Kingdom developments. G. W. A. Dummer. ... 55
- New concepts, techniques and components for transistor circuits. A. W. Rogers. ... 56

- Components suitable for automatic assembly. J. W. Buffington. ... 256
- Components for severe environmental conditions. J. S. Lambert. ... 258
- Component design in relation to printed and potted electronic circuits. H. G. Manfield. ... 304
- Nuclear radiation damage to electronic components. E. H. Cooke-Yarborough. ... 305
- Problems in long-term component reliability. K. E. Latimer. ... 306
- Casting lossy microwave parts in resin aids design work. A. Staniforth and K. A. Steele. ... 692

Interference Noise (621.396.82)

- A simple noise generator. V. Herles. ... 448
- Automatic recorder of the waveforms of atmospherics. B. A. P. Tantry. ... 628
- Some aspects of noise in communications and servo systems. R. M. Huey. ... 748

Navigation Aids—Radar

Aircraft Communications (621.396.933/96)

- The power level control in transmitters for the instrument landing system (ILS). K. May. ... 140
- A new receiver for the Australian DME beacon. B. R. Robinson. ... 188
- A radar sonde system for upper air measurements. N. E. Goddard and H. A. Dell. ... 260
- The flight testing of radio facilities. M. Cassidy. ... 448
- S.A.T.C.O.—a new system for air traffic control. ... 448
- Further progress in the work relating to bandwidth compression for radar p.p.i. pictures. H. Meinke and A. Rihaczek. ... 564
- Radio links for the control of aeronautical air-ground air equipment. W. S. McGuire. ... 692

Broadcasting (621.396.97)

- A new method for the automatic monitoring of broadcasting systems. F. Enkel. ... 320

Television (621.397)

- Assessment of the use of horizontal synchronization for television receivers. Helmut Lutz. ... 68
- A luminous frame around the television screen. J. J. Balder. ... 68
- On the behaviour of synchronization circuits in television broadcast receivers in the presence of interference. E. Ludicke. ... 140
- Transmission of video signals over local telephone lines. J. Appeldoorn and C. Bakker. ... 188
- Television picture tubes for cathode modulation with increased effective perveance. W. Niklas, C. Szegho and J. Wimpfen. ... 260
- Non-linear distortions in television links. J. Muller. ... 260
- The cause and the measurement of level sensitive phase and amplitude fluctuations in the transmission of colour-television chrominance carriers. J. Piening. ... 260

INDEX OF ABSTRACTS

Recording television programmes on film in the German Federal Republic. J. Goldman and H. Funk.	320	Analogue representation of heat exchange circuits. Application to exchangers in nuclear power stations. J. Carteron. ...	188
Method of interlace scanning measurement in television receivers. J. Kamler.	320	The theory and design of a sampled data control systems. S. Bellert.	260
A line transformer with a screened h.t. winding. H. Reker.	384	An electronic differential analyser.	320
Standards conversion with vidicon tube. W. Dillenburger.	384	Automatic input for business data-processing systems. K. R. Eldredge, F. J. Kamp-hoefner and P. H. Wendt.	564
An N.T.S.C. colour modulator for C.C.I.R. standards. F. Jaeschke.	448	Quality Control (621.658)	
The projection of colour-television pictures. T. Poorter and F. W. de Vrijer.	628	The circle concept of quality control applied to tv receiver manufacture. T. J. Brown.	564
Gradation correction in colour television. J. Kaashoek.	692	Control of quality and reliability. M. Ger-vaise.	564
Computers (681.142)		Filing Systems (651.396)	
A.D.A.—a transistor decimal digital differen-tial analyser. M. W. Allen.	188	Marginal punched cards for a reference file in the field of electronics. W. G. Hoyle. ...	564

JOURNALS FROM WHICH ABSTRACTS HAVE BEEN TAKEN DURING 1958

<i>Acta Polytechnica Scandinavica</i>	<i>Journal of the Institution of Telecommunication Engineers (India)</i>
<i>Archiv der Elektrischen Ubertragung (Germany)</i>	<i>Journal of the Royal Astronomical Society of Canada</i>
<i>Automatica si Electronica (Roumania)</i>	<i>L'Onde Electrique (France)</i>
<i>Automatisace (Czechoslovakia)</i>	<i>Nachrichtentechnische Zeitschrift (Germany)</i>
<i>Canadian Electronics Engineering</i>	<i>Philips Technical Review (Holland)</i>
<i>Canadian Journal of Physics</i>	<i>Prace Instytutu Tele-I-Radiotechnicznego (Poland)</i>
<i>Elektrotehniski Vestnik (Yugoslavia)</i>	<i>Proceedings of the Institute of Radio Engineers Australia</i>
<i>Engineering Journal of Canada</i>	<i>P.T.T. Bedrijf (Holland)</i>
<i>Ericsson Technics (Sweden)</i>	<i>Rozprawy Electrotechniczne (Poland)</i>
<i>European Broadcasting Union Review</i>	<i>Slaboproudy Obzor (Czechoslovakia)</i>
<i>Indian Journal of Physics</i>	<i>Telecommunicatii (Roumania)</i>
<i>Journal of Technology, Bengal</i>	<i>Tijdschrift van het Nederlands Radiogenootschap</i>
<i>Journal of the Institution of Electrical Communi-cation Engineers of Japan</i>	<i>Transactions of the Engineering Institute of Canada</i>
<i>Journal of the Institution of Engineers, Australia</i>	

<i>Memoirs of the Faculty of Engineering, Kumamoto University (Japan)</i>	
<i>Proceedings of the International Symposium on Electronic Components, Malvern</i>	
<i>Reports of the National Research Council of Canada</i>	
<i>University of Delft Doctorate Thesis</i>	

INDEX OF PERSONS

The names of authors of papers are indicated by bold numerals for the page references. Biographical references are indicated by italic numerals.

	<i>Page</i>		<i>Page</i>		<i>Page</i>
Abhirama Reddy, C. ...	669	Eccles, Sir David ...	70	Lambert, J. S. ...	258
Akester, H. W. ...	6	Edinburgh, H. R. H. The	...	Lanchester, R. A. ...	142
Alexander, D. A. ...	71, 251	Duke of ...	236	Langton, N. H. ...	663
Allen, D. H. O. ...	510	Ellingham, R. W. ...	348	Latimer, K. E. ...	306, 381
Anderson, J. C. ...	49, 417	Ellis, H. O. ...	496	Lawrence, L. A. J. ...	85
Anslow, N. G. ...	291	Ellis, N. W. ...	630	Lewis, R. ...	6
Ash, W. T. ...	329	Elton, H. J. ...	249	Lockspeiser, Sir Ben ...	94
		Emery, E. J. ...	32		
		Evans, R. B. ...	262		
Barnett, Sir Ben ...	142	Faircloth, R. L. ...	143	Macintosh, A. E. ...	226
Bassett, E. J. ...	510	Fakley, D. C. ...	317	Mahendru, P. D. ...	262
Batchelor, J. H. ...	124	Feather, N. ...	82	Manfield, H. G. ...	304
Beagles, R. E. ...	497	Ferrett, D. J. ...	143	Marriott, G. A. ...	5, 83, 326, 386, 693, 724
Beauchamp, K. G. ...	446	Finden, H. J. ...	249	Matthews, D. ...	663
Beck, G. E. ...	443	Foster, K. ...	715	Meewezen, W. D. ...	714
Bell, D. A. ...	124, 248	Fouweather, K. W. B. ...	443	Mellon, D. C. ...	414
Bennington, T. W. ...	413	Fowler, C. S. ...	292	Melville, H. W. ...	94
Bevc, V. ...	696			Miller, C. W. ...	630
Beynon, W. J. G. ...	401	Ganderton, P. C. ...	331	Mitchell, J. H. ...	304
Binks, J. K. ...	581	Gargini, E. J. ...	174	Mitra, S. K. ...	226, 661
Blackband, W. T. ...	255	Garthwaite, E. ...	387	Moss, H. ...	485
Blair, G. M. ...	581	Garton, G. C. ...	138	Mothersole, P. L. ...	307
Blowers, G. G. ...	357	Gaut, G. L. ...	137	Mott, N. F. ...	70
Boomer, G. I. ...	101	Gilmore, A. G. ...	254	Mountbatten, Admiral of the	...
Booth, A. D.	Glover, B. W. ...	136	Fleet, The Earl ...	70, 323
Booth, F. M. ...	253	Godfrey, A. I. ...	355		
Borley, C. R. ...	252	Gray, T. ...	442	Nemet, A. ...	262
Bose, Sir J. C. ...	661	Griffiths, H. V. ...	412	Nettell, D. F. ...	124, 248
Bragg, Sir Lawrence ...	6	Griffiths, J. W. R. ...	318	Nicholson, C. H. ...	17
Braybrook, C. H. ...	252	Grocott, D. F. H. ...	291	Niklas, W. F. ...	653
Brennand, R. ...	630				
Brinkley, J. R. ...	595	Halton, D. L. ...	510	O'Hanlon, D. M. ...	443
Brown, J. I. ...	630	Harris, I. A. ...	596		
Buffington, J. W. ...	256	Hasson, J. ...	510	Palmer, J. L. ...	696
Burkett, R. W. ...	175	Hayes, N. W. V. ...	714	Parker, J. D. ...	595
Burrows, K. ...	415	Heathcoat Amory, D. ...	630	Peard, Sir Kenyon ...	329
		Heightman, D. W. ...	350, 413	Pengilley, C. J. ...	179
Cane, P. E. ...	621	Henderson, J. G. ...	179	Perkins, W. J. ...	505, 630
Catton, M. ...	443	Hendley, D. A. ...	291	Perry, S. H. ...	341
Chapman, D. G. ...	248	Hill, J. W. ...	581	Peterson, R. J. ...	176
Chisholm, R. O. ...	124	Hilsum, C. ...	595	Peysou, J. ...	178
Clarke, G. M. ...	359	Hinshelwood, Sir Cyril ...	142, 321	Pickavance, T. G. ...	174
Clifford, G. D. ...	83, 629, 630, 693, 724	Hoge, R. R. ...	125	Pickles, J. S. ...	83
Coates, L. ...	252	Holloway, D. R. ...	249	Piddington, V. H. ...	349
Cockcroft, Sir John ...	398	Horlock, B. A. ...	249	Planer, G. V. ...	177
Collins, N. ...	386	Hosburn, J. C. ...	329	Potok, M. H. N. ...	263
Cook, P. F. ...	292	Howard, R. J. F. ...	237	Potter, R. ...	95
Cooke-Yarborough, E. H. ...	305	Howkins, W. E. ...	581	Powell, C. ...	277
Copeland, K. ...	630	Hughes, W. G. ...	151	Price, W. L. ...	6
Coppin, K. J. ...	250	Hytch, J. ...	70	Prince, M. B. ...	583
Cozens, J. H. ...	137				
Craven, J. H. ...	293	Jelonek, Z. J. ...	101	Ramachandra Rao, B. ...	493, 669
Cunningham-Sands, J. ...	595	Jeppesen, P. E. ...	354	Ramsay, D. A. ...	136
		Joslin, V. A. ...	346	Richards, C. E. ...	135
		Joslin, C. A. F. ...	630	Roberts, R. S. ...	386
		Joslin, S. W. ...	82	Robinson, F. H. ...	70
Davies, D. E. N. ...	709	Kendell, R. ...	465	Robson, A. ...	510
Dickenson, C. R. ...	581	Kennard, L. J. ...	17	Rogers, A. W. ...	56
Doherty, S. N. ...	354	Kilham, L. F. ...	253	Rosenbrock, H. H. ...	57
Dorling, Vice-Admiral, J. W. S. ...	6	Kirkpatrick, Sir Ivone ...	386	Ross, C. W. ...	551
Dummer, G. W. A. ...	55	Kiryuk, W. ...	510		
		Kollanyi, M. ...	541		

INDEX OF PERSONS

Scadeng, P.	356	Süsskind, C.	696	Walker, E. G.	425
Seaborne, R. F.	371	Syke, G.	117	Wansbrough-Jones, Sir Owen	328
Sewell, D. W. R.	135			Webb, F. R. G.	355
Seymour, P. W.	446	Taylor, G. A.	695	Wei Kung Hsu	581
Sharp, L. W. D.	175	Taylor, W. E.	621	Welsby, V. G.	465
Shearman, E. D. R.	414, 510	Telford, M.	511	Westcott, J. H.	133
Shepherd, R. B.	227	Tenger, P.	33	Wiegerinck, H. T. J.	142
Sherwood, S.	505	Terry, N. B.	371	Wilkins, A. F.	510
Shipgood, F. J.	363, 510	Tomlinson, T. B.	510	Wilkinson, H.	262
Silver, H. G.	226	Toothill, J. N.	83	Williams, E.	630
Slater, F.	189	Trojanowski, M. S.	414	Williams, H. P.	595
Smith-Rose, R. L.	631	Tucker, D. G.	233, 465	Williams, N. A. F.	248
Sohrabji, N.	297	Tye, L.	352	Wilson, B. L. H.	207
Spears, R. A.	613			Wilson, I.	85, 95
Spencer, H. C.	594	Vallese, L. M.	725	Wimpffen, J.	653
Squires, M.	151	van Trier, A. A. Th. M.	138	Winwood, J. M.	510
Srirama Rao, M.	493, 669	van Weel, A.	510, 525	Wolf, M.	583
Stagg, J. M.	414	von Munch, W.	136, 645	Wolsey, C. L.	351
Sterling, Sir Louis	329, 330			Wray, A. G.	387
Stevens, J. H.	329	Waite, T. A.	248		
Stevenson, D.	227	Waldron, R. A.	361, 510, 597, 677, 733	Zepler, E. E.	630
				Zworykin, V. K.	505

Note.—The authors of papers abstracted in "Radio Engineering Overseas" are not included in this list but are given in the separate Index of Abstracts.